

**SPATIOTEMPORAL CHARACTERISATION OF SOME TRANSCRIPTIONAL
SIGNATURES IN EARLY CEREBELLAR DEVELOPMENT**

by

Ishita Gupta

B. Tech., Indian Institute of Technology Kanpur, 2017

A THESIS SUBMITTED IN PARTIAL FULFILLMENT OF
THE REQUIREMENTS FOR THE DEGREE OF

MASTER OF SCIENCE

in

THE FACULTY OF GRADUATE AND POSTDOCTORAL STUDIES
(Medical Genetics)

THE UNIVERSITY OF BRITISH COLUMBIA

(Vancouver)

August 2020

© Ishita Gupta, 2020

The following individuals certify that they have read, and recommend to the Faculty of Graduate and Postdoctoral Studies for acceptance, a thesis entitled:

Spatiotemporal characterisation of some transcriptional signatures in early cerebellar development

submitted by Ishita Gupta in partial fulfillment of the requirements for

the degree of Master of Science

in Medical Genetics

Examining Committee:

Dr. Daniel Goldowitz, Medical Genetics

Supervisor

Dr. Carles Vilarino-Guell, Medical Genetics

Supervisory Committee Member

Dr. Douglas Allan, Cellular & Physiological Sciences

Supervisory Committee Member

Dr. Timothy O'Connor, Cellular & Physiological Sciences

Additional Examiner

Abstract

The cerebellum is an important part of the central nervous system (CNS). During early embryonic development, the neuroepithelium of the cerebellar primordium consists of two primary progenitor zones – the rhombic lip (RL) and the ventricular zone (VZ). All glutamatergic cells like granule cells arise from the RL while the GABAergic cells like Purkinje cells arise from the VZ. Each of the progenitor zones gives rise to multiple cell types in a distinct spatiotemporal sequence, but it is not clear what are the underlying genetics that control this sequence. Compartmentation of these progenitor zones has been an emerging field in this line of investigation. Using fluorescent RNA *in situ* hybridisation, I have characterised the *Msx* genes, a family of transcription factors downstream of BMP signaling, to show how they spatiotemporally pattern the cerebellar neuroepithelium. *Msx1* is compartmentalised within the RL to likely maintain a progenitor pool, while *Msx3* is compartmentalised within the VZ to likely be involved in the VZ progenitor fate specification. As external signaling molecules, the BMPs have been implicated in the specification of cerebellar cell types but their downstream molecular cascades are unknown. The results of this study present the *Msx* genes as strong candidates facilitating this BMP signaling in cerebellum development. In the second part of the study, I have utilised a time-course transcriptome to identify a catalog of brain specific long non-coding RNAs (lncRNAs) expressed significantly in the developing cerebellum. This class of non-coding RNAs is largely heterogenous and uncharacterised in their function. Recent studies, however, have implicated lncRNAs in the genetic regulation of CNS development. The top candidate lncRNA of the catalog, 6330403K07Rik, has been analysed for its spatiotemporal expression in the developing cerebellum. 6330403K07Rik has strong expression in the RL and nuclear transitory zone at E11.5 and in the glutamatergic cerebellar nuclear neurons at E18.5. This two-part study is aimed to further the genetic resolution of cerebellar development through gene expression studies. Developmental defects in the cerebellum are implicated in neurodevelopmental disorders such as Autism Spectrum Disorder, Schizophrenia and ADHD, and understanding the genetics of cerebellar development is important to developing therapeutic interventions.

Lay Summary

The cerebellum has an important role in brain function to coordinate incoming sensory information that is crucial to motor, emotional and cognitive processing. Not surprisingly, alterations in cerebellar development are linked to several neuropsychiatric disorders. A two-part study was done to better understand gene regulation in cerebellar development. The first part focused on the expression patterns of the *Msx* genes, a family of transcription factors that responds to critical signaling in brain development. The second part focused on one of the largest classes of RNAs that do not code for proteins. We find many long non-coding RNAs enriched during cerebellum development. The top candidate, 6330403K07Rik, was found to be expressed in many cell types of the cerebellum including a distinct class of cerebellar nuclear neurons. This is a first step towards understanding the potential role of the *Msx* genes and long non-coding RNAs in cerebellar development.

Preface

I was responsible for the design of research, design and execution of all experiments, data collection, data analysis, and making of all illustrations and figures. Miguel Ramirez helped me with the FANTOM5 time-course transcriptome analysis to generate Appendix Table 1 and the Z-score analysis to generate Table 3.1. Daniel Goldowitz was the supervisory author on this project and was involved in the design of research, data analysis and thesis edits.

Table of Contents

Abstract	iii
Lay Summary	iv
Preface	v
Table of Contents	vi
List of Tables	viii
List of Figures	ix
List of Abbreviations	xi
Acknowledgements	xiii
Chapter 1 - Introduction	1
1.1 Introduction to the Cerebellum	1
1.2 Signaling from the isthmus organiser to generate the cerebellar primordium	2
1.3 Progenitor zones and molecular compartmentation of the cerebellum in early development	3
1.4 <i>Atoh1</i> -null, <i>Ptf1a</i> -null, and <i>Pax6</i> -null mice as tools to better understand cell types emerging from the progenitor zones: phenotypes from the molecular defects	8
1.5 Importance of BMP signaling in cerebellum development.....	9
1.6 Introduction to the <i>Msx</i> genes	10
1.7 Introduction to FANTOM5 time-course transcriptome	13
1.8 Introduction to long non-coding RNAs in cerebellum development	14
Chapter 2 - Materials & Methods	16
2.1 Animal husbandry	16
2.2 Tissue preparation and histology.....	16
2.3 Fluorescence immunohistochemistry	16

2.4 BrdU labelling	17
2.5 RNA <i>in situ</i> hybridization	17
2.6 RNAscope® fluorescence <i>in situ</i> hybridization	18
2.7 Organotypic E11.5 cerebellum explant culture	19
2.8 Microscopy	22
Chapter 3 - Results.....	23
3.1 <i>Msx</i> genes are expressed only in the progenitor zones at early time-points	23
3.2 <i>Msx1</i> and <i>Msx2</i> are compartmentalised within the rhombic lip at E12.5	24
3.3 <i>Msx3</i> expression in the VZ creates a demarcation between the <i>Atoh1</i> and <i>Ptfla</i> domains at E12.5	27
3.4 <i>Msx3</i> is compartmentalised within the ventricular zone at later time-points	28
3.5 Catalog of brain specific lncRNA expressed in the cerebellum during development	31
3.6 Characterizing spatial-temporal expression of 6330403K07Rik	33
3.7 LncRNA 6330403K07Rik is expressed in the <i>Tbr1</i> -positive glutamatergic CN neurons ..	37
Chapter 4 - Conclusion.....	42
4.1 <i>Msx</i> genes pattern the early cerebellar neuroepithelium.....	42
4.2 There are brain specific long non-coding RNAs expressed in the cerebellum during development	44
4.3 The functionally unannotated lncRNA 6330403K07Rik shows cell type specific expression in the developing cerebellum	44
4.4 Single cell RNA-seq data supports findings for <i>Msx</i> genes and 6330403K07Rik	45
References	48
Appendices.....	58
Appendix Figures	58
Appendix Tables	63

List of Tables

Table 3.1. Highly expressed lncRNAs enriched during cerebellar development.....	32
Table 4.1. List of cell type clusters identified for <i>Msx</i> genes and lncRNA 6330403K07Rik using a single cell RNA-seq study by Vladoiu et al. (2019).....	47
Appendix Table 1. Expression levels of robustly expressed lncRNAs during cerebellum development.....	65

List of Figures

Figure 1.1. Illustration of the cerebellar progenitor zones in a sagittal view of E12.5 cerebellum.....	5
Figure 1.2. Illustration of molecular compartmentation in the RL as studied by Yeung et al. (2014).....	6
Figure 1.3. Illustration of molecular compartmentation in the VZ.....	7
Figure 2.1. Schematic drawing taken from Kapfhammer (2009) showing the arrangement of the interface-type explant culture.....	19
Figure 2.2. Schematic illustration taken from Kawabata et al. (2004) showing the arrangement of the electroporation.....	20
Figure 2.3. Characterizing the organotypic E11.5 cerebellum explant culture.....	21
Figure 2.4. <i>Msx3</i> expression in an electroporated organotypic cerebellum culture.....	22
Figure 3.1. Higher <i>Msx</i> expression at early time-points in the cerebellum is limited to the progenitor zones.....	24
Figure 3.2. <i>Msx1</i> is compartmentalised within the RL.....	26
Figure 3.3. <i>Msx3</i> does not overlap with <i>Atoh1</i> . <i>Msx3</i> overlaps with <i>Ptf1a</i> but their boundaries near the RL do not coincide.....	28
Figure 3.4. <i>Msx3</i> is compartmentalised within the VZ at E14.5 and this expression is spatially dynamic.....	30
Figure 3.5. <i>Msx3</i> is expressed strictly within the proliferative neuroepithelium.....	30
Figure 3.6. Temporal expression of 6330403K07Rik across cerebellar time-course.....	33
Figure 3.7. Spatial expression of 6330403K07Rik in the cerebellar primordium across multiple embryonic ages.....	34
Figure 3.8. LncRNA 6330403K07Rik co-expresses with glutamatergic lineage marker <i>Atoh1</i> in the RL at E11.5.....	36
Figure 3.9. 6330403K07Rik expression in the CN neurons is perturbed in <i>Pax6</i> -null mutant E18.5 cerebellum.....	39
Figure 3.10. 6330403K07Rik expression in the cerebellum at P0.....	41
Figure 4.1. Schematic illustration of <i>Msx</i> compartmental expression in the early embryonic cerebellar neuroepithelium.....	43

Appendix Figure 1. <i>Msx1</i> and <i>Msx2</i> expression in postnatal age.....	58
Appendix Figure 2. Negative control for RNA <i>in situ</i> hybridisation (ISH) for (a) E11.5, (b) E12.5 and (c) E14.5.....	59
Appendix Figure 3. <i>Msx1</i> and <i>Atoh1</i> expression at E11.5.....	60
Appendix Figure 4. Negative control for RNAscope FISH for (a) E11.5, (b) E12.5 and (c) E14.5.....	60
Appendix Figure 5. <i>Msx3</i> expression in postnatal ages localises to Purkinje cells.....	61
Appendix Figure 6. LncRNA 6330403K07Rik is conserved across multiple species.....	61
Appendix Figure 7. Weak 6330403K07Rik expression in the VZ at E11.5.....	62

List of Abbreviations

ACC	Animal Care Committee
bHLH	basic Helix-Loop-Helix
BrdU	5-bromo-deoxyuridine
CAGE	Cap Analysis of Gene Expression
CN	Cerebellar nuclei
CNS	Central Nervous system
CP	Choroid plexus
DAPI	4',6-diamidino-2-phenylindole
DNA	Deoxyribonucleic acid
E	Embryonic day
eGFP	Enhanced green fluorescent protein
EGL	External granule cell layer
EP	Electroporation
eRL	Exterior rhombic lip
FANTOM5	Functional Annotation of Mammalian Genome 5
FISH	Fluorescent <i>in situ</i> hybridisation
GC	Granule cell
GRN	Gene regulatory network
HH	Hamburger-Hamilton stage
HRP	Horseradish peroxidase
IGL	Internal granule cell layer
IN	Interneurons
iRL	Interior rhombic lip
ISH	<i>In situ</i> hybridisation
IsO	Isthmic organiser
KO	Knock out
lncRNA	Long non-coding RNA
MHB	Midbrain-Hindbrain boundary
N	Neonatal day
NTZ	Nuclear transitory zone
OCT	Optimal cutting temperature
P	Postnatal day
PBS	Phosphate buffer saline
PBS-T	Phosphate buffer saline - Tween20
PC	Purkinje cell
PFA	Paraformaldehyde
r1	Rhombomere 1
RL	Rhombic lip

RNA	Ribonucleic acid
RP	Roofplate
scRNA-seq	Single cell RNA sequencing
TFs	Transcription factors
TPM	Transcripts per million mapped
UBC	Unipolar Brush cell
VZ	Ventricular zone

Acknowledgements

I would like to express sincere and heartfelt gratitude to my supervisor, Dr. Dan Goldowitz, for taking me in as a student in his group and training me. Thank you for introducing me to the world of the cerebellum and neurodevelopment. I have learnt so much from you, and you are truly a source of inspiration for me.

I would like to extend my gratitude to my committee members, Dr. Douglas Allan and Dr. Sara Mostafavi, for their valuable supervision throughout my project.

I am deeply grateful to the members of the Goldowitz lab. Thank you, Dr. Joanna Yeung, for your mentorship and training in all the experiments I have enjoyed doing so much. Thank you, Miguel Ramirez, for all your help and support. I thank Anita Chiu, Dr. Maryam Rahimi Balaei, Jeffy Rajan Soundararajan, Cheryl Tan, Nayrouz El-azzabi, Yuliya Badayeva, Brian Daly and Erin Yang for their continued friendship and help.

I would also like to thank my parents, family and friends for their constant support.

In the unprecedented times of the COVID19 pandemic, I would like to acknowledge the hardships being faced by the world. I am incredibly grateful that I was safe and had comfortable access to basic utilities in the past few months as I drafted my thesis.

Chapter 1 - Introduction

1.1 Introduction to the Cerebellum

Cerebellum, or the “little brain”, is an important part of the central nervous system (CNS) in all vertebrates, accounting for over 80% of the neurons in the human brain (Andersen, Korbo, and Pakkenberg 1992). It is involved in motor coordination and cognitive functions (Schmahmann and Caplan 2006). Developmental defects in the cerebellum are implicated in neurodevelopmental disorders like Autism Spectrum Disorder (Fatemi et al. 2012).

The cortex of the adult cerebellum is organised into three major layers across all species. The molecular layer is the outermost layer of the cerebellar cortex and is low in cell density, primarily consisting of the parallel fibers of the Granule cells (GCs) and dendrites of the Purkinje cells (PCs), along with interneurons like Stellate and Basket cells. The Purkinje cell layer is the second layer, composed of a monolayer of the large cell bodies of the Purkinje cells along with the cell bodies of Bergmann glia and candelabrum cells. The next layer contains Granule cells, the most abundant neuron type in the brain, which are densely packed as the internal granular layer (IGL) along with the Unipolar Brush cells (UBCs), the Golgi cells, and the Lugaro cells. Underneath the cortical layers is the white matter (consisting of fibres coming into and going out of the cerebellar cortex), and then deep to the white matter are situated four major pairs (humans) of cerebellar nuclear (CN) neurons that are identified based on their positions from lateral to medial - dentate, emboliform, globose and fastigial nuclei. Emboliform and globose nuclei are not distinct in mice and thus are together referred to as interposed nuclei.

A major source of signal input comes from the pontine nuclei via the mossy fibers that project onto the GCs that further synapse with the PCs. PCs also receive input signals directly from the climbing fibers that originate in the inferior olive. The PCs then project onto the CN neurons as a modulatory inhibitory signal, as the CN neurons also receive excitatory signals from the collaterals of the mossy fibers and the climbing fibers. The CN neurons are the only output cells of the cerebellum.

The major molecular players and signaling pathways have been established and functionally characterized in the embryonic development of the cerebellum (Butts, Green, and Wingate 2014; Goldowitz and Hamre 1998). In mice (*Mus musculus*) the cerebellum primordium emerges around embryonic day (E) 9.5 and is influenced by many signaling centers, including the isthmus organiser and the fourth ventricle roof plate as it develops. Two progenitor zones - the rhombic lip (RL) and the ventricular zone (VZ) - are established and all cell types emerge from these two zones in a spatio-temporal sequence. The RL gives rise to all the excitatory or glutamatergic neurons like granule cells, glutamatergic nuclear neurons, and unipolar brush cells (UBCs) (Goldowitz and Hamre 1998). The VZ gives rise to all the inhibitory or GABAergic neurons like Purkinje cells, GABAergic nuclear neurons, and interneurons (Stellate, Basket and Golgi cells) (Goldowitz and Hamre 1998). The well-known neuronal circuitry, morphology and cellular organisation makes the cerebellum an excellent model to study the genetics of neurodevelopmental processes like cell specification, progenitor pool maintenance, cell migration and cell differentiation.

1.2 Signaling from the isthmus organiser to generate the cerebellar primordium

During early development, the neural tube is divided into 3 major neural vesicles along the rostral-caudal axis - prosencephalon (forebrain), mesencephalon (midbrain) and rhombencephalon (hindbrain). The rhombencephalon is further divided into 7 rhombomeres (r1-r7) based on morphological features. Rhombomere 1 (r1) is immediately caudal to the morphological midbrain-hindbrain boundary (MHB) between the mesencephalon and the rhombencephalon, and it was believed that r1 gives rise to the cerebellar primordium with the MHB forming the rostral boundary of the cerebellar primordium. Chick-Quail transplant experiments showed otherwise; the morphological MHB does not coincide with the boundary between the midbrain primordium and hindbrain primordium (Hallonet, Teillet, and Le Douarin 1990). Later it was shown that this boundary can be molecularly defined, that being between the complementary expression of *Otx2* and *Gbx2*. *Otx2* is expressed in the midbrain region and its expression ends slightly rostral to the morphological MHB in E9.5 mouse and Hamburger-Hamilton (HH) 10 chick (Millet et al. 1996). The *Gbx2-Otx2* boundary marks the rostral boundary of the cerebellar primordium, which arises from the *Gbx2*-positive, *Otx2*-negative and *Hoxa2*-negative part of r1 (Wassarman et al. 1997; Wingate and Hatten 1999). This *Gbx2-Otx2*

expression patterning sets up the expression of other genes like *Wnt1* and *Fgf8* and forms a signaling center called the Isthmus Organizer (IsO) (Broccoli, Boncinelli, and Wurst 1999; Millet et al. 1999). The IsO is responsible for signaling the r1 and the adjacent mesencephalon that induces the cerebellar primordium and midbrain primordium, respectively.

Deletion of either *Fgf8* or *Wnt1* in developing mice leads to the loss of midbrain and cerebellar structures (McMahon and Bradley 1990; Meyers, Lewandoski, and Martin 1998; Thomas and Capecchi 1990). In E8 mice, *Fgf8* is expressed all over the hindbrain region that gives rise to the cerebellar primordium later, while *Wnt1* is expressed all over the midbrain primordium. By E9.5 their expression regions get limited to specific bands near the MHB. While *Wnt1* is necessary but not sufficient for midbrain organogenesis (Matsunaga, Katahira, and Nakamura 2002; Panhuysen et al. 2004), ectopic expression of the protein FGF8 leads to the formation of cerebellar-midbrain structures indicating that FGF8 as a secretory molecule plays a key role in the organising of the IsO (Crossley, Martinez, and Martin 1996; Martinez et al. 1999). It is evident that the *Gbx2-Otx2* patterning is crucial to inducing the cerebellum primordium in early development.

1.3 Progenitor zones and molecular compartmentation of the cerebellum in early development

Establishment of the cerebellum primordium gives way to the formation of two primary germinal zones - the rhombic lip (RL) and the ventricular zone (VZ). All neuronal cell types emerge from these two progenitor zones in a temporal order beginning from E10.0. The RL and VZ are spatially and molecularly distinct regions of the neuroepithelium. RL is the dorsal-most part of the cerebellar neuroepithelium situated right next to the roof plate (Figure 1.1). All glutamatergic lineages arise from the RL, which include the large CN neurons, granule cells and UBCs (Machold and Fishell 2005; V. Y. Wang, Rose, and Zoghbi 2005). The temporal order of the emergence of the cell types was identified using Cre-mediated recombination with Tamoxifen in the *Atoh1*-CreERT2 reporter line mouse at various stages. The birthdating of *Atoh1* cells revealed that the first set of cells to emerge are the glutamatergic CN neurons at E10-E12 from the RL which then migrate to the nuclear transitory zone (NTZ) before migrating to their final positions in postnatal cerebellum. This is followed by the granule cells that are generated from E12.5 to E17 (Machold and Fishell 2005). Using a slice culture system and birthdating analysis

showed that the UBCs emerge from the RL at E15.5-E17.5 as the third set of cells (Englund et al. 2006).

The remaining part of the cerebellar neuroepithelium ventral to the RL is the cerebellar VZ (Figure 1.1). All the GABAergic lineages arise from the VZ, which includes the small CN neurons, Purkinje cells and interneurons (Stellate cells, Basket cells, Golgi cells) (Hoshino et al. 2005; Pascual et al. 2007). Genetic fate mapping analysis of *Ascl1* positive cells which coincide with the *Ptfla* positive cells in the VZ revealed the temporal order of neurogenesis in the VZ. The first wave of cells are the GABAergic CN neurons that emerge at E10.5-E11.5 in mouse, followed by the second wave of cells that are the Purkinje cells, born around E10.5-E11.5 and lasting until E13.5 (Hashimoto and Mikoshiba 2003; Kim et al. 2008; Sudarov et al. 2011). The third wave is the set of interneurons that emerge from E13.5 until postnatal day P7 (Leto et al. 2006; Sudarov et al. 2011). The various types of interneurons emerge in a temporal sequence akin to their inner-to-outer spatial positions - first being Golgi cells that reside in the IGL, second being Basket cells that reside in the inner molecular layer and the third being Stellate cells that sit in the outer molecular layer (Sudarov et al. 2011).

These two progenitor zones are molecularly defined by non-overlapping expressions of two basic Helix-Loop-Helix (bHLH) transcription factors - *Atoh1* (formerly termed *Math1*) for the RL and *Ptfla* for the VZ (Figure 1.1). Since these progenitor zones give rise to many cell types over time, a molecular compartmentation within the RL and the VZ has been explored although this is an emerging field of study and the present study aims to contribute to this ongoing analysis.

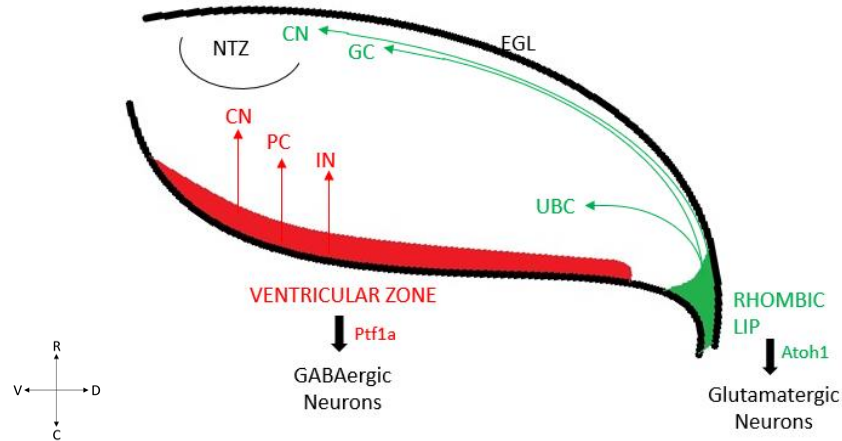


Figure 1.1. Illustration of the cerebellar progenitor zones in a sagittal view of E12.5 cerebellum.

Cerebellar neurons arise from two primary germinal zones. The glutamatergic lineage comes from the *Atoh1* expressing rhombic lip which includes the CN neurons that migrate to the nuclear transitory zone (NTZ), the Granule cells (GC) that migrate along the sub-pial stream and form the external granular layer (EGL) and finally the Unipolar Brush cells (UBCs). The GABAergic lineage comes from the *Ptf1a* expressing ventricular zone that gives rise to the CN neurons, Purkinje cells (PC) and the interneurons (IN). *Atoh1* and *Ptf1a* suppress each other. R, rostral; C, caudal; V, ventral; D, dorsal.

In the RL, compartmentation has been studied by Yeung et al. (2014) via the gene *Wntless* (*Wls*), a crucial player of WNT signaling. This study shows that at E11.5 the RL can be divided into 2 compartments divided across the rostral-caudal axis. The caudal-most tip of the RL, along with the choroid plexus (CP), consists of cells that are *Wls*-positive, *Lmx1a*-positive and *Atoh1*-negative. The rest of the RL is *Wls*-negative and *Atoh1*-positive with some cells at the boundary expressing *Lmx1a* (Figure 1.2). The *Wls* expression is unchanged in the *Atoh1*-null RL showing that this domain is independent of the regulation of *Atoh1*. By E15.5 a new compartmentation emerges dividing the RL into the interior face of RL (iRL) and exterior face of the RL (eRL). In the iRL, *Wls* expression is strong with weak expression of *Atoh1* whereas eRL is marked by strong expression of *Atoh1*, and later-on these two regions are completely segregated (Yeung et al. 2014) (Figure 1.2).

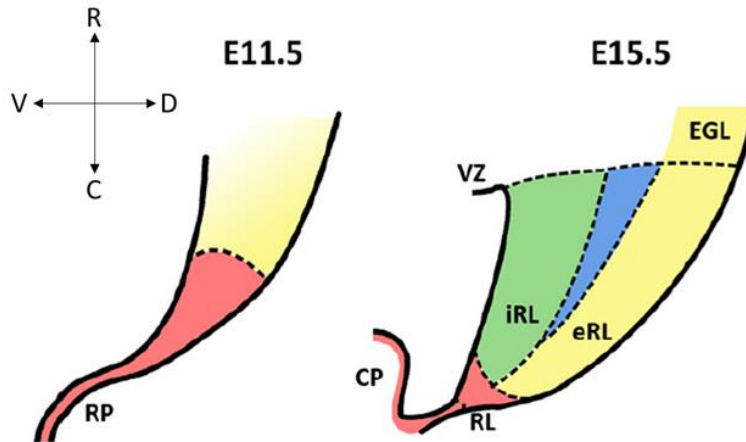


Figure 1.2. Illustration of molecular compartmentation in the RL as studied by Yeung et al. (2014). Figure taken from Yeung et al. (2014) showing two distinct types of compartmentation at different developmental stages. At E11.5 the caudal tip of the RL (red region) along with the roof plate (RP) are *Wls*-positive and *Atoh1*-negative. The yellow region is marked by strong *Atoh1* expression and is *Wls*-negative. By E15.5 a new division emerges, as marked by the iRL and eRL. The yellow eRL is marked by strong *Atoh1* and *Pax6* expression and very weak *Wls* expression. The green iRL has strong *Wls* expression and very weak *Atoh1* and *Pax6* expression. The blue region between these two is marked by *Tbr2*, *Lmx1a*, *Pax6* and is negative for *Wls*. RP, roofplate; CP, choroid plexus; RL, rhombic lip; EGL, external granule layer; VZ, ventricular zone; iRL, interior rhombic lip; eRL, exterior rhombic lip; R, Rostral; C, Caudal; V, Ventral; D, Dorsal.

Compartmentation has also been studied in the VZ. Zordan et al. (2008) studied the expression of proneural genes *Ngn1* and *Ngn2* within the *Ptf1a*-positive and *Ascl1*-positive domain of the VZ of the developing cerebellum (Zordan et al. 2008). Two compartments emerge at E13.5, a ventral sub-domain that is *Ngn2*-positive but *Ngn1*-negative, and the remaining VZ that is positive for both *Ngn1* and *Ngn2* (Figure 1.3 a). Genetic fate mapping of *Ngn1* and *Ngn2* expressing cells showed different cell fates. *Ngn1*-positive cells give rise to Purkinje cells and interneurons (Lundell, Zhou, and Doughty 2009; Obana et al. 2015). On the other hand, *Ngn2*-positive cells give rise GABAergic CN neurons, Purkinje cells and extra-cerebellar interneurons (Florio et al. 2012). Seto et al. (2014) studied compartmentation of the *Ptf1a* domain in the VZ with the non-overlapping expression of *Gsx1* in the ventral VZ and *Olig2* in the dorsal VZ (Seto et al. 2014). At E12.5 the *Gsx1* domain is much smaller and forms a boundary with the *Olig2* domain. Lineage tracing analysis showed that the *Gsx1*-positive cells are Pax2-positive interneuron progenitors (PIPs) and the *Olig2*-positive cells are Purkinje cell progenitors (PCPs). Interestingly, these domains change over developmental time. *Gsx1* expression expands dorsally, overtaking the *Olig2* domain while *Olig2* expression recedes in a complementary fashion,

causing the *Gsx1-Olig2* boundary to shift dorsally. By E14.5 the *Olig2* expression is gone, with *Gsx1* expressing in the entire domain. The *Olig2*-positive progenitors that were giving rise to PCPS at E12.5 have an identity transition to *Gsx1*-positive PIPs by E14.5 (Figure 1.3(b)).

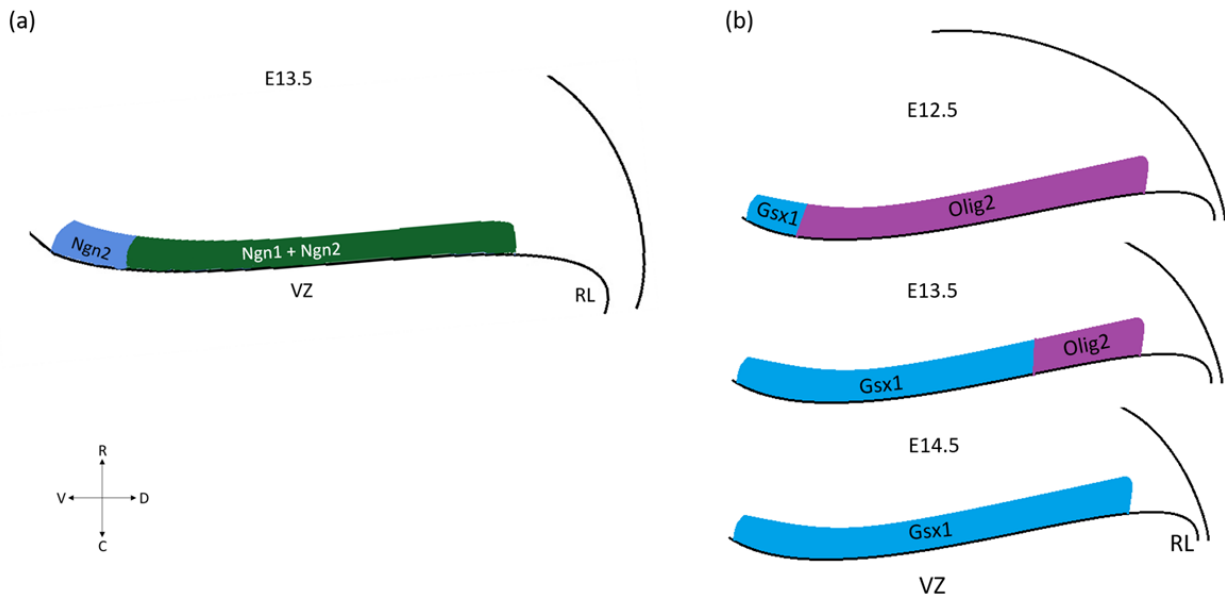


Figure 1.3. Illustration of molecular compartmentation in the VZ. (a) Within the *Ptf1a*-positive and *Ascl1*-positive domain, the VZ is split into two parts based on *Ngn1* and *Ngn2* expression. The green region has expression of both *Ngn1+Ngn2*. *Ngn1* cells give rise to Purkinje cells and interneurons. The blue region is positive only for *Ngn2*. *Ngn2* cells give rise to GABAergic CN neurons, Purkinje cells and extracerebellar interneurons. (b) Spatiotemporal compartmentation based on dynamic expression of *Gsx1* (blue) and *Olig2* (purple). With time the *Gsx1-Olig2* boundary shifts dorsally. *Gsx1* cells give rise to interneuron progenitors and *Olig2* cells give rise to Purkinje cell progenitors. RL, rhombic lip; VZ, ventricular zone; R, Rostral; C, Caudal; V, Ventral; D, Dorsal.

The demarcation between the RL and VZ is genetically not well understood. A possible explanation may come from the fact that *Atoh1* and *Ptf1a* mutually suppress each other. As shown by Yamada et al. (2014), the *Ptf1a^{Atoh1}* mouse mediates expression of *Atoh1* in the VZ leading to a reduction in *Ptf1a*-positive cells, and likewise expressing *Ptf1a* in the RL using the *Atoh1^{Ptf1a}* mouse leads to a reduction of *Atoh1*-positive cells (Yamada et al. 2014). While *Atoh1* and *Ptf1a* expressing domains are non-overlapping, there is no *Atoh1-Ptf1a* boundary observed. This leaves a possibility that other molecular players may be involved in conjunction with *Atoh1* and *Ptf1a* to separate the cerebellar neuroepithelium into the glutamatergic and GABAergic progenitor zones.

1.4 Atoh1-null, Ptf1a-null, and Pax6-null mice as tools to better understand cell types emerging from the progenitor zones: phenotypes from the molecular defects

Atoh1 and *Ptf1a* not only just pattern the neuroepithelium but are also important fate determinants of the cell types emerging from the two progenitor zones. *Atoh1* has been shown to be necessary for the generation of cerebellar glutamatergic cell types. *Atoh1*-null mutants show missing granule cells and the external germinal layer (EGL) (Ben-Arie et al. 1997). Later studies showed that *Atoh1*-null mutants are also missing CN neurons and UBCs (Englund et al. 2006; Machold and Fishell 2005; V. Y. Wang, Rose, and Zoghbi 2005). *Atoh1* is also sufficient to induce glutamatergic cell fate. Yamada et al. (2014) expressed *Atoh1* under the *Ptf1a* promoter, by creating the *Ptf1a^{Atoh1}* transgenic mice. This led to the ectopic expression of *Atoh1* in the *Ptf1a* positive region of the VZ and the production of glutamatergic neurons from the VZ was observed (Yamada et al. 2014).

Complementary to this, *Ptf1a* has been shown to be necessary for the generation of cerebellar GABAergic cell types. *Ptf1a*-null mutant (*cerebelless*) mice show the absence of all GABAergic neurons in the cerebellum (Hoshino et al. 2005). *Ptf1a* is also sufficient to induce a GABAergic cell fate. The study by Yamada et al. (2014) expressed *Ptf1a* under the *Atoh1* promoter by creating *Atoh1^{Ptf1a}* transgenic mice. The ectopic expression of *Ptf1a* in the *Atoh1*-positive RL region gave rise to cells expressing markers of VZ-lineage cells and getting committed to VZ-derived identities. *Ptf1a* also plays a role in preventing VZ cells from acquiring other identities influenced from neighboring regions. Genetic fate mapping of *Ptf1a* lineage cells in *Ptf1a*-null mutant cerebellum showed that some of the cells aberrantly migrated to the EGL and expressed markers of granule cells, which normally arise from the nearby *Atoh1*-positive RL (Pascual et al. 2007). Also, some of the *Ptf1a*-lineage cells in *Ptf1a*-null get fated to become extra cerebellar ventral brainstem neurons typically arising from the *Ascl*-positive and *Ptf1a*-negative neuroepithelium that is ventral to the cerebellar VZ (Millen et al. 2014).

Pax6 is a paired homeobox transcription factor known to play a significant role in the development of major parts of the central nervous system like the spinal cord, hindbrain, forebrain and the eye. *Pax6* is expressed in the RL early on about E13.5 and onwards, and is also expressed sequentially by the CN neurons, granule cells and UBCs as they emerge from the RL.

In the cerebellum, the role of *Pax6* is prominent in later development. Loss of *Pax6* leads to aberrant organisation of the EGL and the foliation, primarily including the Granule cells (Engelkamp et al. 1999; Swanson and Goldowitz 2011; Swanson, Tong, and Goldowitz 2005). Later studies also showed that *Pax6*-null mutant cerebellum has a loss of glutamatergic CN neurons due to enhanced cell death, as well as a loss of UBCs due to enhanced cell death and decreased neurogenesis (Yeung et al. 2016).

1.5 Importance of BMP signaling in cerebellum development

The roof plate produces BMP (bone morphogenetic protein) signaling molecules among other secretory molecules like WNT and retinoic acid signaling that covers the dorsal part of the developing cerebellum primordium. BMP ligands are part of the larger TGF-Beta family and are secreted as extracellular proteins that can be involved in autocrine or paracrine signaling. BMP receptors (*Bmpr*) are heteromers and functional receptors consist of type I and type II receptors to form a hetero tetramer. The intracellular mediators in the canonical signaling pathway are the *Smad* group of genes - *R-smads* or the receptor regulated *Smads*, *I-smads* or the inhibitory *Smads* and *Co-smad* or the common partner *Smad*.

Canonical BMP signaling (*Smad* dependent pathway) has been studied in cerebellar development and is shown to be necessary for normal development of both glutamatergic and GABAergic lineages. Activated *R-smad* is expressed in both the RL and the VZ (Fernandes, Antoine, and Hébert 2012; Tong and Kwan 2013). Studies have shown that loss of both BMP signaling components *Smad1* and *Smad5* (*R-smads*) in cerebellum results in defects in RL stem cell specification, loss of NTZ and reduced EGL; and activation of the BMP antagonist NBL1 suppresses RL cell specification (Krizhanovsky and Ben-Arie 2006; Tong and Kwan 2013). Overexpressing *Smad7* (*I-smad* that inhibits BMP signaling) in the MHB via *Wnt1*-Cre leads to loss of the choroid plexus and cerebellar morphologic anomalies (Tang et al. 2010). *Smad7* (*I-smad*) is expressed in the EGL hinting that activated BMP signaling is not required or suppressed in later development processes like EGL formation (Lai et al. 2011). An *ex vivo* culture-based study by Alder et al. (1999) also showed that E8 ventral neural plate cells could differentiate into mature cerebellar granule cells with BMP7 treatment (Alder et al. 1999).

Involvement of BMP signaling in the VZ lineages has not been explored as much. While the loss of *Smad4* (*Co-smad*) does not affect the glutamatergic lineage, *En1*-Cre knock-out of *Smad4* results in reduced number of Purkinje cells (Zhou et al. 2003). At an earlier age of E11.5, conditional knock-out of *Smad4* using *En1*-Cre significantly reduces the proliferative KI67-positive VZ progenitors (Fernandes, Antoine, and Hébert 2012). Recently, a study by Ma et al. (2020) has shown that the gradual spatiotemporal decline in the BMP/*Smad* gradient across the dorso-ventral axis of the VZ directs the identity transition of the VZ progenitor cells from *Olig2*-positive Purkinje progenitors to *Gsx1*-positive interneuron progenitors (T. C. Ma, Vong, and Kwan 2020). While it is clear that BMP signaling is important to the developing cerebellum, it is not clear what are the downstream genetic and transcriptional changes that mediate this signaling in the cerebellum, particularly in the RL and VZ.

1.6 Introduction to the *Msx* genes

Msx (muscle segment homeobox) genes are a family of highly conserved transcription factors that were first studied in the fruit fly (*Drosophila melanogaster*) as *msh* genes. In the fly, *msh* genes are known to be involved in neurogenesis, myogenesis and dorso-ventral patterning of the wing. They are directly activated by BMP signaling in mice and are suitable candidates for mediating BMP signaling in cerebellar development (Suzuki, Ueno, and Hemmati-Brivanlou 1997; Takahashi et al. 1998). These homeobox containing genes are known transcriptional repressors (Catron et al. 1995; Catron et al. 1996; Newberry et al. 1997; Zhang, Catron, and Abate-Shen 1996). The mouse family consist of three members - *Msx1*, *Msx2* and *Msx3*. These 3 genes share 98% sequence similarity in their homeodomains (Ekker et al. 1997). Mouse *Msx3* and the putative human ortholog *VENTX* (based on NCBI's Eukaryotic Genome Annotation pipeline) do not share sequence homology, hinting towards a species-based difference in functions and redundancy of the *Msx* family. In mice, *Msx1* and *Msx2* have been extensively studied in the context of craniofacial morphogenesis and limb organogenesis, while in neural development they are known to be expressed in overlapping patterns in many regions including roof plate cells and the adjacent neural tube. *Msx3* has been relatively less studied in the context of development although it is exclusively expressed only in the dorsal CNS in mouse, particularly the developing spinal cord and the cerebellum (Sunkin et al. 2013). Based on the expression of the *Msx* genes in the E9.5-E10.5 murine neural tube, along with strong expression

in the neural plate of cephalochordates (Sharman, Shimeld, and Holland 1999) and ascidians (Ma et al. 1996), this family of genes seems to have a strong conserved function in dorsal neural tube patterning.

Msx1 and *Msx2* have been widely studied in the context of craniofacial and tooth development (Foerst-Potts and Sadler 1997). *Msx1* expression is noted in the boundary region of the neural plate set to produce neural crest cells and is also required to induce markers of neural crest cells. *Msx* genes along with co-factors from the WNT signaling pathway are necessary for neural crest specification (Tríbulo et al. 2003). While *Msx1*-knock out (KO), *Msx2*-KO or a double-KO do not show major anomalies in neural crest formation, they do show major effects in neural crest derived tissue, such as craniofacial tissue and CNS tissue (Bach et al. 2003; Han et al. 2003; Satokata et al. 2000; Satokata and Maas 1994). Loss of function of *Msx1* shows neural phenotypes. *Msx1*-KO shows abnormal brain morphology, hypoplasia of the cerebral cortex, abnormal dorsal prosomere1 (Bach et al. 2003; Ramos et al. 2004), whereas anti-sense mediated knockdown (KD) of *Msx1* shows wavy or kinked neural tube and a small forebrain (Foerst-Potts and Sadler 1997). Gain of function analysis of *Msx1* shows induction of apoptosis (Bach et al. 2003) and reduction of neuronal differentiation and proliferation (Liu, Helms, and Johnson 2004). In the study by Liu et al. (2004), overexpression of *Msx1* in chick dorsal neural tube at HH10-12 disrupted and/or reduced the expression of pro-neural and pro-differentiation genes like *Cath1* (*Atoh1*) among others like *Cash1* (*Ascl1*), *Ngn1*, *Ngn2* and *Pax7* which was phenocopied by constitutive BMP signaling at that same stage (Liu, Helms, and Johnson 2004). *Msx1* mutations also affect the expression of genes like *Bmp6*, *Wnt1*, *Caspases*, *Pax* genes, *Lmx* genes and bHLH genes most notably as these have a known or implicated function in the cerebellum, as discussed above in various sections (Bach et al. 2003; Y. Liu, Helms, and Johnson 2004; Tríbulo et al. 2004). *Msx1*-KO reduces *Atoh1*-positive cells by more than half in the dorsal-most progenitor pool of the developing mouse spinal cord, while *Msx2*-KO reduces *Atoh1* to some extent and *Msx1*-*Msx2* double KO completely abolishes *Atoh1* expression throughout the dorsal spinal cord observed in E10.5 mice (Duval et al. 2014). This same study showed through lineage tracing analysis of *Msx1* that almost all *Atoh1*-positive cells at E10.5 arise from progenitors expressing *Msx1* as early as E9.25 in the murine dorsal spinal cord. This reveals that *Atoh1* is a downstream target of *Msx1*, and *Msx1* has an important regulatory role towards *Atoh1*.

A key question is whether this *Msx1-Atoh1* relationship is retained in the cerebellum. Despite a strong indication of a possible role, *Msx1* has not been studied in the context of cerebellum development yet.

Msx2 expression regions tend to overlap with *Msx1* expression regions, so there is a possibility of redundancy in function, although the *Msx1-Msx2* double KO displays more severe brain defects than either single gene mutants (Bach et al. 2003). Foerst-Potts and Sadler (1997) carried out anti-sense mediated disruption for *Msx2* as well and found similar phenotypes as *Msx1*, such as small forebrain and kinked neural tube (Foerst-Potts and Sadler 1997). Interestingly, *Msx2*-KO mice show a very severe cerebellar phenotype (Satokata et al. 2000). Satokata et al. (2000) noted a hypoplastic cerebellar vermis, severely reduced cerebellar lobules and foliation, and at a more histological level, disorganised layers of Purkinje cells and internal granule cells (Satokata et al. 2000). Gain of function analysis of *Msx2* reveals results similar to those of *Msx1* - induction of apoptosis, and reduction of neuronal differentiation and proliferation (Takahashi et al. 1998). While it is known that the upstream factors affecting *Msx2* include the BMPs (Y. Liu, Helms, and Johnson 2004; Takahashi et al. 1998) and *Pax3* (Kwang et al. 2002), downstream targets in neural development are not well identified, apart from the *Bmps* (Wu et al. 2003), *Atoh1* (Duval et al. 2014) and potentially *Wnt1* (Bach et al. 2003).

Msx3 is the least studied gene of the family, with no published *Msx3*-KO studies or any loss-of-function studies yet. We do know that BMP signaling activates *Msx3* - BMP4 can induce ectopic expression of *Msx3* in hindbrain explants (Shimeld, McKay, and Sharpe 1996). In the study by Liu et al. (2004), overexpressing *Msx3* in the chick dorsal neural tube at HH14-16 affected the cell fate of dorsal progenitors as they adopted a more dorsal identity at the expense of generating ventral neurons, which was phenocopied by constitutive BMP signaling but not by *Msx1* overexpression at that stage. The study also demonstrated that *Msx3* overexpression in the chick developing neural tube at HH10-12 could not replicate the effects shown by *Msx1* overexpression (Y. Liu, Helms, and Johnson 2004). Notably, *Msx3* protein has been functionally established to directly regulate *Msx1* transcription by recruiting a histone deacetylase to downregulate the *Msx1* promoter in a myoblast cell culture assay (Mehra-Chaudhary, Matsui, and Raghov 2001). Taken together, it is unlikely that *Msx3* and *Msx1* have redundant or similar

functional roles despite being closely related family members, and instead indicate distinct and stage-dependent roles. Unlike *Msx1* and *Msx2* which are expressed not only in CNS but also in the craniofacial tissue and the limb-buds, *Msx3* expression is restricted to the dorsal CNS only, specifically the cerebellum and the spinal cord (Shimeld, McKay, and Sharpe 1996; W. Wang et al. 1996). This warrants further studies of *Msx3* in the cerebellum.

These transcription factors can be expressed in a specific temporal window that associate with critical time periods in development. Hence, there is a need for understanding *Msx* patterning in cerebellum development as a first step towards understanding their function and readdressing the molecular compartmentation of the developing cerebellum. This is one goal of the thesis.

1.7 Introduction to FANTOM5 time-course transcriptome

Molecular patterning and regulatory pathways in development have an important temporal component that dictates the sequence of events required for correct development. This stresses the importance of understanding the genetic underpinnings of critical time windows. To this end, transcriptomic expression data across a time-course can help us capture gene regulatory elements with developmentally crucial dynamics. The Goldowitz group participated in the international FANTOM5 consortium led by RIKEN to create a transcriptomic expression dataset for the cerebellum; whole cerebellar tissue was collected from 12 developmental time-points (3 biological replicates per time-point) - embryonic days (E) 11.5 to E18.5 and postnatal (P) days 0, 3, 6 and 9 – and processed for cap analysis of gene expression (CAGE) sequencing (Forrest et al. 2014; Kodzius et al. 2006). With CAGE, every RNA molecule that is 5' capped is captured and sequenced at a single-nucleotide resolution towards its 5' end. Once mapped back to the genome, this gives us not only the transcriptional expression levels, but also transcriptional start sites, or promoters, due to the 5' sequence information (Kodzius et al. 2006).

In an unbiased approach, we can use bioinformatic analyses on this transcriptome to identify potential candidates involved in cerebellar development based on gene expression levels within the cerebellar time-points. Associative expression patterns across time can help us predict genes that are co-regulated, which can be modelled using algorithms on existing gene regulatory networks (GRNs), like the Regnetworks, to give us predicted GRNs (Liu et al. 2015). GRNs typically have clusters or hubs of genes each with a central hub gene that shows the highest

correlations with other genes. These hub genes can help us to potentially identify novel master regulatory genes. In a similar bioinformatic analysis by the Goldowitz group (unpublished), a cerebellum GRN was predicted based on the FANTOM5 cerebellum time-course using a skeletal network from Regnetworks and previously established algorithms (Gui et al. 2017). One of the hub genes that emerged from this cerebellar GRN was *Msx1*.

We can also identify tissue specific candidates using metrics that compare the expression levels of the transcripts across all the different tissue samples submitted to FANTOM5. This approach has been used to identify cerebellum specific transcripts during development. In a different approach, this dataset can be used to focus on the temporal expression dynamics of a candidate gene or family of genes and help us identify the potentially most important developmental stage(s) of the cerebellum that the candidate gene is involved in.

More recently single-cell RNA sequencing (scRNA-seq) has made it possible to look at transcriptional gene expression at a single cell level. Differential gene expression analysis on such a dataset has proved to be useful in identifying new cell types, and identifying transcriptional signatures for established cell types, as they emerge during development. Many scRNA-seq based studies on the cerebellum recently have furthered the cellular and molecular resolution of our understanding of cerebellum development (Carter et al. 2018; Vladioiu et al. 2019; Wizeman et al. 2019). Since the morphological information in such a study is absent, the need for spatial characterisation to understand gene patterning remains, complementary to the information obtained from scRNA-seq based studies.

1.8 Introduction to long non-coding RNAs in cerebellum development

Tools utilising sensitive RNA-based sequencing to obtain unbiased transcriptomics like the ones mentioned above also offer an opportunity to study the non-coding RNAs involved in the genetic regulation of CNS development.

Among the many categories of regulatory non-coding RNAs, the class of long non-coding RNAs (lncRNAs) remains largely heterogeneous and uncharacterised in their function. They are defined as long (>200 nucleotides) RNAs with no protein coding potential. They are capped, poly-adenylated, undergo splicing and are derived from genomic regions that are antisense, intronic, intergenic, and overlapping protein-coding loci. The proportion of non-coding DNA

seems to increase with developmental complexity (G. Liu, Mattick, and Taft 2013). LncRNAs have diverse interactions with DNA, RNA, and proteins which aligns with potential function in organizing and regulating cellular processes (Tim R Mercer and Mattick 2013). This has led to the idea that gene regulation by lncRNAs might have been important in giving rise to the diversity of cell differentiation programmes underlying development in multicellular organisms (Amaral and Mattick 2008; Taft, Pheasant, and Mattick 2007). As expression of mammalian lncRNAs shows greater tissue specificity than that of coding genes (Cabili et al. 2011), it seems likely that they might contribute to tissue-specific regulation. As part of FANTOM5, studies by the RIKEN group have created a massive atlas of lncRNAs in humans (Hon et al. 2017) and again showed strong support for tissue specific roles (Kawaji et al. 2017).

Expression of lncRNAs in the mammalian brain is impressive - it has been estimated that most of the lncRNAs are expressed in the mouse brain (T. R. Mercer et al. 2008) and about 40% in the human brain (Briggs et al. 2015; Derrien et al. 2012). LncRNAs have been shown to be vital for neuronal differentiation, neuron cell maintenance and neurogenesis (Ng, Johnson, and Stanton 2012). The functional role of lncRNAs in the context of brain development is thus an exciting direction of research.

To test the hypothesis that there are cerebellum specific lncRNAs involved in its development, the second aim of this thesis is to use the FANTOM5 time-course transcriptome to construct a catalog of lncRNAs that are highly and specifically expressed in the cerebellum. The top functionally unannotated candidate lncRNA would then be validated with spatial characterisation to give a cellular and molecular context to its possible function in cerebellar development.

Chapter 2 - Materials & Methods

2.1 Animal husbandry

For obtaining wildtype embryos, timed pregnancies were set up using wildtype C57/BL6 mice and the pregnant females were sacrificed in keeping with the guidelines of the Animal Care Committee (ACC).

For obtaining *Pax6*-null embryos, timed pregnancies were set up using Pax6^{Sev} mice (obtained from Robert Grainger and Marilyn Fisher, University of Virginia). The mice were bred, phenotyped and genotyped as described previously (Swanson, Tong, and Goldowitz 2005) and sacrificed in accordance with the guidelines of the ACC.

2.2 Tissue preparation and histology

Embryos harvested between E10.5 and E14.5 were immersion-fixed in 4% paraformaldehyde made in 0.1M PB for 1 hour on ice. Embryos harvested at E18.5 and onwards were first transcardially perfused with 0.1M PBS and 4% paraformaldehyde in 0.1M PB, brains were dissected out, and then immersion-fixed in 4% paraformaldehyde in 0.1M PB for 1 hour on ice. Fixed tissues were rinsed thrice with 0.1M PBS followed by cryoprotection in 30% sucrose solution in 0.1M PBS overnight at 4°C before embedding them in optimal cutting temperature (OCT) compound. Tissue was cryosectioned either in sagittal or coronal orientation at -20°C at 12 µm thickness, mounted on Superfrost slides (Thermo Fisher), air dried at room temperature and stored at -80°C until use.

2.3 Fluorescence immunohistochemistry

Tissue sections were prepared as described above. Slides were incubated at 37°C for 10 minutes before rehydrating in 0.1M PBS washes. Slides were then washed in 0.1M PBS-T before blocking in a solution of 1% BSA and 10% normal goat serum in PBS-T for an hour, followed by overnight incubation with the primary antibody in a humid chamber at room temperature. After 0.1M PBS-T washes, slides were incubated with fluorophore conjugated secondary antibodies (AlexaFluor, 1:500) and DAPI for an hour followed by PB washes and then coverslipped with FluorSave mounting medium (Vector Laboratories). Primary antibodies used: RbαOlig2 (1:500, AbCam), RbαLmx1a (1:2000, Millipore), RatαBrdU (1:500, AbCam)

2.4 BrdU labelling

To look at proliferative cells in the cerebellar ventricular zone, pregnant female mouse with E14.5 embryos was intraperitoneally injected with 5-bromo-deoxyuridine (BrdU, Sigma; 50 µg/g body weight) 1 hour before collecting the embryos. The pulse duration was 1 hour because the cells are rapidly dividing at this age, and the aim was to capture proliferative cells in the neuroepithelium only. Tissue sections were prepared as described above. Tissue sections underwent fluorescence immunohistochemistry with Rat α BrdU antibody (1:500), with an added step of 1M HCl incubation at 37°C for 30 minutes after the very first 0.1M PBS wash.

2.5 RNA *in situ* hybridization

Digoxigenin-UTP labelled riboprobes (antisense and sense) were generated corresponding to the cDNA of *Msx1*, *Msx2*, *Msx3* and 6330403K07Rik. The cDNA was amplified from a cDNA library made from E12.5 mouse cerebellum using Invitrogen SuperScript IV synthesis kit. The following primers were used:

Gene Name	Forward Primer 5'-3'	Reverse Primer 5'-3'	Riboprobe Position (NCBI Reference)
Msx1	CCGAAAGCCCCGAGA AACTA	GCTGGGGACCACGGAT AAAT	653-1470 (NM_010835.2)
Msx2	GCGGTGACTTGTTTTTC GTCG	TTTGTGAGAGGAAAGG GGGC	90-1095 (NM_013601.2)
Msx3	CCCTCCGCAAACACA AAACC	CTTCCAAGTCCATCCA GCGT	396-1344 (NM_001347609.1)
6330403K07Rik (ENSMUST00000156068)	AGAGGAATGAGAAGC GTAGCC	TCCATCAGACATGCTG CAAT	632-1570 (NM_134022.2)

This cDNA was cloned into pGEM-T Easy vector (Promega) and a combination of gene-specific primers and M13 primers were used to generate DNA templates which were then reverse transcribed using T7 and SP6 polymerases to generate the probes. The probes were denatured for 10 minutes at 72°C before being added to the hybridization buffer (Ambion). The tissue sections were acetylated with acetic anhydride in 0.1M triethanolamine and dehydrated with increasing concentrations of ethanol before hybridizing them with the probes overnight at 68°C in a humid chamber. Then, they were washed in saline sodium citrate (SSC) solutions: 4xSSC, 2xSSC, 1xSSC and 0.5xSSC at 55°C followed by anti-Dig antibody (Roche, 1:500) incubation for 2 hours at room temperature. After washes, sections were colorized with NBT/BCIP (Roche), fixed in 4% PFA, dehydrated and cleared in graded ethanols and Xylene, and coverslipped with Permount diluted in Xylene.

2.6 RNAscope® fluorescence *in situ* hybridization

To look at RNA level expression of 2 genes simultaneously, and at higher resolution, Bio-technique ACD's RNAscope Multiplex Fluorescent V2 Assay kit (single molecule RNA fluorescent *in situ* hybridization) was used according to manufacturer's instructions. The RNAscope technology uses tyramide signal amplification which suppresses background and boosts the signal such that individual RNA molecules can be detected as single dot punctae - The "ZZ" probe design only allows amplification to build upon consecutively bound probes on the target, thereby ensuring that each punctate dot represents only real signal (F. Wang et al. 2012; Z. Wang et al. 2013). Briefly, the slides were post-fixed in 4% PFA for 30 minutes, dehydrated in graded ethanol solutions and permeabilized with a protease treatment for 15-30 minutes depending on the tissue age. Slides were then hybridized with the probes overnight at 40°C. After this, the signal amplification tree was built by sequentially incubating slides in Amplifiers 1,2 and 3 at 40°C. The first amplification strand, Amplifier 1, only hybridizes to the "ZZ" s. This was followed by developing the fluorescent channels that involved incubation with HRP attached to the channel-specific sequence, adding the fluorescent dye, and then adding HRP blockers so the other channels can be developed similarly. All these incubations were done at 40°C for durations based on the user manual guide provided by the manufacturer. After the final HRP blocking step, slides were incubated in DAPI to counterstain for 5 minutes before coverslipping with FluorSave mounting medium. RNAscope protocol dictates a short DAPI treatment to ensure that the

punctate dots (real signal) are visible and not visually overpowered by the much larger nuclear DAPI staining.

2.7 Organotypic E11.5 cerebellum explant culture

Brain slice cultures are commonly used in electrophysiology and are a standard tool in neuroscience. Explant cultures of the mouse or rat cerebellum have been used to study development of specific cell types like Purkinje cells (Metzger and Kapfhammer 2000), and even genes transfected into the neurons of such cultures (Boukhtouche et al. 2006). The protocol is based on the chapter “Cerebellar Slice Cultures” in ‘Protocols for neural cell culture’ (Kapfhammer 2009) for postnatal cerebellum which I adapted for E11.5 cerebellum . The key difference was the tissue age, so instead of slicing a postnatal cerebellum into 350 μm thick slices, I dissected and cultured the whole E11.5 cerebellum primordium which is about 250 μm thick.

E11.5 cerebellum tissue has been previously shown to be cultured in vitro (de Diego et al. 2002). The equipment and reagents used are as described in the chapter by Kapfhammer (2009), while the media used to culture these explants was made according to previously described protocols (de Diego et al. 2002; Holland et al. 2012). Explants were dissected out of E11.5 embryo in clear HBSS on ice and placed on a Millipore membrane insert in a plate with 3 ml of media (Figure 2.1) (Kapfhammer 2009).

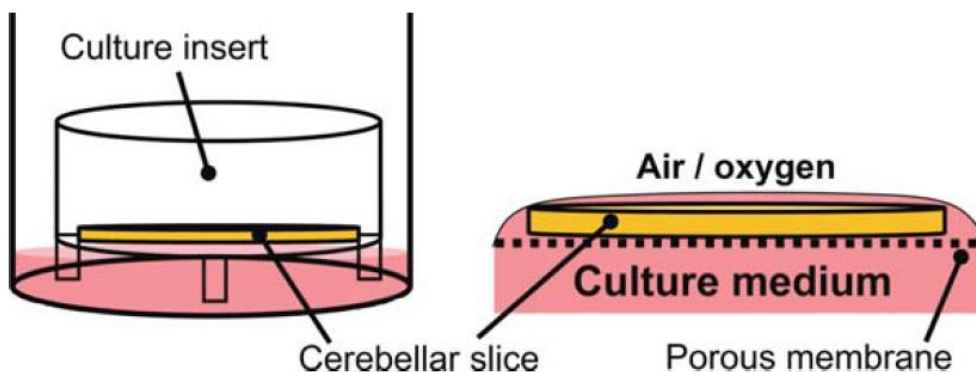


Figure 2.1. Schematic drawing taken from Kapfhammer (2009) showing the arrangement of the interface-type explant culture. The explant lies on a porous membrane in a tissue culture insert with the culture medium provided underneath such that the tissue has access to medium components through the large pores (0.4 μm) and also to oxygen from above which diffuses into the thin film of medium that coats the top of the tissue due to capillary action.

These explants were cultured for 2 hours at 37°C before electroporation. 10 µl of EP buffer with plasmid DNA containing eGFP of 1-2 µmg/µl concentration was electroporated on the tissue using a Petri dish-type circular platinum electrode and rod-type circular platinum electrode along with a CUY21EDIT electroporator (Figure 2.2) (Kawabata et al. 2004). The following parameters were used:

Voltage: 30 mV

Pulse ON: 5 ms

Pulse OFF: 500 ms

No. of pulses: 5

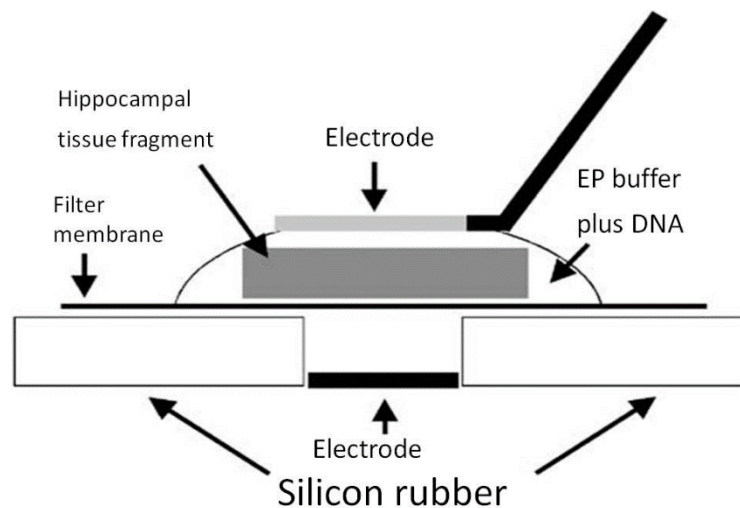


Figure 2.2. Schematic illustration taken from Kawabata et al. (2004) showing the arrangement of the electroporation. The membrane along with the tissue is transferred to a petri-dish type electrode with HBSS underneath the membrane. DNA mixed in EP Buffer is added on top and a rod-type electrode is used to then electroporate.

The explant along with the membrane insert was placed back in the culture dish containing the media and cultured for 24 or 48 hours at 37°C. The culture was stopped by immersing the explants in 0.1M PBS for a wash followed by immersing in 4% PFA for 1 hour at room temperature. Then 3 washes of 0.1M PBS were given and explants were stored in 0.1M PBS at 4°C.

The 24-hour cultures were then characterised with previously described protocols of immunohistochemistry and RNAscope fluorescence in situ hybridization, with the tissue being

free-floating in a 6-well plate. The ventricular zone is visualised by OLIG2 and *Msx3* expression, while the nuclear transitory zone is visualised by LMX1A expression (Figures 2.3, 2.4).

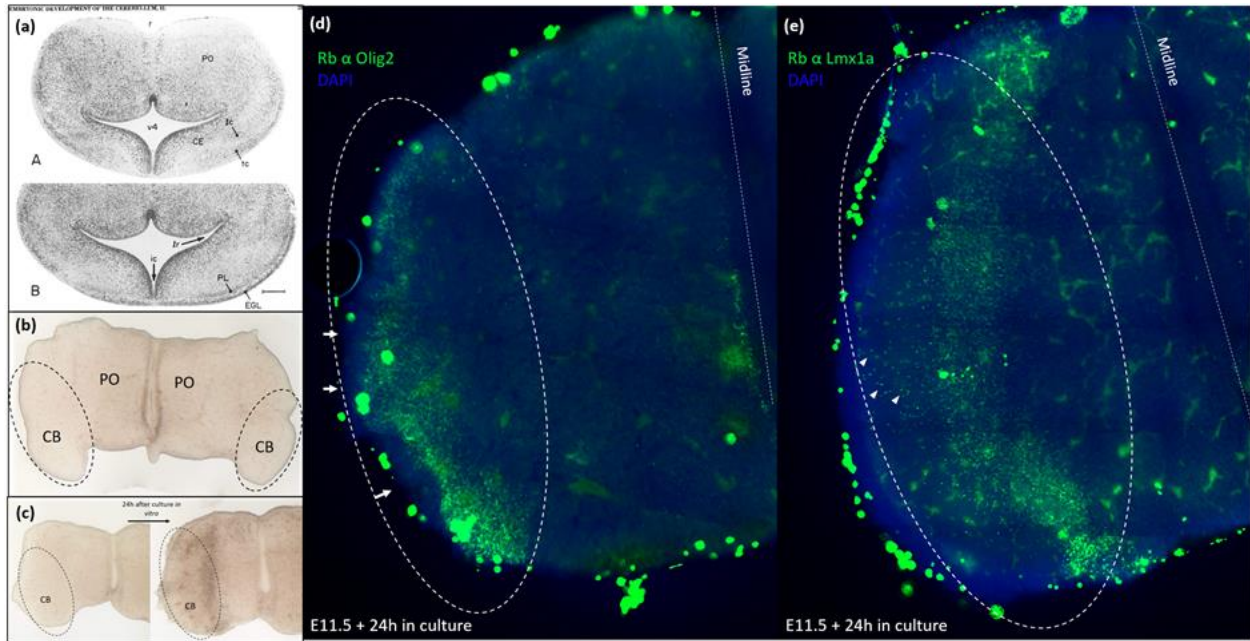


Figure 2.3. Characterizing the organotypic E11.5 cerebellum explant culture. (a) A and B show rat E17 cerebellum horizontal sections, from Altman & Bayer, 1985 which point out landmarks like the pons, the midline and the two halves of the cerebellum primordium. (b) and (c) show dissected E11.5 mouse cerebellum and how it looks after 24 hours in culture. (d) and (e) are two different cerebellum explants from two different embryos of the same litter, cultured for 24 hours and stained for (d) OLIG2 or (e) LMX1A protein expression using immunohistochemistry. (d) OLIG2 stains the ventricular zone at E11.5 and is not present in the rhombic lip (arrows). (e) LMX1A stains the roof plate, which is absent in the culture, and the nuclear transitory zone (NTZ) as highlighted by the dashed circle, with some LMX1A-positive cells seen to be migrating towards the NTZ (arrow heads).

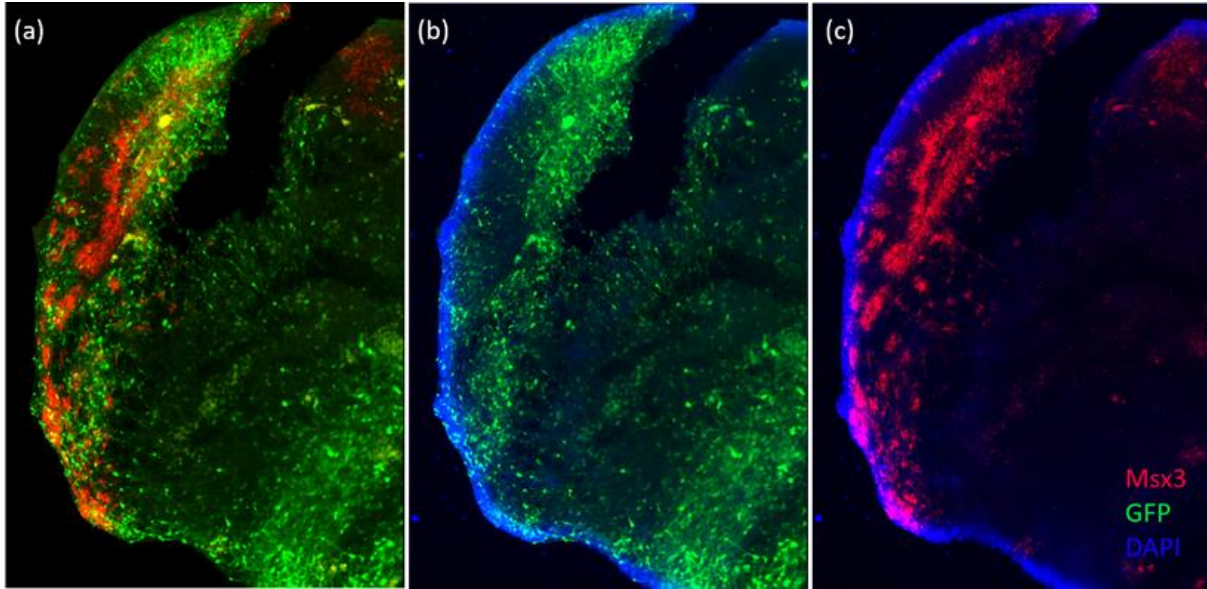


Figure 2.4. *Msx3* expression in an electroporated organotypic cerebellum culture. (a) *Msx3* expression (red) and eGFP positive cells (green) that show successful electroporation. (b) electroporated cells (eGFP positive) with DAPI counterstain. (c) *Msx3* expression, labelled by RNAscope fluorescence *in situ* hybridization, with the circled area highlighting the cerebellar ventricular zone. This was cultured for 24 hours.

2.8 Microscopy

Analysis and photomicroscopy was performed with a Zeiss Axiovert 200M microscope with the AxioCam/Axiovision hardware-software components (Carl Zeiss). Single-tiled fluorescent images were generated with auto-exposure. Multiple-tiled fluorescent images (Figures 3.9 and 3.10) were generated with manual exposure set to the same level.

Chapter 3 - Results

3.1 *Msx* genes are expressed only in the progenitor zones at early time-points

As a first step towards understanding the spatiotemporal expression patterns of the *Msx* transcription factors (TFs), I employed the use of the FANTOM5 time-course transcriptome for the developing cerebellum. This gives us an idea of how the *Msx* expression changes across developmental time in the cerebellum. All three *Msx* TFs have a highly dynamic temporal expression signature, with a steep decline after E11.5-E12.5 (Figure 3.1 a-c). The most dynamic part of the *Msx1* and *Msx3* graphs is at the early embryonic stages, hinting to their possible roles in events occurring during these time-points. While *Msx2* also shows dynamic expression during early development, *Msx2* additionally shows a temporally dynamic expression at neonatal (N) or postnatal stages as well. As detected by the transcriptome, *Msx2* expression rises at P3 corresponding to its expression detected in the granule cells (Appendix Figure 1 c-d).

To evaluate spatial expression of the *Msx* genes at E11.5-E12.5, I used chromogenic RNA *in situ* hybridization to probe for the mRNA levels on E11.5 and E12.5 sagittal cerebellum tissue sections (See Materials and Methods for probe details and tissue details). The histological images presented in this thesis henceforth represent observations made from at least 3 embryos with multiple sections stained from each embryo. *Msx1* expressed in the rhombic lip (RL) at both E11.5 and E12.5 (Figure 3.1 d, g). In contrast, *Msx3* expression is reserved to the ventricular zone (VZ) (Figure 3.1 f, i). *Msx2* expression is nonspecific but above noise level in the neuroepithelium (Figure 3.1 e, h; Appendix Figure 2 a, b). Expressions of *Msx1* and *Msx3* get more specific with better defined boundaries at E12.5 compared to E11.5. All the *Msx* genes are concentrated in the progenitor zones of the neuroepithelium and are absent from the rest of the cerebellar primordium at E12.5. See Appendix Figure 2 for negative control staining.

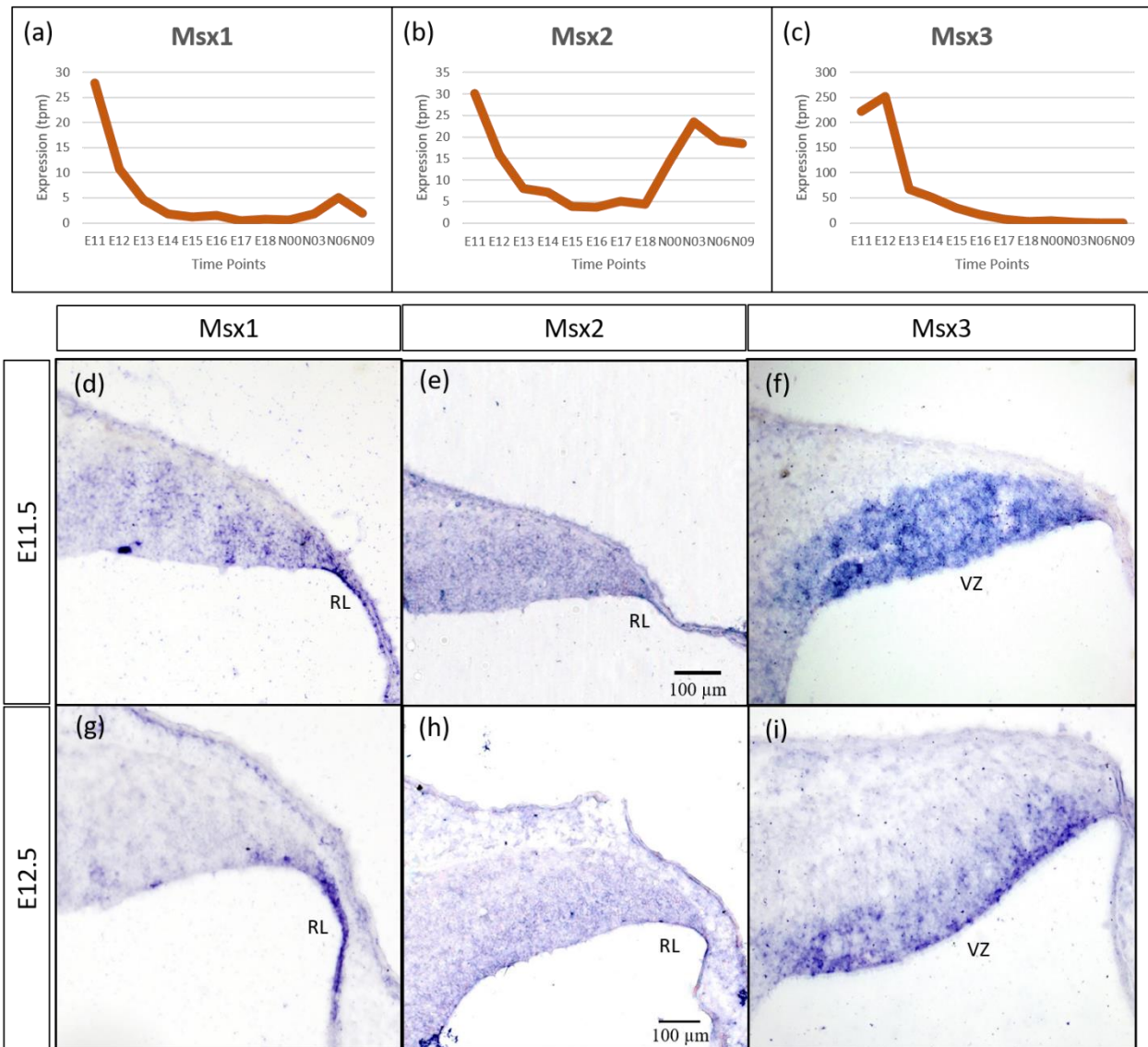


Figure 3.1. Higher *Msx* expression at early time-points in the cerebellum is limited to the progenitor zones. (a-c). Graphs show the dynamic nature of *Msx* expression in the cerebellum across 12 developmental time-points as observed from the RIKEN FANTOM5 transcriptome time-course data. (d-i). RNA *in situ* hybridization showing *Msx* genes expressed in the progenitor zones in (d-f) E11.5 sagittal sections and (g-i) E12.5 sagittal sections. *Msx1* expression is limited to the RL whereas *Msx3* is limited to the VZ. *Msx2* expression is nonspecific but above noise level in the neuroepithelium. See Appendix Figure 2 for negative control staining. RL, Rhombic Lip; VZ, Ventricular Zone. Scale bar, 100 μm.

3.2 *Msx1* and *Msx2* are compartmentalised within the rhombic lip at E12.5

As discussed in section 1.6, *Msx1* and *Msx2* have been previously shown to have overlapping expression domains with sometimes similar and/or redundant functions. To investigate this in the cerebellar RL, I used the highly sensitive RNAscope fluorescent RNA *in situ* hybridization (FISH) multiplex assay to double-label mRNAs of *Msx1* and *Msx2*, in the context of the *Atoh1*

positive RL. This histological technique, unlike traditional RNA *in situ* hybridization, has a signal amplification system that also quenches background, so that each sharp punctate dot represents only real signal (See Materials & Methods section 2.6 for more details). Interestingly, both *Msx1* and *Msx2* are expressed in compartments within the RL but these compartments are distinct. At E12.5 *Msx1* is expressed most strongly in the dorsal-most tip of the RL that is *Atoh1* negative (Figure 3.2 a) with much weaker expression in the rest of the RL. This is also observed at E11.5 (Appendix Figure 3). This compartmentation at E12.5 is illustrated in Figure 3.2 d. At E11.5 and E12.5, the *Atoh1*-negative compartment is *Wls*-positive and remains intact structurally upon ablation of *Atoh1*, with continued expression of *Wls* after complete loss of *Atoh1* (Yeung et al. 2014). *Msx2* expression is within the *Atoh1* expression domain and is not expressed in the *Atoh1*-negative *Msx1*-positive compartment (Figure 3.2 b-c). *Msx1* and *Msx2* expression regions are non-overlapping and form an *Msx1*-*Msx2*-*Msx1* banding pattern (Figure 3.2 c). Based on different expression compartments within the RL, *Msx1* and *Msx2* may have different functional roles in the cerebellum. At postnatal ages, *Msx2* expression is detected in the granule cells unlike *Msx1* (Appendix Figure 1). Whether these two TFs can functionally compensate for each other in the RL will require further studies in the cerebellum with *Msx1*-KO, *Msx2*-KO and double KO.

Later at E14.5, chromogenic RNA *in situ* hybridization of *Msx1* reveals that *Msx1* expression is stronger in the iRL compartment (Figure 3.2 e) which is also marked by stronger *Wls* expression (Yeung et al. 2014). This compartmentation is illustrated in Figure 3.2 d at E14.5. Yeung et al. (2014) proposed a cellular model wherein the iRL houses a pool of progenitors that migrate out of the RL via the eRL when they become *Atoh1* positive. *Msx1* expression supports this model. *Msx1* is a transcriptional repressor and represses pro-neural and pro-differentiation markers such as *Atoh1*, *Ascl1*, *Ngn1*, *Ngn2* and *Pax7* in the dorsal neural tube (Liu et al. 2004). Thus, it is likely that *Msx1* also represses pro-differentiation markers in the cerebellar iRL to keep the progenitor pool in a less-specified state, in tandem with *Wls* (Figure 3.2 d).

Previously, Duval et al. (2014) have shown through lineage tracing analysis of *Msx1* that almost all *Atoh1*-positive cells at E10.5 arise from progenitors expressing *Msx1* as early as E9.25 in the murine dorsal spinal cord. As *Msx1* is expressed in the same compartments as *Wls* in the RL, this

expression pattern of *Msx1* also supports the possible upstream regulatory role of *Msx1* towards *Atoh1* in the cerebellum.

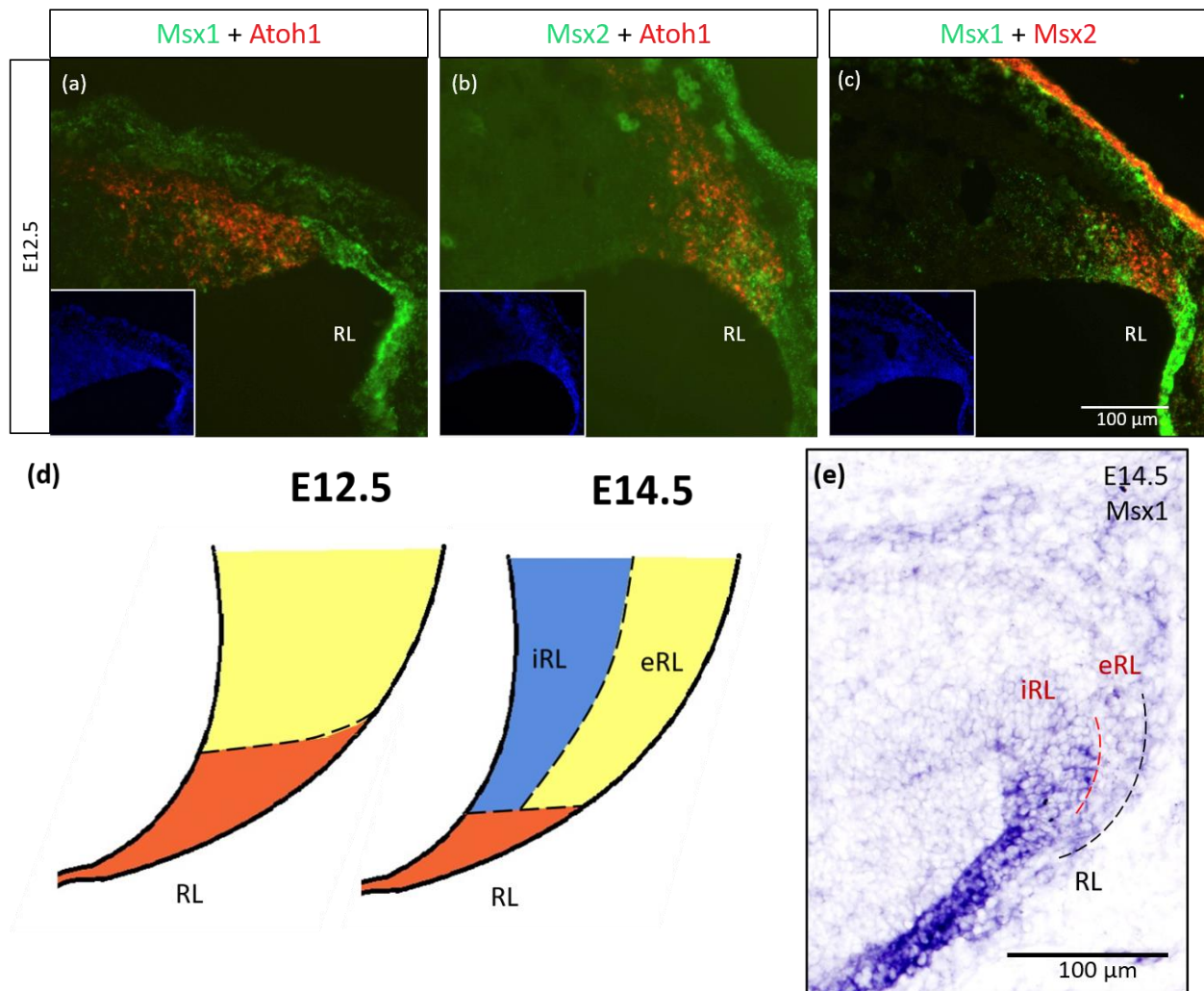


Figure 3.2. *Msx1* is compartmentalised within the RL. (a-c, e) Sagittal sections of the RL with the right-side of panels denoting dorsal and the bottom-side denoting caudal. (a-c) RNAscope fluorescent RNA *in situ* hybridization (FISH) double-label on sagittal E12.5 cerebellum. (a) *Msx1* (green) is expressed highest in a compartment more dorsal to *Atoh1* (red). This compartment is *Atoh1*-negative and *Wls*-positive compartment as shown in (d) at E12.5. (b) *Msx2* (green) and *Atoh1* (red) are largely overlapping in their expression regions. (c) *Msx1* (green) and *Msx2* (red) expression regions form an alternative banding pattern and do not overlap with each other. (a-c) Inset shows DAPI (blue) counterstain of the respective cerebellar tissue sections. Roof plate epithelium auto-fluoresces with the fluorescent dyes. (d) Schematic illustrating the compartments within the RL at E12.5 and E14.5 based on results by Yeung et al. (2014). At both ages, red represents *Wls*-positive, *Msx1*-positive and *Atoh1*-negative, yellow represents *Atoh1*-positive, *Wls*-negative, *Msx1*-negative. At E14.5 the blue iRL is *Wls*-positive and *Atoh1*-negative. (e) RNA *In situ* hybridization of *Msx1* on sagittal E14.5 section shows stronger expression in the *Wls*-positive iRL than the eRL. Refer to Appendix Figures 2c and 4b for negative control staining. RL, Rhombic Lip; iRL, interior RL; eRL, exterior RL. Scale bars, 100 μm.

3.3 *Msx3* expression in the VZ creates a demarcation between the *Atoh1* and *Ptf1a* domains at E12.5

I utilised RNAscope FISH double-label to visualize *Msx3* expression in the VZ of E12.5 cerebellum. As seen with chromogenic RNA *in situ* analysis (Figure 3.1 f, i), *Msx3* is expressed throughout the VZ at E11.5 and E12.5. To see if *Msx3* expression extends to the RL, *Msx3* was RNAscope double-labelled with the RL marker *Atoh1* at E12.5. This revealed that *Msx3* expression does not overlap with *Atoh1* expression and a boundary can be observed between their respective domains (Figure 3.3 a-c). RNAscope double-label of *Msx3* with *Ptf1a* at the same age revealed that they largely overlap in their expression domains in the VZ, with a notable exception that their dorsal most expression boundaries near the RL do not coincide (Figure 3.3 d-f). This is also observed at E11.5 (Figure 3.3 g-i). *Msx3* expression extends more dorsally compared to *Ptf1a* expression at E11.5 and E12.5, and *Msx3* expression at its dorsal edge creates a molecular demarcation between the non-overlapping *Atoh1* and *Ptf1a* regions.

The question arises - do the cells originating from this *Msx3*-positive, *Ptf1a*-negative, and *Atoh1*-negative region in the neuroepithelium become glutamatergic or GABAergic? Lineage tracing of *Msx3* cells would be required as a first step towards answering this question. This also points to the open question of what genetic and molecular events divide the cerebellar neuroepithelium into a glutamatergic and a GABAergic zone in the first place.

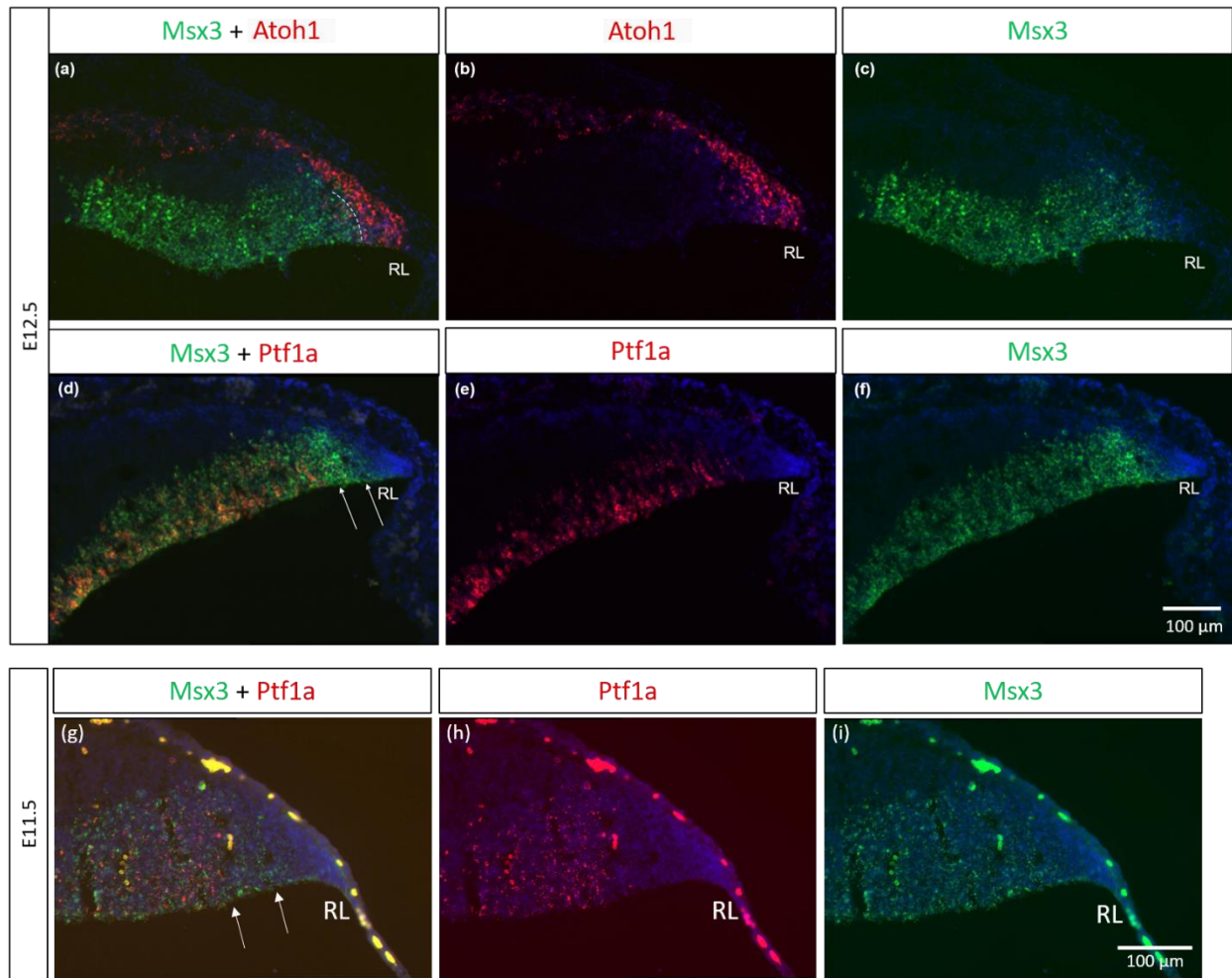


Figure 3.3. *Msx3* does not overlap with *Atoh1*. *Msx3* overlaps with *Ptf1a* but their boundaries near the RL do not coincide. (a-i) All sections are sagittal with right side of the panels denoting dorsal and bottom side denoting caudal. (a-f) RNAscope FISH double-label on E12.5 cerebellum. (a-c) *Msx3* (green) and *Atoh1* (red) co-stain showing a boundary (dashed line) between their expression regions. *Msx3* and *Atoh1* do not overlap. (d-f) *Msx3* (green) and *Ptf1a* (red) co-stain showing a large overlap in their expression regions in the VZ but the *Msx3* boundary extends further than the *Ptf1a* boundary towards the RL (arrows). (g-i) RNAscope FISH double-label on sagittal E11.5 sections with *Msx3* (green) and *Ptf1a* (red) also shows the same boundary feature near the RL (arrows). (g-i) E11.5 roof plate epithelium auto-fluoresces with the fluorescent dyes giving rise to the blob-like artefacts (refer to Appendix Figure 4a for negative control staining). All panels have DAPI (blue) as counterstain. RL, Rhombic Lip. Scale bars, 100 μm .

3.4 *Msx3* is compartmentalised within the ventricular zone at later time-points

While *Msx3* is expressed throughout the VZ at E11.5 and E12.5, *Msx3* expression gets highly restricted within the VZ at later time-points. Chromogenic RNA in situ analysis reveals that *Msx3* domain gets compartmentalised within the VZ at E14.5. Interestingly the *Msx3* expression is spatially dynamic along the lateral-medial axis at E14.5. In the most lateral section, *Msx3*

occupies a small region in the dorsal part of the VZ near the RL and progressively occupies the entire VZ at the most medial section (Figure 3.4).

I used the RNAscope FISH along with BrdU immunohistochemistry to mark the expression boundaries of *Msx3* more precisely, and to co-label with BrdU, a proliferative marker at E14.5 (Figure 3.5). The *Msx3* expression along the lateral-medial axis was replicated with RNAscope and was also strictly within the proliferative region of the neuroepithelium, as marked by the one-hour pulsed BrdU (See Materials & Methods section 2.4 for details on BrdU labelling).

This type of compartmentation in the lateral VZ has been observed by Seto et al. (2014) wherein *Olig2* is expressed in the compartment similar to *Msx3* (Seto et al. 2014) (Figure 1.3 b). *Olig2* and *Gsx1* compartmentalise within the VZ to control cell fate of the VZ progenitors that produce PCPs from the *Olig2* domain and PIPs from the *Gsx1* domain (Figure 1.3 b). Recently, Ma et al. (2020) showed that the BMP and p-SMAD1/5 show a gradient in the VZ with higher expression in the dorsal VZ region that also shows high *Olig2* and *Msx3* expression. This study shows that the BMP p-SMAD1/5 gradient directs the *Olig2-Gsx1* based progenitor fate transition by virtue of p-SMAD1/5 suppressing *Gsx1* expression in the *Olig2* domain of the dorsal VZ (Ma, Vong, and Kwan 2020). As discussed earlier in Section 1.6, *Msx3* is a transcriptional repressor directly induced by BMP signaling. Taken together, this places *Msx3* as a candidate gene mediating the BMP/SMAD orchestration of the *Olig2-Gsx1* based progenitor fate transition in the VZ. If *Msx3* works downstream of BMP signaling to maintain the *Olig2* domain, an interesting question is whether *Msx3* can suppress interneuron fate or enable Purkinje cell fate or both? In the study by Liu et al. (2004), a decrease in *Pax2* positive interneurons was observed upon *Msx3* overexpression in the chick dorsal neural tube (Liu, Helms, and Johnson 2004). Additionally, in the postnatal mouse cerebellum, *Msx3* expression can be detected in the Purkinje cells but not in the interneurons (Appendix Figure 5). Studies looking at ablation of *Msx3* in the cerebellar VZ are required to answer this line of enquiry.

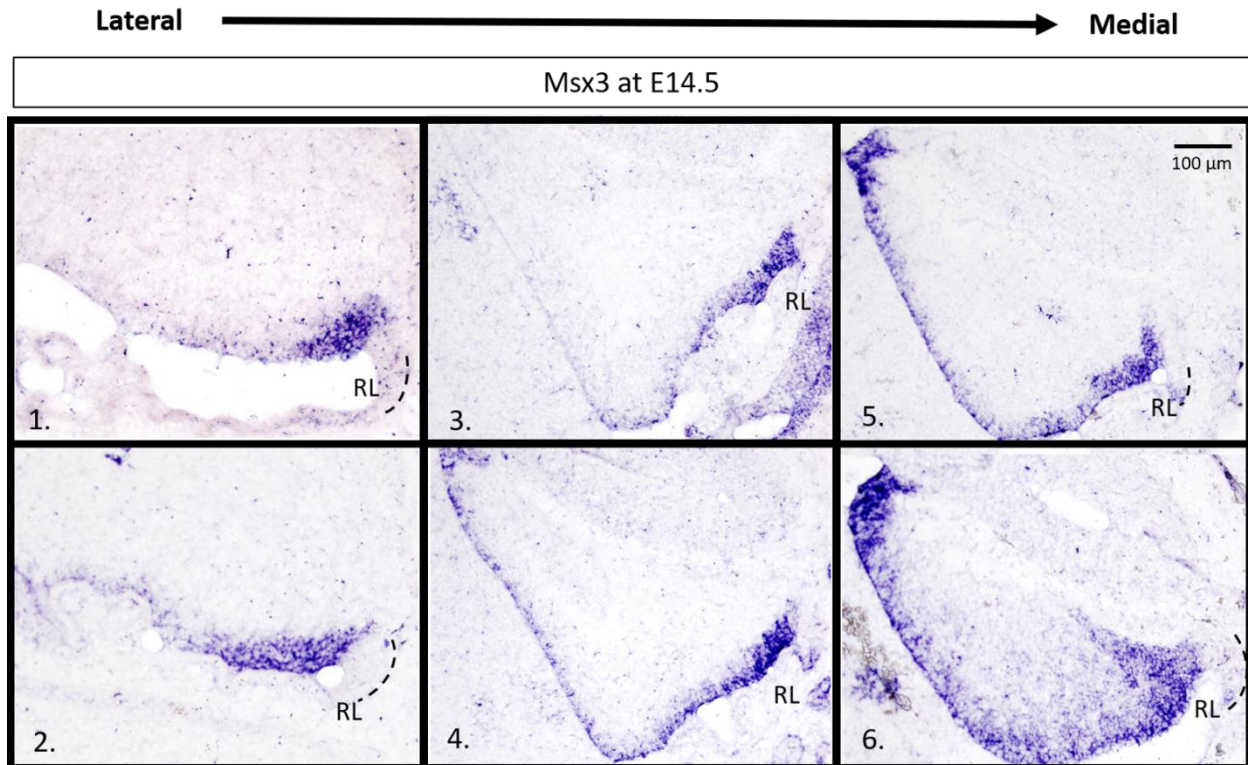


Figure 3.4. *Msx3* is compartmentalised within the VZ at E14.5 and this expression is spatially dynamic. All are sagittal sections at E14.5, with right side of the panels denoting dorsal and bottom side denoting caudal. *Msx3* gets restricted to the dorsal end of the lateral VZ and progressively occupies the entire VZ in the medial sections. (1-6) RNA *in situ* hybridization of *Msx3* in increasing order of relative lateral-medial positions with 1 being the most lateral, 2 being more medial than 1, and so on with 6 being the most medial. Refer to Appendix Figure 2c for negative control staining. RL, Rhombic Lip. Scale bar, 100 μ m.

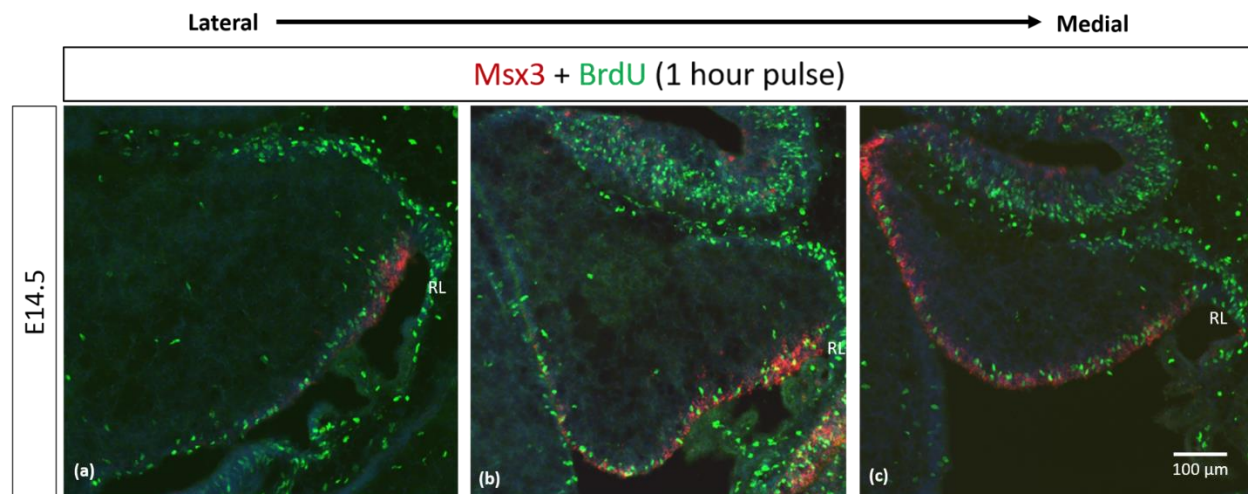


Figure 3.5. *Msx3* is expressed strictly within the proliferative neuroepithelium. All are sagittal sections at E14.5, with right side of the panels denoting dorsal and bottom side denoting caudal (a-c) RNAscope FISH of *Msx3* (red) with fluorescence immunohistochemistry of BrdU (green) for mouse pulsed with BrdU one hour before E14.5 embryos were harvested. Relatively (a) is the most lateral and (c) is the most medial. RL, Rhombic Lip. Scale bar, 100 μ m.

3.5 Catalog of brain specific lncRNA expressed in the cerebellum during development

CAGE sequencing captures all 5' capped mouse RNA transcripts. Thus, we wanted to utilize the FANTOM5 transcriptome to build a catalog of lncRNAs as these non-coding elements are 5' capped (Carninci et al. 2005). Out of a total of over 150,000 unique transcripts identified by the RIKEN FANTOM5 consortium across all tissue and cell samples, the subset that is robustly expressed in the cerebellar time-course samples consists of 16,138 unique transcript entries. To distinguish a subset of these transcripts that are identified as lncRNAs, we used the GENCODE atlas of annotated mouse lncRNAs (version M16) consisting of 13,154 unique transcripts (removing splice variants). GENCODE assigns the biotype 'lncRNA' based on a combination of factors - genomic location such as intergenic, intronic, or antisense together with the absence of an ORF, experimental data and/or literature showing no protein-coding power (Frankish et al. 2019; Lagarde et al. 2017; Mudge and Harrow 2015). Overlapping this list of GENCODE annotations with the list of 16,138 expressed transcripts in the cerebellum time-course, we identified 180 transcripts to be lncRNAs expressed in the developing cerebellum (Appendix Table 1). Z-score is a widely used metric for tissue specificity (Kryuchkova-Mostacci and Robinson-Rechavi 2017; Yao et al. 2015). To capture cerebellum tissue specific transcripts, Z-scores were generated per transcript based on the average expression of the transcript across all 399 mouse samples submitted to the FANTOM5 consortium, spanning 271 tissue types and 128 primary cell types, including the 12 cerebellar time-points as independent samples (Arner et al. 2015; Forrest et al. 2014). A transcript with a Z-score of 3 in E11.5 cerebellum, for example, would mean it is expressed in E11.5 cerebellum at a level that is 3 standard deviations above its most expected expression value across tissue types. Of the 180 lncRNA transcripts, only the ones having a Z-score ≥ 3 in at least one of the 12 cerebellar time-points were retained; their high expression values at those time-points being cerebellum enriched with a p-value < 0.003 . A caveat of FANTOM5 is that the tissue types apart from the cerebellum are mostly non-neuronal, so we are unable to compare the cerebellum to other parts of the brain.

This analysis resulted in a list of 66 hits that can be ranked based on the average or age-specific expression levels, or alternatively the average or age-specific Z-scores, based on a researcher's interests. For our interests, this list was ranked in decreasing order of average expression level across the cerebellar time-course (Table 3.1). The topmost hit was the transcript

ENSMUST00000156068 that has now been assigned the annotation of 6330403K07Rik. Like many other lncRNAs on the list, this lncRNA is conserved in humans, among other mammals (Appendix Figure 6). This lncRNA has a sequence of ~350 bases in its Exon 1 that has high positive conservation (Appendix Figure 6).

S.No.	Name	Average Expression (TPM)	Z-score												Average Z-score
			E11.5	E12.5	E13.5	E14.5	E15.5	E16.5	E17.5	E18.5	P0	P3	P6	P9	
1	p1.ENSMUST00000156068	196.47	2.59	3.16	3.02	2.63	2.24	2.21	2.02	1.75	1.10	0.68	0.52	0.01	1.83
2	p1.Miat	85.15	3.04	5.01	3.22	1.92	1.95	1.76	1.55	1.75	2.25	1.90	1.39	1.06	2.23
3	p1.Peg13	80.64	0.90	1.54	2.24	2.29	1.69	1.50	2.07	3.18	1.72	1.43	1.58	2.95	1.92
4	p1.C130071C03Rik	54.62	5.91	5.21	5.46	4.46	4.13	3.77	3.22	3.32	4.97	3.82	3.53	1.99	4.15
5	p1.Meg3	48.82	0.00	-0.14	0.40	0.59	1.87	1.91	1.27	3.62	3.01	0.54	0.65	0.15	1.16
6	p1.ENSMUST00000131907	46.39	2.91	4.53	4.51	4.10	3.06	2.97	3.62	3.32	3.23	3.78	5.25	2.66	3.66
7	p1.Gm2694	39.41	1.80	3.17	3.99	4.08	4.24	4.78	4.83	4.27	4.32	5.73	6.62	7.92	4.65
8	p1.C230004F18Rik	39.36	-0.05	0.34	0.79	1.55	1.64	1.31	2.44	2.42	1.66	0.97	0.84	3.34	1.44
9	p1.Xist	37.89	0.20	1.59	2.72	3.00	1.01	1.27	1.77	1.35	3.26	2.43	1.44	2.00	1.84
10	p1.ENSMUST00000098868	29.75	1.31	2.98	5.83	4.80	4.35	2.60	2.14	2.19	1.47	0.56	0.01	-0.06	2.35
11	p1.C630043F03Rik	24.13	1.18	2.85	5.45	7.24	5.38	3.46	3.13	2.67	1.59	1.36	1.31	0.62	3.02
12	p1.A730094K22Rik	22.92	0.73	2.16	3.29	4.84	4.88	3.82	6.32	5.45	5.22	5.64	6.92	3.90	4.43
13	p1.ENSMUST00000139356	22.86	3.42	3.40	3.69	2.85	2.73	2.57	2.54	4.05	3.18	2.97	2.44	0.67	2.88
14	p2.Dig2	20.12	0.04	0.86	2.17	4.32	3.89	3.47	4.89	4.37	3.35	2.63	2.98	4.82	3.15
15	p1.1700020I14Rik	19.71	0.15	0.19	0.32	0.34	0.30	1.05	0.80	0.84	1.01	0.95	0.97	3.40	0.86
16	p9.Dig2	18.58	-0.20	-0.13	1.87	4.47	6.82	6.07	5.70	6.82	6.92	3.49	2.21	3.00	3.92
17	p3.Peg13	17.56	1.29	2.07	2.64	2.88	2.03	2.11	2.80	3.81	1.97	1.39	1.48	1.80	2.19
18	p2.ENSMUST00000098868	17.47	2.05	5.68	8.21	6.26	4.13	2.11	2.20	2.68	0.87	0.28	-0.05	-0.11	2.86
19	p1.ENSMUST00000128121	17.00	3.82	5.77	5.46	4.38	5.10	3.74	3.19	4.49	3.60	3.53	3.92	2.01	4.08
20	p1.ENSMUST00000133630	16.17	0.54	1.18	2.19	2.81	3.63	3.91	4.08	3.99	3.85	3.77	3.66	1.39	2.92
21	p1.2900079G21Rik	15.16	-0.11	0.50	1.29	1.30	1.52	1.65	2.11	3.04	3.83	3.74	6.85	5.25	2.58
22	p7.Dig2	14.97	-0.20	-0.13	1.65	4.34	5.71	4.91	5.16	6.53	4.84	2.95	2.64	3.27	3.47
23	p1.ENSMUST00000139835	14.50	0.29	1.14	2.10	2.19	2.28	2.44	2.75	2.75	2.55	3.32	3.07	0.49	2.11
24	p2.Miat	13.84	1.89	3.02	4.32	2.76	3.09	3.00	2.66	3.05	4.80	3.53	4.40	2.34	3.24
25	p3.ENSMUST00000131907	13.50	5.99	6.87	5.38	4.57	4.33	2.77	3.75	4.03	3.02	3.21	3.68	1.48	4.09
26	p1.ENSMUST00000134624	11.74	3.20	2.76	1.86	1.64	0.82	0.86	0.73	0.75	0.32	0.08	-0.10	-0.38	1.04
27	p5.Dig2	11.48	-0.26	-0.10	2.14	1.83	2.01	1.99	2.37	3.91	4.73	5.06	5.35	7.41	3.04
28	p3.Cct6a	11.32	3.18	3.25	1.95	2.17	1.89	1.75	0.89	1.97	1.02	0.56	-0.21	0.24	1.56
29	p1.ENSMUST00000155166	10.96	1.63	2.70	3.00	3.10	2.50	2.29	2.86	1.90	1.63	1.45	1.23	1.64	2.16
30	p1.2610316D01Rik	10.12	1.34	1.64	2.61	2.59	2.28	2.58	3.20	2.21	1.75	2.10	1.43	0.92	2.05
31	p1.ENSMUST00000123016	9.91	1.46	3.77	6.36	5.25	4.24	3.65	3.18	2.83	2.25	1.86	1.59	0.66	3.09
32	p1.ENSMUST00000151778	9.31	4.48	6.68	6.71	5.83	5.85	4.09	3.30	2.66	2.80	2.26	1.35	0.29	3.86
33	p3.ENSMUST00000098868	8.98	1.30	4.71	7.13	5.60	4.62	2.18	2.54	3.37	1.27	0.45	0.39	0.00	2.80
34	p2.ENSMUST00000131907	8.68	3.24	4.22	3.21	3.56	2.69	2.07	3.20	3.86	3.34	2.43	3.83	3.32	3.25
35	p1.ENSMUST00000170849	7.92	4.73	2.72	1.31	0.78	0.47	0.22	0.09	0.02	-0.10	-0.12	-0.05	-0.16	0.82
36	p1.A230056P14Rik	7.68	2.83	3.23	4.16	3.86	4.33	2.84	3.81	2.54	1.25	0.93	1.37	1.89	2.75
37	p1.ENSMUST00000159155	7.40	-0.11	0.24	0.44	1.39	1.91	2.97	4.21	5.09	4.82	7.70	8.78	2.32	3.31
38	p1.D430036J16Rik	7.23	1.46	1.05	0.48	1.74	2.18	3.63	4.49	4.30	5.04	3.32	1.38	1.88	2.58
39	p1.ENSMUST00000148743	6.81	3.51	1.91	2.05	1.11	1.00	1.16	1.33	0.62	0.66	1.00	0.88	-0.12	1.26
40	p1.ENSMUST00000129089	6.51	5.39	3.18	3.25	2.62	1.46	1.61	1.19	0.63	0.47	-0.11	0.11	-0.38	1.62
41	p1.ENSMUST00000144350	6.44	0.54	2.40	2.40	3.26	3.63	4.45	5.88	6.12	5.35	7.83	7.05	3.85	4.40
42	p1.ENSMUST00000151229	6.37	5.67	3.60	2.79	2.76	1.41	0.73	0.78	0.81	0.21	-0.18	-0.28	-0.42	1.49
43	p1.ENSMUST00000124378	6.11	0.22	1.52	2.57	3.03	3.26	2.92	2.27	1.85	1.74	1.24	0.57	0.52	1.81
44	p3.Meg3	6.00	0.09	-0.15	0.34	0.56	1.98	2.33	1.02	3.26	2.18	0.20	0.42	0.17	1.03
45	p1.2810429I04Rik	5.94	3.21	2.93	2.35	2.94	2.72	3.15	2.34	3.04	2.41	1.60	0.92	1.32	2.41
46	p4.Peg13	5.91	0.86	1.10	1.76	1.97	1.63	1.85	2.20	2.52	2.09	1.37	2.36	3.75	1.96
47	p1.ENSMUST00000129868	5.85	-0.14	0.38	1.96	5.48	6.67	6.27	9.10	9.55	4.98	2.32	1.71	0.15	4.03
48	p1.2610027F03Rik	5.32	7.51	9.22	5.93	2.98	1.07	0.59	0.44	0.06	-0.11	-0.08	-0.11	-0.11	2.28
49	p4.ENSMUST00000098868	5.11	2.14	4.95	7.76	6.47	4.44	2.68	2.28	1.50	1.92	0.58	0.25	0.01	2.91
50	p17.Dig2	4.29	-0.29	-0.09	0.82	0.60	1.58	2.03	3.56	6.05	5.79	5.76	5.10	6.16	3.09
51	p1.ENSMUST00000098678	4.25	8.06	3.36	2.67	1.78	0.76	0.82	0.03	-0.05	-0.16	-0.19	-0.19	-0.19	1.39
52	p12.Dig2	4.16	-0.24	-0.23	1.41	1.45	1.68	2.01	1.90	3.58	5.07	4.14	5.40	5.54	2.64
53	p6.Meg3	4.04	-0.02	-0.15	0.17	0.73	1.02	1.28	1.12	2.30	1.35	0.58	0.84	3.71	1.08
54	p1.A330076H08Rik	3.83	-0.06	0.23	0.18	0.50	0.59	0.29	0.57	1.16	1.42	1.39	2.56	11.29	1.68
55	p3.9430053O09Rik	3.74	0.90	2.98	10.67	9.80	6.94	4.13	2.50	1.14	1.63	0.67	0.36	-0.19	3.46
56	p1.ENSMUST00000126472	3.44	4.70	4.20	2.08	1.80	1.76	1.03	1.43	1.01	0.55	0.23	-0.27	0.10	1.55
57	p2.2610027F03Rik	3.29	12.16	9.55	6.12	2.42	0.87	0.46	0.36	0.87	-0.05	-0.12	-0.12	-0.12	2.70
58	p1.ENSMUST00000147294	2.90	3.45	2.31	1.81	1.30	0.84	0.16	-0.02	-0.21	-0.09	-0.19	-0.21	-0.18	0.75
59	p1.ENSMUST00000137258	2.89	12.68	8.08	3.52	0.96	-0.12	0.08	-0.12	-0.12	-0.12	-0.12	-0.12	-0.12	2.04
60	p4.2610203C20Rik	2.81	1.01	1.06	3.47	4.93	4.65	2.99	1.49	5.10	1.82	1.62	2.25	0.55	2.58
61	p1.ENSMUST00000128815	2.79	3.49	4.99	5.67	3.98	2.23	1.68	0.48	0.61	0.29	0.05	0.40	-0.17	1.97
62	p1.ENSMUST00000160099	2.59	0.62	1.01	1.10	1.06	1.39	0.55	1.99	3.14	1.02	0.94	2.32	0.11	1.27
63	p3.2900079G21Rik	2.15	-0.09	-0.09	-0.09	-0.09	0.00	0.03	0.82	0.57	0.97	5.32	9.56	12.06	2.41
64	p1.ENSMUST00000130362	1.98	-0.17	-0.14	-0.09	-0.10	0.15	0.51	0.87	0.50	1.12	2.60	5.83	1.56	1.05
65	p1.ENSMUST00000159595	1.18	-0.09	0.22	0.42	0.53	0.40	0.16	0.45	0.55	0.21	1.49	4.41	9.31	1.50
66	p20.Meg3	1.11	-0.04	-0.04	0.34	0.68	1.32	1.59	0.46	5.96	2.69	0.09	1.44	-0.14	1.20

Table 3.1. Highly expressed lncRNAs enriched during cerebellar development. Robustly expressed lncRNAs in the FANTOM5 cerebellar time-course (Appendix Table 1) were filtered with the criteria of Z-score ≥ 3 in at least 1 out of 12 cerebellar timepoints and considered enriched for that corresponding timepoint. This analysis yielded 66 hits that were ranked according to their average expression levels across the 12 cerebellar timepoints, shown here in this table.

3.6 Characterizing spatial-temporal expression of 6330403K07Rik

The FANTOM5 time-course transcriptome for the developing cerebellum gives us the temporal expression pattern of 6330403K07Rik (Figure 3.6). The normalised expression of this lncRNA peaks at E13.5, and hence I probed for spatial expression using chromogenic RNA *in situ* hybridization (See Materials & Methods section 2.5 for probe details) beginning at E13.5 and at E15.5 and E18.5 to track its embryonic expression pattern (Figure 3.7). Qualitatively, more cells express this lncRNA at E18.5 compared to E13.5. But there are far less cells at E13.5 compared to E18.5, so when the expression levels are normalised, the proportion of cells in the cerebellar primordium at E13.5 expressing this transcript is the highest. As can be seen from Figure 3.7 a, 6330403K07Rik at E13.5 stains the rhombic lip, the nuclear transitory zone (NTZ) and the ventricular zone, showing that this transcript marks both glutamatergic and GABAergic zones. By E15.5 and E18.5, the most prominent region marked by this lncRNA is the NTZ and the cerebellar nuclear (CN) neurons, respectively (Figure 3.7 b-c, e-g).

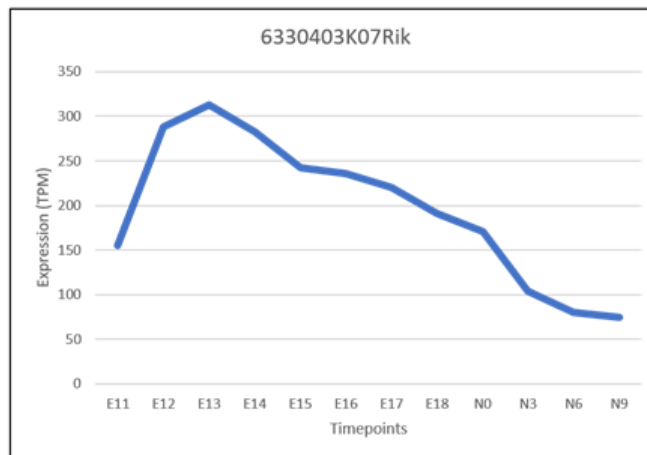


Figure 3.6. Temporal expression of 6330403K07Rik across cerebellar time-course. Temporal expression for lncRNA 6330403K07Rik across 12 developmental timepoints of the mouse cerebellum, from the FANTOM5 cerebellum time-course. Expression of the lncRNA is higher in early embryonic ages with a peak at E13.5. TPM, transcripts per million mapped.

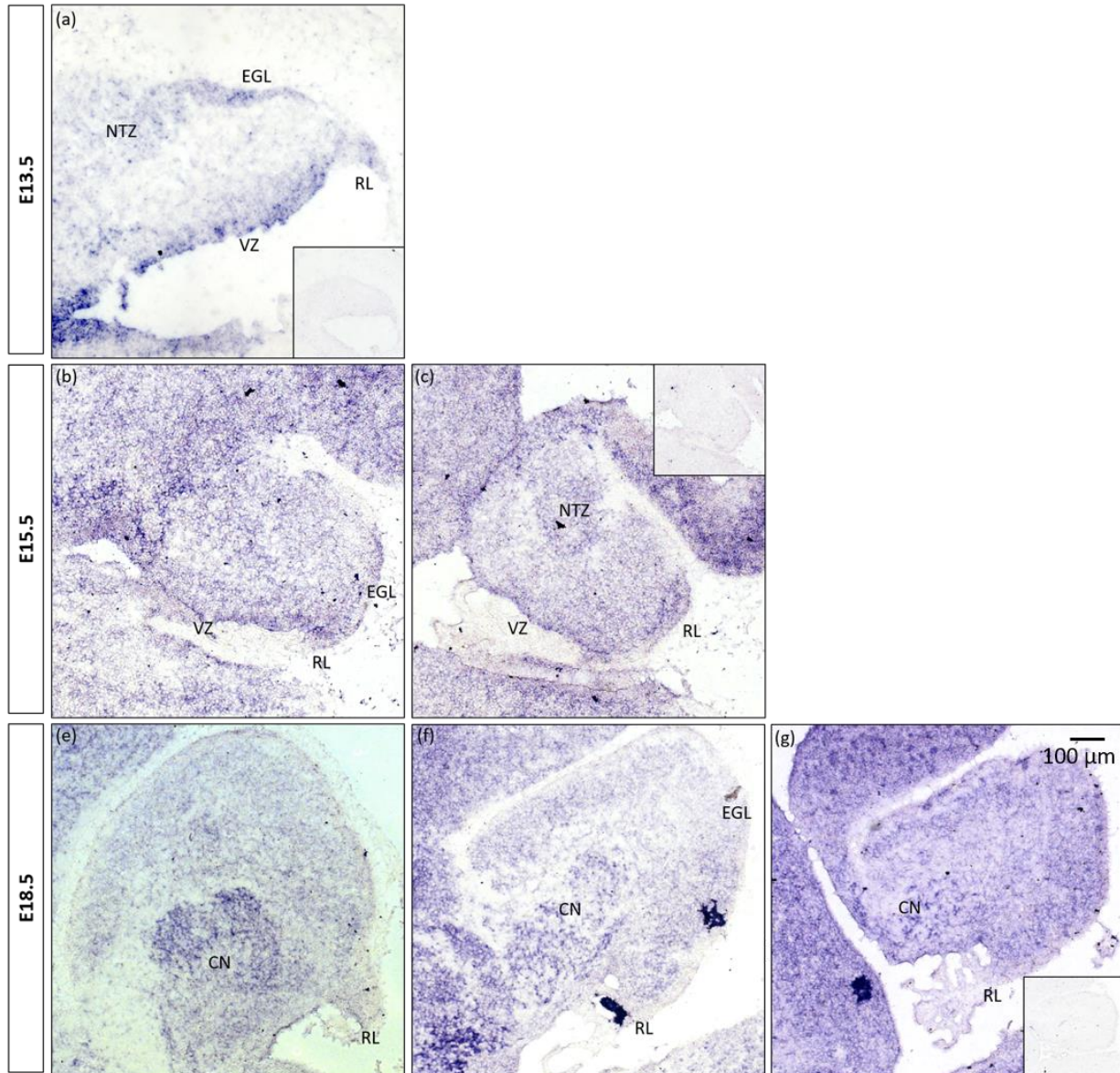


Figure 3.7. Spatial expression of 6330403K07Rik in the cerebellar primordium across multiple embryonic ages. Chromogenic RNA *in situ* hybridization of the lncRNA 6330403K07Rik using 1 kilobase long probe complementary to the sequence. Right side of all panels denotes dorsal and bottom side denotes caudal. (a) E13.5 cerebellum sagittal section. Inset is negative control for the staining using probe with same sequence as the lncRNA. (b-c) E15.5 cerebellum sagittal sections. (c) is more medial to (b) and inset is negative control for the staining. (e-g) E18.5 cerebellum sagittal sections, (e) being most lateral to (g) being most medial with an inset in (g) of negative control for the staining. From the 3 ages, the lncRNA seems to be expressed in specific clusters of cells in the NTZ and the CN. EGL, external granular layer; NTZ, nuclear transitory zone; RL, rhombic lip; VZ, ventricular zone; CN, cerebellar nuclei. Scale bar, 100 μ m.

To place 6330403K07Rik expression in the context of primary progenitor zone markers, I utilised RNAscope FISH double label to co-stain this lncRNA with *Atoh1* and *Ptf1a* at E11.5. 6330403K07Rik expression is strongest in the rhombic lip and the NTZ at this age, and co-expresses with *Atoh1* in the RL (Figure 3.8). The expression of this lncRNA in the VZ is very weak, but some expression in the VZ was detected (Appendix Figure 7). Most notably, these results show that at E11.5 the strongest expression of this lncRNA is in the NTZ, with *Atoh1* co-expression in the RL. These results indicate that the lncRNA 6330403k07Rik is most prominently expressed in the CN neurons, and that these CN neurons marked by 6330403K07Rik can be glutamatergic.

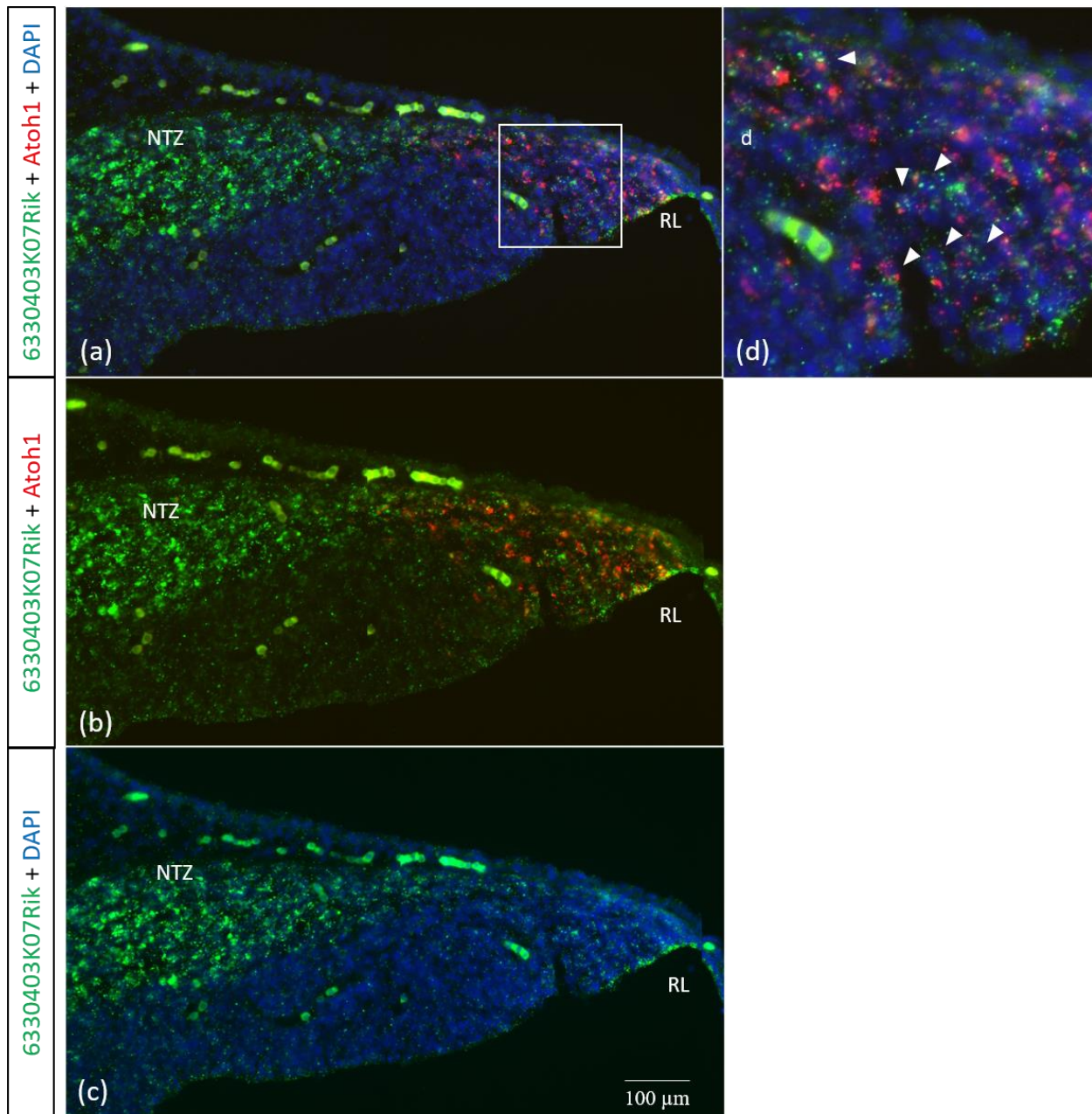


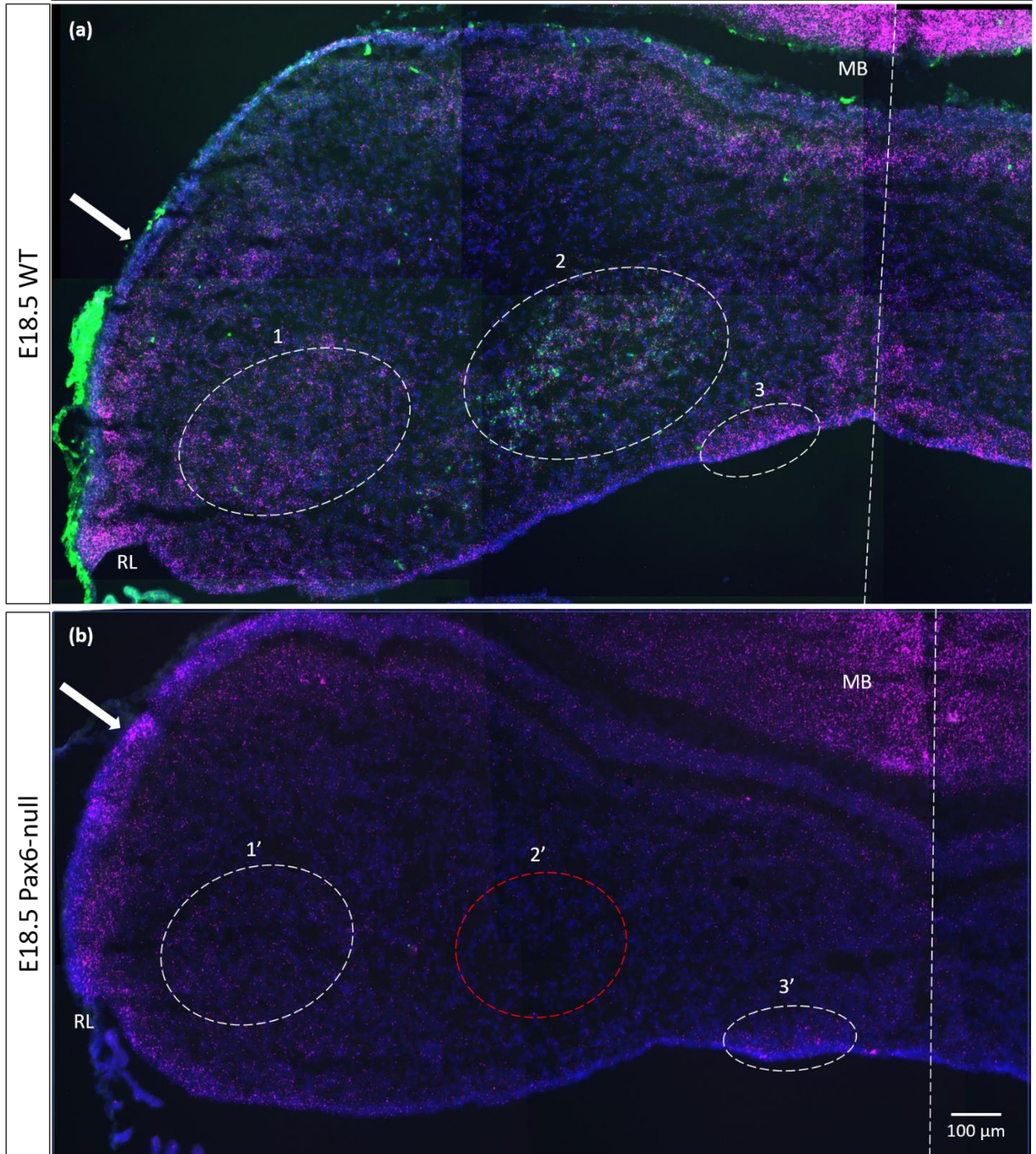
Figure 3.8. LncRNA 6330403K07Rik co-expresses with glutamatergic lineage marker *Atoh1* in the RL at E11.5. (a-c) RNAscope FISH double-label of lncRNA 6330403K07Rik (green) along with *Atoh1* (red). (d) is a close-up of (a) showing co-labeled cells (arrowheads). NTZ, nuclear transitory zone; RL, rhombic lip. Scale bar, 100 μm.

3.7 LncRNA 6330403K07Rik is expressed in the *Tbr1*-positive glutamatergic CN neurons

To confirm the expression of this lncRNA in the glutamatergic CN neurons, I probed for its expression along with a cell type marker at a later stage using RNAscope FISH. At E18.5, the lncRNA 6330403K07Rik marks 2 distinct clusters in the white matter, and one cluster close to the midline. The middle cluster (Cluster 2) in the white matter overlaps with the *Tbr1*-positive cluster (Figure 3.9 a, 2). *Tbr1* is the most well-known marker for glutamatergic CN neurons, and it is known that the *Tbr1*-positive cluster is lost in *Pax6*-null mutant (Yeung et al. 2016). Interestingly, 6330403K07Rik expression in Cluster 2 is lost in the *Pax6*-null mutant cerebellum at E18.5, along with *Tbr1* expression (Figure 3.9 2, 2'). 6330403K07Rik expression is detectable but perturbed in Clusters 1 and 3 (Figure 3.9 1, 3, 1', 3'). 6330403K07Rik expression that is noted in the RL, the cerebellar cortex and the midbrain in the wildtype remains intact in *Pax6*-null mutant (Figure 3.9 a,b).

These results indicate that the 6330403K07Rik expression in the CN neurons is *Pax6* dependent, with 6330403K07Rik-positive Cluster 2 marking the *Tbr1*-positive glutamatergic CN neurons.

6330403K07Rik + Tbr1 + DAPI



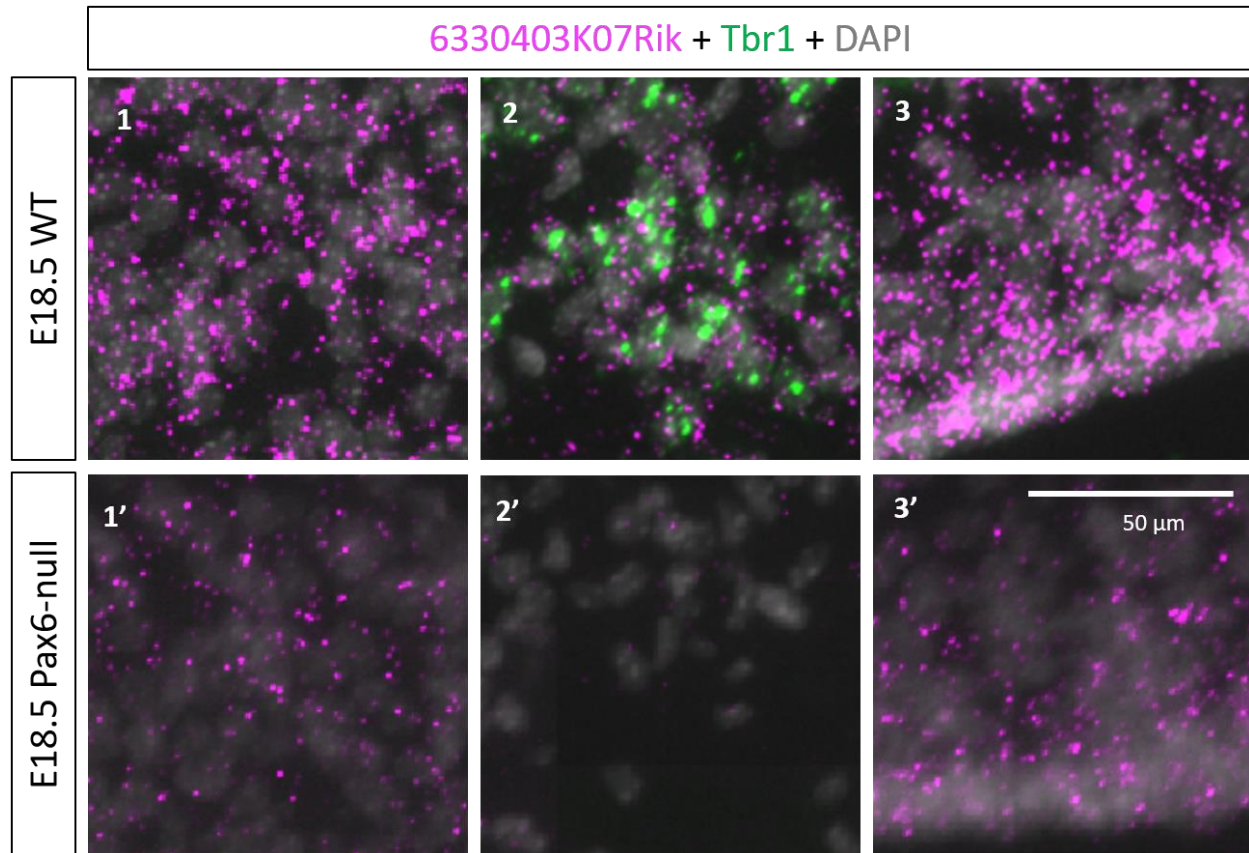


Figure 3.9. 6330403K07Rik expression in the CN neurons is perturbed in *Pax6*-null mutant E18.5 cerebellum. RNAscope FISH double-label on coronal sections with the midline (dashed line) on the right and lateral end on the left. Top is anterior. (a) 6330403K07Rik (magenta) in wildtype (WT) E18.5 cerebellum is expressed in the cortex (white arrow), the rhombic lip (RL), the midbrain (MB) and in 3 distinct clusters (dashed circles). Clusters 1 and 2 are in the white matter while Cluster 3 is very close to the midline. Cluster 2 overlaps with the *Tbr1* (green) cluster. Closeup of the clusters in 1,2 and 3 with DAPI in grey. (b) In *Pax6*-null mutant E18.5 cerebellum, 6330403K07Rik expression (magenta), along with *Tbr1* expression (green), in Cluster 2 is lost, while expression appears to be reduced in Clusters 1 and 3. 6330403K07Rik expression in the cortex (white arrow), RL and MB remains intact. Closeups of clusters in 1',2' and 3' with DAPI in grey. RL, rhombic lip; MB, midbrain. Scale bars indicated.

Since loss of PAX6 is embryonic lethal, E18.5 is the oldest age of viability for *Pax6*-null mutants. By P0, in wildtype cerebellum the 6330403K07Rik expression is strongest in a region earlier identified as Cluster 3 at E18.5 (Figure 3.10 a,b). Whether the expression of the lncRNA in the cells of Clusters 1 and 2 is reduced or do those cells migrate to the region of Cluster 3, or even outside the cerebellum, needs to be further studied with lineage tracing and birthdating analyses. 6330403K07Rik expression persists in the RL and the cortex (Figure 3.10 b).

The strongest expressing 6330403K07Rik cluster is positioned close to the *Tbr1* cluster in the medial portion of the cerebellum, but it does not overlap with the *Tbr1* cluster (Figure 3.10 a). Interestingly, 6330403K07Rik expression is detected in *Tbr1*-positive cells (Figure 3.10 c). It is possible that this expression persists from Cluster 2 as seen at E18.5. This can be compared to *Irx3* which is another CN neuron marker (Morales and Hatten 2006). The *Irx3* cluster is more lateral to the 6330403K07Rik cluster (Figure 3.10 b) where weak expression of 6330403K07Rik is detected (not shown). The GABAergic CN neurons are an under-studied cell population which do not have a well-known genetic marker yet, so it is unclear if any subset of the CN neuron populations marked by 6330403K07Rik are GABAergic or not. Continued expression of the lncRNA in the RL at E18.5 and P0 indicates that it is expressed in the UBCs as they are the only cell type to emerge from the RL at these ages. Overall, these results indicate an association of this lncRNA with multiple cell types in the cerebellum including the *Tbr1*-positive glutamatergic CN neurons.

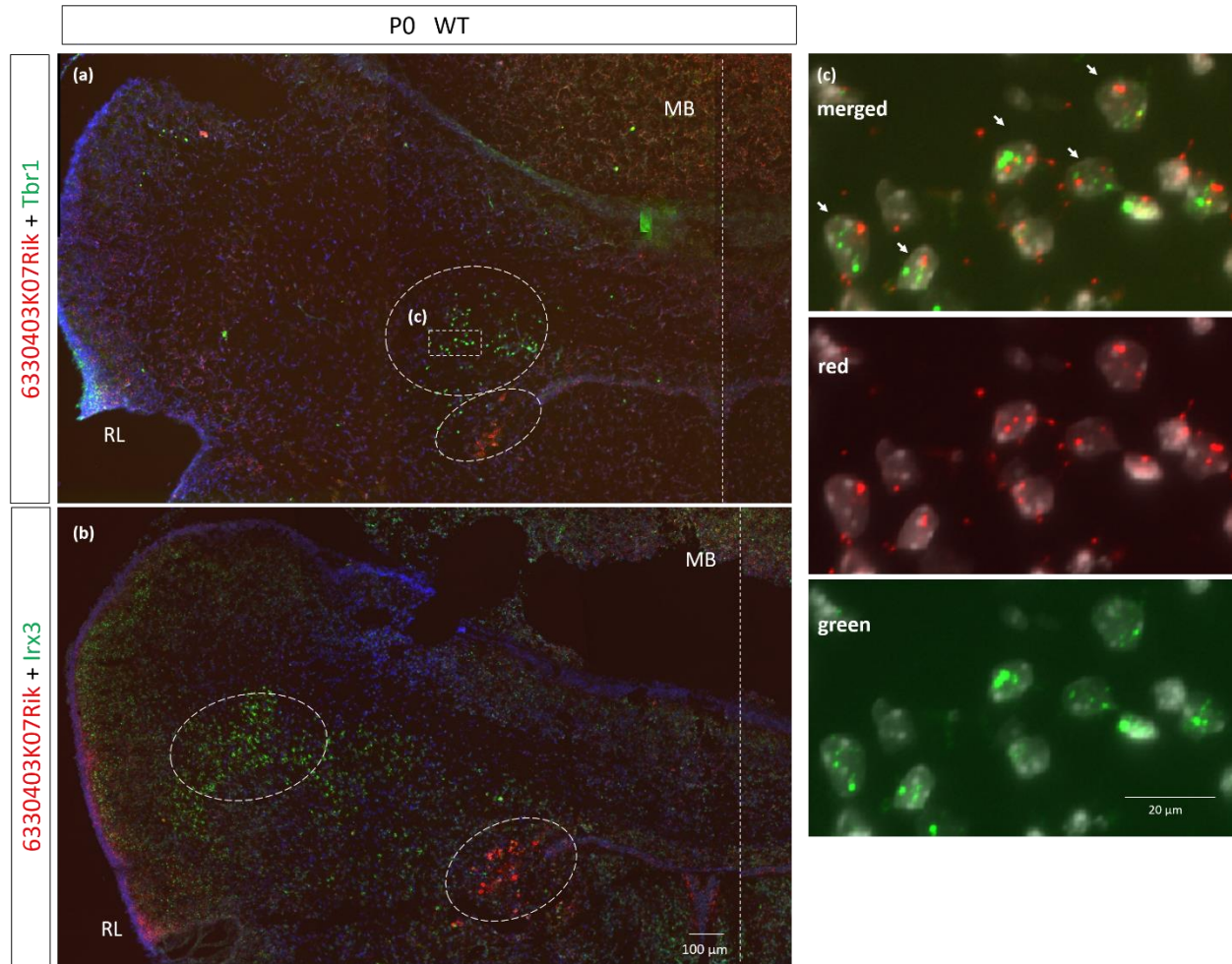


Figure 3.10. 6330403K07Rik expression in the cerebellum at P0. RNAscope FISH double-label on coronal sections of P0 wildtype cerebellum with the midline (dashed line) on the right and lateral end on the left. Top is anterior. DAPI is a nuclear counterstain in blue (a,b) and in grey (c). (a,b) 6330403K07Rik (red) expression is strongest in a specific cluster (dashed circle) that appears to be in the same location as Cluster 3 seen at E18.5. 6330403K07Rik expression is also noted in the RL that houses UBCs at this age. (a) 6330403K07Rik positive cluster (dashed circle) is positioned close to the *Tbr1* (green) positive glutamatergic CN neuron cluster. (c) is a closeup within the *Tbr1* positive cluster to show cells co-expressing *Tbr1* and 6330403K07Rik (arrows). (b) *Irx3* cluster (green) is positioned more lateral to the 6330403K07Rik (red) positive cluster. RL, rhombic lip; MB, midbrain. Scale bars indicated.

Chapter 4 - Conclusion

This two-part study aims to further our understanding of the genetic regulation of cerebellar development. In the first part, I focus on the spatial patterning of the cerebellar progenitor zones by the *Msx* genes in the specific time windows in which they are expressed. These are homeobox-containing, highly conserved transcription factors, previously unexplored in the context of the cerebellum. The *Msx* genes were found to pattern the proliferative neuroepithelium of the early embryonic cerebellar primordium. Expression patterns of *Msx1* and *Msx3* allude to their potential function in progenitor cell maintenance and specification, and present as strong candidates for facilitating BMP signaling in cerebellum development. In the second part, I utilize cerebellar transcriptomic data to create a catalog of brain specific long non-coding RNAs enriched during cerebellum development and spatiotemporally characterise the top candidate, 6330403K07Rik in the developing cerebellum. 6330403K07Rik is identified to be involved in the *Pax6* dependent *Tbr1*-positive glutamatergic cerebellar nuclear neurons. Here I summarise the findings from Chapter 3 and discuss their implications.

4.1 *Msx* genes pattern the early cerebellar neuroepithelium

At E12.5 the proliferative neuroepithelium of the cerebellar primordium is divided into two distinct primary progenitor zones - the *Atoh1*-positive rhombic lip that produces glutamatergic or excitatory neurons and the *Ptf1a*-positive ventricular zone that produces GABAergic or inhibitory neurons. Each of these zones gives rise to multiple cell types in a specific spatio-temporal sequence. High resolution RNAscope FISH of mRNA levels revealed that *Msx1* and *Msx2* are largely non-overlapping markers of rhombic lip domains, while *Msx3* is expressed in the ventricular zone that demarcates the *Ptf1a* and *Atoh1* domains. This spatial patterning fine tunes our understanding of compartmentation of the neuroepithelium and can be summarized in Figure 4.1.

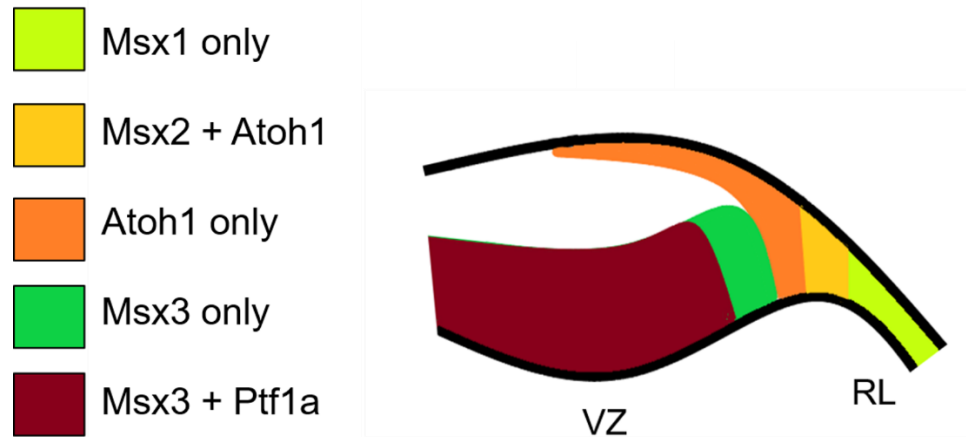


Figure 4.1. Schematic illustration of *Msx* compartmental expression in the early embryonic cerebellar neuroepithelium. RL, rhombic lip; VZ, ventricular zone.

At E14.5, further interesting spatial expression patterns of *Msx1* and *Msx3* emerge. *Msx1* is expressed in the interior face of the rhombic lip (iRL) a compartment marked by *Wls*. Given that this compartment is considered to house a progenitor pool of cells and that *Msx1* is known as a transcriptional repressor of neuronal differentiation, it is likely that *Msx1* is involved in maintaining this progenitor pool by suppressing pro-differentiation genes. *Msx3* expression gets more restrictive at E14.5, receding to the dorsal most part of the ventricular zone. This receding expression pattern in the ventricular zone is also shown by *Olig2* that specifies the Purkinje cell progenitors, as well as the canonical BMP/*Smad5* gradient which directs the *Olig2-Gsx1* based progenitor fate in the ventricular zone. From the limited studies on *Msx3*, we know that this gene is directly induced by BMP signaling but whether it is a direct target is yet to be confirmed. Further studies are required to decipher if *Msx3* is a molecular player directly downstream of the BMP/*Smad5* gradient which orchestrates the *Olig2-Gsx1* progenitor identity control.

Msx1 and *Msx2* are direct targets of BMP signaling. Research on the roles of *Msx1* and *Msx2* in limb and tooth organogenesis points to an association between *Msx* genes and how extracellular signaling controls the balance of proliferation and differentiation (Maxson, Ishii, and Merrill 2003). *Msx3* is the most understudied member of the family. *Msx3* is yet to be confirmed as a direct target of BMP signaling, although ectopic BMP expression can induce *Msx3* (Shimeld, McKay, and Sharpe 1996). Unlike the other family members, *Msx3* is present exclusively in the

dorsal CNS tissue. Liu et al. (2004) showed that perturbing *Msx3* expression can affect the population sizes of different interneuron cell types along the dorso-ventral axis in the chick neural tube. A key question is whether *Msx3* plays a similar role in specifying the cell populations coming from the cerebellar ventricular zone in a dorso-ventral specific pattern. In neural development, the *Msx* family of genes have been previously implicated in CNS patterning, with conserved expression in the CNS across multiple species. This is the first study that examines the patterning and potential roles of the *Msx* genes in cerebellar development. The results place the *Msx* genes as strong candidates for facilitating BMP signaling in the cerebellum. As transcription factors that are immediate effectors of external BMP signaling from the roof plate, the *Msx* genes are likely to be upstream players of molecular cascades underlying transcriptional regulation of cell types emerging during cerebellar development, given that they play similar roles in limb and tooth development. Further studies cementing the regulation of the *Msx* genes by the BMPs in cerebellum would help illuminate this direction.

4.2 There are brain specific long non-coding RNAs expressed in the cerebellum during development

We have constructed a catalog of annotated long non-coding RNAs (lncRNAs) that are significantly expressed at specific cerebellar timepoints, and may be crucial to cerebellum development, based on their expression levels and tissue specificity. LncRNAs that are enriched in the developing cerebellum, compared to other tissue types and cell types, were identified with Z-scores calculated for each of the 12 cerebellar timepoints for all the transcripts. Our aim was to capture all possible cerebellum enriched lncRNAs that were previously annotated, so if a transcript has a Z-score of 3 or above in any of the 12 time-points, they were counted as showing tissue specificity for those time-points. This catalog can be re-ranked according to either expression levels or Z-scores at any time-point, giving the flexibility to focus on specific developmental stages.

4.3 The functionally unannotated lncRNA 6330403K07Rik shows cell type specific expression in the developing cerebellum

I characterised the spatio-temporal expression pattern of our top candidate from the catalog, 6330403K07Rik, a long non-coding RNA that has not been functionally described in any context

previously. 6330403K07Rik shows sequence conservation across multiple species including humans, with a specific stretch of ~120 bases perfectly conserved, hinting to an evolutionarily conserved binding sequence (Appendix Figure 6). In the cerebellum, strong and specific expression is identified in the *Pax6* dependent, *Tbr1*-positive excitatory cerebellar nuclear neurons. Long non-coding RNAs are known to contribute to cell type specificity and 6330403K07Rik may be defining a sub-population of cerebellar nuclear neurons. 6330403K07Rik is also expressed in the unipolar brush cells (UBCs), as its expression is noted in the rhombic lip until P0, which only produces UBCs by that stage. Interestingly, 6330403K07Rik expression is unaffected in the *Pax6*-null E18.5 rhombic lip and cerebellar cortex. 6330403K07Rik at early stages is expressed in both glutamatergic and GABAergic zones, implying potential function in multiple cell types from both lineages. Further studies are required to understand the function of the lncRNA 6330403K07Rik in the cerebellar nuclear neurons, and other cerebellar cell types it is expressed in. These results set this lncRNA as an example to show the potential involvement of lncRNAs in brain development, a field largely uncharted currently. We have only begun to understand the functional roles of non-coding elements of the genome like lncRNAs. Functionally heterogeneous, lncRNAs add another dimension to genetic regulation and cellular biology. The second part of this thesis is a step towards understanding the potential roles of lncRNAs in cerebellar development.

GENCODE continuously updates and changes the mouse lncRNA annotation list and recently 6330403K07Rik was not assigned the biotype “lncRNA” due to a possible open reading frame in its sequence, although the predicted peptide has not been identified yet. The nature of the transcript 6330403K07Rik is thus unclear. Nevertheless, this transcript does have high and significantly enriched expression in the cerebellum. As the lncRNA annotations are updated, our pipeline can be reapplied to obtain an updated catalog.

4.4 Single cell RNA-seq data supports findings for *Msx* genes and 6330403K07Rik

In a recent study by Vladiou et al. (2019), unsupervised clustering analysis of scRNA-seq data of mouse developing cerebellum from 9 time points (E10, E12, E14, E16, E18, P0, P5, P7 and P14) was done to identify molecularly distinct cell types (Vladiou et al. 2019). Transcriptionally distinct cell populations from 62,040 single cells from 9 developmental time points were

annotated by cluster identity (n=34). For each cluster, a transcriptionally unique profile was generated that lists genes (transcripts) differentially expressed for that cluster, available as a table in the study's supplementary data. Table 4.1 shows the annotated clusters that were unique to *Msx1*, *Msx2*, *Msx3* and 6330403K07Rik taken from the supplementary data mentioned. *Msx1* and *Msx2* are identified in roof plate-like stem cells, which not only points to the spatial location but also the likelihood of *Msx1* and *Msx2* expressing in a stem cell pool or a progenitor pool identified in the present study based on the compartments of *Msx1* and *Msx2*. *Msx3* is identified in clusters identified as neural stem cells, VZ progenitors and proliferating VZ progenitors and that supports the findings of the present study. Notably, 6330403K07Rik specific clusters identified in this scRNA-seq study also corroborates our spatio-temporal expression findings - excitatory cerebellar nuclei neurons, unipolar brush cells (UBCs), NTZ neurons, VZ progenitors and other GABAergic cells. Transcriptional expression patterns from scRNA-seq studies like these can be further analysed to predict cell type specific molecular partners or target genes for the *Msx* genes or the lncRNAs as a future direction.

p_val	avg_logFC	p_val_adj	cluster	gene	Annotations
0	1.03	0	13	<i>Msx1</i>	Mesenchymal stem cells
1.29E-264	1.09	2.59E-260	29	<i>Msx1</i>	Meninges
4.68E-270	1.66	9.39E-266	30	<i>Msx1</i>	Roof plate-like stem cells
8.72E-16	0.37	1.75E-11	33	<i>Msx1</i>	Postnatal gliogenic progenitors
p_val	avg_logFC	p_val_adj	cluster	gene	Annotations
2.00E-247	0.84	4.03E-243	19	<i>Msx2</i>	Astrocytes/Bergmann glia
0	0.68	0	21	<i>Msx2</i>	Astrocyte/ Bergmann glial precursors
2.29E-122	0.87	4.61E-118	30	<i>Msx2</i>	Roof plate-like stem cells
p_val	avg_logFC	p_val_adj	cluster	gene	Annotations
0	1.03	0	4	<i>Msx3</i>	Neural stem cells
0	1.28	0	12	<i>Msx3</i>	VZ progenitors
0	1.22	0	17	<i>Msx3</i>	Proliferating VZ progenitors
1.78E-79	0.42	3.57E-75	25	<i>Msx3</i>	Red blood cells
p_val	avg_logFC	p_val_adj	cluster	gene	Annotations
0	0.89	0	0	6330403K07Rik	Excitatory cerebellar nuclei neurons
6.28E-192	0.30	1.26E-187	1	6330403K07Rik	Unilar brush cells
0	0.75	0	8	6330403K07Rik	Brainstem progenitors
1.73E-135	0.37	3.48E-131	10	6330403K07Rik	GABA interneurons
3.62E-92	0.31	7.28E-88	12	6330403K07Rik	VZ progenitors
2.05E-72	0.27	4.11E-68	14	6330403K07Rik	Differentiating Purkinje cells
4.89E-61	0.32	9.83E-57	15	6330403K07Rik	Differentiating GABA interneurons
9.03E-147	0.46	1.81E-142	16	6330403K07Rik	Purkinje cells
6.50E-237	0.82	1.31E-232	23	6330403K07Rik	Postmitotic NTZ neurons

Table 4.1 List of cell type clusters identified for *Msx* genes and lncRNA 6330403K07Rik using a single cell RNA-seq study by Vladoiu et al (2019). Transcriptional signatures unique to each cluster in mouse developing cerebellum were identified in the scRNA-seq study. These data help in identifying clusters or cell types unique to a particular gene or transcript. The clusters identified for *Msx1*, *Msx2*, *Msx3* and 6330403K07Rik shown in this table corroborate findings of the present thesis. p_val, p-value; avg_logFC, average of logarithmic fold change; p_val_adj, p-value adjusted.

References

- Alder, Janet, Kevin J. Lee, Thomas M. Jessell, and Mary E. Hatten. 1999. "Generation of Cerebellar Granule Neurons in Vivo by Transplantation of BMP-Treated Neural Progenitor Cells." *Nature Neuroscience* 2(6): 535–40. http://www.nature.com/articles/nn0699_535 (July 24, 2019).
- Amaral, Paulo P., and John S. Mattick. 2008. "Noncoding RNA in Development." *Mammalian Genome* 19(7–8): 454–92.
- Andersen, Birgitte Bo, Lise Korbo, and Bente Pakkenberg. 1992. "A Quantitative Study of the Human Cerebellum with Unbiased Stereological Techniques." *Journal of Comparative Neurology* 326(4): 549–60. <https://pubmed.ncbi.nlm.nih.gov/1484123/> (June 24, 2020).
- Arner, Erik et al. 2015. "Transcribed Enhancers Lead Waves of Coordinated Transcription in Transitioning Mammalian Cells." *Science* 347(6225): 1010–14. <http://www.ncbi.nlm.nih.gov/pubmed/25678556> (October 30, 2018).
- Bach, Antoine et al. 2003. "Msx1 Is Required for Dorsal Diencephalon Patterning." *Development* 130(17): 4025–36.
- Ben-Arie, Nissim et al. 1997. "Math1 Is Essential for Genesis of Cerebellar Granule Neurons." *Nature* 390(6656).
- Boukhtouche, Fatiha et al. 2006. "Retinoid-Related Orphan Receptor α Controls the Early Steps of Purkinje Cell Dendritic Differentiation." *Journal of Neuroscience* 26(5): 1531–38.
- Briggs, James A. et al. 2015. "Mechanisms of Long Non-Coding RNAs in Mammalian Nervous System Development, Plasticity, Disease, and Evolution." *Neuron* 88(5): 861–77. <http://www.ncbi.nlm.nih.gov/pubmed/26637795> (October 30, 2018).
- Broccoli, Vanla, Edoardo Boncinelli, and Wolfgang Wurst. 1999. "The Caudal Limit of Otx2 Expression Positions the Isthmic Organizer." *Nature* 401(6749).
- Butts, Thomas, Mary J. Green, and Richard J.T. Wingate. 2014. "Development of the Cerebellum: Simple Steps to Make a 'Little Brain.'" *Development (Cambridge)* 141(21): 4031–41. <https://dev.biologists.org/content/141/21/4031> (June 24, 2020).
- Cabili, M. N. et al. 2011. "Integrative Annotation of Human Large Intergenic Noncoding RNAs Reveals Global Properties and Specific Subclasses." *Genes & Development* 25(18): 1915–27. <http://www.ncbi.nlm.nih.gov/pubmed/21890647> (October 30, 2018).

- Carninci, P. et al. 2005. "Molecular Biology: The Transcriptional Landscape of the Mammalian Genome." *Science* 309(5740): 1559–63.
- Carter, Robert A. et al. 2018. "A Single-Cell Transcriptional Atlas of the Developing Murine Cerebellum." *Current Biology* 28(18): 2910-2920.e2.
<https://doi.org/10.1016/j.cub.2018.07.062> (July 8, 2020).
- Catron, K M et al. 1995. "Transcriptional Repression by Msx-1 Does Not Require Homeodomain DNA-Binding Sites." *Molecular and Cellular Biology* 15(2).
- Catron, Katrina M. et al. 1996. "Comparison of MSX-1 and MSX-2 Suggests a Molecular Basis for Functional Redundancy." *Mechanisms of Development* 55(2): 185–99.
<https://pubmed.ncbi.nlm.nih.gov/8861098/> (July 6, 2020).
- Crossley, Philip H., Salvador Martinez, and Gail R. Martin. 1996. "Midbrain Development Induced by FGF8 in the Chick Embryo." *Nature* 380(6569).
- Derrien, T. et al. 2012. "The GENCODE v7 Catalog of Human Long Noncoding RNAs: Analysis of Their Gene Structure, Evolution, and Expression." *Genome Research* 22(9): 1775–89. <http://www.ncbi.nlm.nih.gov/pubmed/22955988> (October 30, 2018).
- de Diego, I, K Kyriakopoulou, D Karagogeos, and M Wassef. 2002. "Multiple Influences on the Migration of Precerebellar Neurons in the Caudal Medulla." *Development* 129(2): 297–306.
<http://www.ncbi.nlm.nih.gov/pubmed/11807023> (April 3, 2020).
- Duval, N. et al. 2014. "Msx1 and Msx2 Act as Essential Activators of Atoh1 Expression in the Murine Spinal Cord." *Development* 141(8): 1726–36.
<http://dev.biologists.org/cgi/doi/10.1242/dev.099002>.
- Ekker, Marc et al. 1997. "Relationships among Msx Gene Structure and Function in Zebrafish and Other Vertebrates." *Molecular Biology and Evolution* 14(10).
- Engelkamp, Dieter, Penny Rashbass, Anne Seawright, and Veronica Van Heyningen. 1999. "Role of Pax6 in Development of the Cerebellar System." *Development* 126(16).
- Englund, Chris et al. 2006. "Unipolar Brush Cells of the Cerebellum Are Produced in the Rhombic Lip and Migrate through Developing White Matter." *Journal of Neuroscience* 26(36).
- Fatemi, S. Hossein et al. 2012. "Consensus Paper: Pathological Role of the Cerebellum in Autism." *Cerebellum* 11(3): 777–807.
- Fernandes, Marie, Michelle Antoine, and Jean M. Hébert. 2012. "SMAD4 Is Essential for

- Generating Subtypes of Neurons during Cerebellar Development.” *Developmental Biology* 365(1).
- Florio, Marta et al. 2012. “Neurogenin 2 Regulates Progenitor Cell-Cycle Progression and Purkinje Cell Dendritogenesis in Cerebellar Development.” *Development (Cambridge)* 139(13).
- Foerst-Potts, L., and T.W. Sadler. 1997. “Disruption of Msx1 and Msx2 Reveals Roles for These Genes in Craniofacial, Eye, and Axial Development.” *Developmental Dynamics* 209(1).
- Forrest, Alistair R. R. et al. 2014. “A Promoter-Level Mammalian Expression Atlas.” *Nature* 507(7493): 462–70. <http://www.nature.com/articles/nature13182> (October 26, 2018).
- Frankish, Adam et al. 2019. “GENCODE Reference Annotation for the Human and Mouse Genomes.” *Nucleic Acids Research* 47(D1): D766–73.
- Goldowitz, D, and K Hamre. 1998. “The Cells and Molecules That Make a Cerebellum.” *Trends in neurosciences* 21(9): 375–82. <http://www.ncbi.nlm.nih.gov/pubmed/9735945> (October 30, 2018).
- Gui, Shupeng et al. 2017. “A Scalable Algorithm for Structure Identification of Complex Gene Regulatory Network from Temporal Expression Data.” *BMC Bioinformatics* 18(1): 74. <http://bmcbioinformatics.biomedcentral.com/articles/10.1186/s12859-017-1489-z> (March 11, 2019).
- Hallonet, M.E., M.A. Teillet, and N.M. Le Douarin. 1990. “A New Approach to the Development of the Cerebellum Provided by the Quail-Chick Marker System.” *Development* 108(1).
- Han, Jun et al. 2003. “Cranial Neural Crest-Derived Mesenchymal Proliferation Is Regulated by Msx1-Mediated P19INK4d Expression during Odontogenesis.” *Developmental Biology* 261(1).
- Hashimoto, Mitsuhiro, and Katsuhiko Mikoshiba. 2003. “Mediolateral Compartmentalization of the Cerebellum Is Determined on the ‘Birth Date’ of Purkinje Cells.” *Journal of Neuroscience* 23(36).
- Holland, Patrick J., Angela M. George, Leslie T.C. Worrell, and Rebecca L. Landsberg. 2012. “In Vitro Electroporation of the Lower Rhombic Lip of Midgestation Mouse Embryos.” *Journal of Visualized Experiments* (66): e3983.
- Hon, Chung Chau et al. 2017. “An Atlas of Human Long Non-Coding RNAs with Accurate 5’

- Ends.” *Nature* 543(7644): 199–204. <http://dx.doi.org/10.1038/nature21374>.
- Hoshino, Mikio et al. 2005. “Ptf1a, a BHLH Transcriptional Gene, Defines GABAergic Neuronal Fates in Cerebellum.” *Neuron* 47(2): 201–13.
- Kapfhammer, Josef P. 2009. “Cerebellar Slice Cultures.” In *Protocols for Neural Cell Culture*, Humana Press, 285–98. https://link.springer.com/protocol/10.1007/978-1-60761-292-6_17 (July 9, 2020).
- Kawabata, Izumi, Tatsuya Umeda, Kazuhiro Yamamoto, and Shigeo Okabe. 2004. “Electroporation-Mediated Gene Transfer System Applied to Cultured CNS Neurons.” *NeuroReport* 15(6): 971–75.
- Kawaji, Hideya et al. 2017. “The FANTOM5 Collection, a Data Series Underpinning Mammalian Transcriptome Atlases in Diverse Cell Types.” *Scientific Data* 4: 170113. <http://www.ncbi.nlm.nih.gov/pubmed/28850107> (October 30, 2018).
- Kim, Euseok J., James Battiste, Yasushi Nakagawa, and Jane E. Johnson. 2008. “Ascl1 (Mash1) Lineage Cells Contribute to Discrete Cell Populations in CNS Architecture.” *Molecular and Cellular Neuroscience* 38(4).
- Kodzius, Rimantas et al. 2006. “CAGE: Cap Analysis of Gene Expression.” *Nature Methods* 3(3): 211–22. <http://www.nature.com/doi/10.1038/nmeth0306-211> (October 30, 2018).
- Krizhanovsky, Valery, and Nissim Ben-Arie. 2006. “A Novel Role for the Choroid Plexus in BMP-Mediated Inhibition of Differentiation of Cerebellar Neural Progenitors.” *Mechanisms of Development* 123(1): 67–75.
- Kryuchkova-Mostacci, Nadezda, and Marc Robinson-Rechavi. 2017. “A Benchmark of Gene Expression Tissue-Specificity Metrics.” *Briefings in Bioinformatics* 18(2): 205–14.
- Kwang, Stanford J. et al. 2002. “Msx2 Is an Immediate Downstream Effector of Pax3 in the Development of the Murine Cardiac Neural Crest.” *Development* 129(2).
- Lagarde, Julien et al. 2017. “High-Throughput Annotation of Full-Length Long Noncoding RNAs with Capture Long-Read Sequencing.” *Nature Genetics* 49(12).
- Lai, Helen C. et al. 2011. “In Vivo Neuronal Subtype-Specific Targets of Atoh1 (Math1) in Dorsal Spinal Cord.” *Journal of Neuroscience* 31(30).
- Leto, Ketty et al. 2006. “Different Types of Cerebellar GABAergic Interneurons Originate from a Common Pool of Multipotent Progenitor Cells.” *Journal of Neuroscience* 26(45).

- Liu, Ganqiang, John S Mattick, and Ryan J Taft. 2013. "A Meta-Analysis of the Genomic and Transcriptomic Composition of Complex Life." *Cell cycle (Georgetown, Tex.)* 12(13): 2061–72. <http://www.ncbi.nlm.nih.gov/pubmed/23759593> (October 30, 2018).
- Liu, Y., Amy W Helms, and Jane E Johnson. 2004. "Distinct Activities of Msx1 and Msx3 in Dorsal Neural Tube Development." *Development* 131(5): 1017–28. <http://www.ncbi.nlm.nih.gov/pubmed/14973289> (November 1, 2018).
- Liu, Zhi Ping, Canglin Wu, Hongyu Miao, and Hulin Wu. 2015. "RegNetwork: An Integrated Database of Transcriptional and Post-Transcriptional Regulatory Networks in Human and Mouse." *Database* 2015.
- Lundell, T. G., Q. Zhou, and M. L. Doughty. 2009. "Neurogenin1 Expression in Cell Lineages of the Cerebellar Cortex in Embryonic and Postnatal Mice." *Developmental Dynamics* 238(12).
- Ma, Liang et al. 1996. "Expression of an Msx Homeobox Gene in Ascidians: Insights into the Archetypal Chordate Expression Pattern." *Developmental Dynamics* 205(3).
- Ma, Tsz Ching, Keng Ioi Vong, and Kin Ming Kwan. 2020. "Spatiotemporal Decline of BMP Signaling Activity in Neural Progenitors Mediates Fate Transition and Safeguards Neurogenesis." *Cell Reports* 30(11).
- Machold, Rob, and Gord Fishell. 2005. "Math1 Is Expressed in Temporally Discrete Pools of Cerebellar Rhombic-Lip Neural Progenitors." *Neuron* 48(1): 17–24. <http://linkinghub.elsevier.com/retrieve/pii/S0896627305007038> (October 30, 2018).
- Martinez, Salvador et al. 1999. "FGF8 Induces Formation of an Ectopic Isthmic Organizer and Isthmocerebellar Development via a Repressive Effect on Otx2 Expression." *Development* 126(6).
- Matsunaga, Eiji, Tatsuya Katahira, and Harukazu Nakamura. 2002. "Role of Lmx1b and Wnt1 in Mesencephalon and Metencephalon Development." *Development* 129(22).
- Maxson, Robert E., Mamoru Ishii, and Amy Merrill. 2003. "Msx Genes in Organogenesis and Human Disease." In *Murine Homeobox Gene Control of Embryonic Patterning and Organogenesis*, ed. Thomas Lufkin. Elsevier, 43–68.
- McMahon, Andrew P., and Allan Bradley. 1990. "The Wnt-1 (Int-1) Proto-Oncogene Is Required for Development of a Large Region of the Mouse Brain." *Cell* 62(6).
- Mehra-Chaudhary, Ritcha, Hideo Matsui, and Rajendra Raghov. 2001. "Msx3 Protein Recruits

- Histone Deacetylase to Down-Regulate the Msx1 Promoter.” *Biochemical Journal* 353(1): 13–22. <http://biochemj.org/lookup/doi/10.1042/bj3530013>.
- Mercer, T. R. et al. 2008. “Specific Expression of Long Noncoding RNAs in the Mouse Brain.” *Proceedings of the National Academy of Sciences* 105(2): 716–21. <http://www.ncbi.nlm.nih.gov/pubmed/18184812> (October 30, 2018).
- Mercer, Tim R, and John S Mattick. 2013. “Structure and Function of Long Noncoding RNAs in Epigenetic Regulation.” *Nature Structural & Molecular Biology* 20(3): 300–307. <http://www.ncbi.nlm.nih.gov/pubmed/23463315> (October 30, 2018).
- Metzger, Friedrich, and Josef P. Kapfhammer. 2000. “Protein Kinase C Activity Modulates Dendritic Differentiation of Rat Purkinje Cells in Cerebellar Slice Cultures.” *European Journal of Neuroscience* 12(6): 1993–2005.
- Meyers, Erik N., Mark Lewandoski, and Gail R. Martin. 1998. “An Fgf8 Mutant Allelic Series Generated by Cre-and Flp-Mediated Recombination.” *Nature Genetics* 18(2).
- Millen, Kathleen J., Ekaterina Y. Steshina, Igor Y. Iskusnykh, and Victor V. Chizhikov. 2014. “Transformation of the Cerebellum into More Ventral Brainstem Fates Causes Cerebellar Agenesis in the Absence of Ptf1a Function.” *Proceedings of the National Academy of Sciences of the United States of America* 111(17).
- Millet, Sandrine et al. 1999. “A Role for Gbx2 in Repression of Otx2 and Positioning the Mid/Hindbrain Organizer.” *Nature* 401(6749).
- Millet, Sandrine, Evelyne Bloch-Gallego, Antonio Simeone, and Rosa Magda Alvarado-Mallart. 1996. “The Caudal Limit of Otx2 Gene Expression as a Marker of the Midbrain/Hindbrain Boundary: A Study Using in Situ Hybridisation and Chick/Quail Homotopic Grafts.” *Development* 122(12).
- Morales, Daniver, and Mary E. Hatten. 2006. “Molecular Markers of Neuronal Progenitors in the Embryonic Cerebellar Anlage.” *Journal of Neuroscience* 26(47): 12226–36.
- Mudge, Jonathan M., and Jennifer Harrow. 2015. “Creating Reference Gene Annotation for the Mouse C57BL6/J Genome Assembly.” *Mammalian Genome* 26(9–10): 366–78.
- Newberry, Elizabeth P., Tammy Latifi, John T. Battaile, and Dwight A. Towler. 1997. “Structure-Function Analysis of Msx2-Mediated Transcriptional Suppression.” *Biochemistry* 36(34).
- Ng, Shi-Yan, Rory Johnson, and Lawrence W Stanton. 2012. “Human Long Non-Coding RNAs

- Promote Pluripotency and Neuronal Differentiation by Association with Chromatin Modifiers and Transcription Factors.” *The EMBO Journal* 31(3): 522–33.
<http://www.ncbi.nlm.nih.gov/pubmed/22193719> (October 30, 2018).
- Obana, Edwin A. et al. 2015. “Neurog1 Genetic Inducible Fate Mapping (GIFM) Reveals the Existence of Complex Spatiotemporal Cyto-Architectures in the Developing Cerebellum.” *Cerebellum* 14(3).
- Panhuysen, Markus et al. 2004. “Effects of Wnt1 Signaling on Proliferation in the Developing Mid-/Hindbrain Region.” *Molecular and Cellular Neuroscience* 26(1).
- Pascual, Marta et al. 2007. “Cerebellar GABAergic Progenitors Adopt an External Granule Cell-like Phenotype in the Absence of Ptf1a Transcription Factor Expression.” *Proceedings of the National Academy of Sciences of the United States of America* 104(12): 5193–98.
- Ramos, Casto et al. 2004. “Msx1 Disruption Leads to Diencephalon Defects and Hydrocephalus.” *Developmental Dynamics* 230(3).
- Satokata, Ichiro et al. 2000. “Msx2 Deficiency in Mice Causes Pleiotropic Defects in Bone Growth and Ectodermal Organ Formation.” *Nature Genetics* 24(4): 391–95.
- Satokata, Ichiro, and Richard Maas. 1994. “Msx1 Deficient Mice Exhibit Cleft Palate and Abnormalities of Craniofacial and Tooth Development.” *Nature Genetics* 6(4).
- Schmahmann, Jeremy D., and David Caplan. 2006. “Cognition, Emotion and the Cerebellum.” *Brain : a journal of neurology* 129(Pt 2).
- Seto, Yusuke et al. 2014. “Temporal Identity Transition from Purkinje Cell Progenitors to GABAergic Interneuron Progenitors in the Cerebellum.” *Nature Communications* 5.
- Sharman, Anna C., Sebastian M. Shimeld, and Peter W.H. Holland. 1999. “An Amphioxus Msx Gene Expressed Predominantly in the Dorsal Neural Tube.” *Development Genes and Evolution* 209(4).
- Shimeld, Sebastian M., Ian J. McKay, and Paul T. Sharpe. 1996. “The Murine Homeobox Gene Msx-3 Shows Highly Restricted Expression in the Developing Neural Tube.” *Mechanisms of Development* 55(2): 201–10.
- Sudarov, Anamaria et al. 2011. “Ascl1 Genetics Reveals Insights into Cerebellum Local Circuit Assembly.” *The Journal of Neuroscience* 31(30): 11055–69.
<http://www.jneurosci.org/cgi/doi/10.1523/JNEUROSCI.0479-11.2011> (October 30, 2018).
- Sunkin, Susan M. et al. 2013. “Allen Brain Atlas: An Integrated Spatio-Temporal Portal for

- Exploring the Central Nervous System.” *Nucleic Acids Research* 41(D1).
- Suzuki, Atsushi, Naoto Ueno, and Ali Hemmati-Brivanlou. 1997. “Xenopus Msx1 Mediates Epidermal Induction and Neural Inhibition by BMP4.” *Development* 124(16).
- Swanson, Douglas J., and Dan Goldowitz. 2011. “Experimental Sey Mouse Chimeras Reveal the Developmental Deficiencies of Pax6-Null Granule Cells in the Postnatal Cerebellum.” *Developmental Biology* 351(1).
- Swanson, Douglas James, Yiai Tong, and Dan Goldowitz. 2005. “Disruption of Cerebellar Granule Cell Development in the Pax6 Mutant, Sey Mouse.” *Developmental Brain Research* 160(2): 176–93. <http://www.ncbi.nlm.nih.gov/pubmed/16289327> (October 30, 2018).
- Taft, Ryan J., Michael Pheasant, and John S. Mattick. 2007. “The Relationship between Non-Protein-Coding DNA and Eukaryotic Complexity.” *BioEssays* 29(3): 288–99. <http://www.ncbi.nlm.nih.gov/pubmed/17295292> (October 30, 2018).
- Takahashi, Katsu et al. 1998. “Adenovirus-Mediated Ectopic Expression of Msx2 in Even-Numbered Rhombomeres Induces Apoptotic Elimination of Cranial Neural Crest Cells in Ovo.” *Development* 125(9).
- Tang, Sunyong, Paige Snider, Antony B. Firulli, and Simon J. Conway. 2010. “Trigenic Neural Crest-Restricted Smad7 over-Expression Results in Congenital Craniofacial and Cardiovascular Defects.” *Developmental Biology* 344(1).
- Thomas, Kirk R., and Mario R. Capecchi. 1990. “Targeted Disruption of the Murine Int-1 Proto-Oncogene Resulting in Severe Abnormalities in Midbrain and Cerebellar Development.” *Nature* 346(6287).
- Tong, K. K., and K. M. Kwan. 2013. “Common Partner Smad-Independent Canonical Bone Morphogenetic Protein Signaling in the Specification Process of the Anterior Rhombic Lip during Cerebellum Development.” *Molecular and Cellular Biology* 33(10): 1925–37. <http://mcb.asm.org/cgi/doi/10.1128/MCB.01143-12>.
- Tríbulo, Celeste et al. 2003. “Regulation of Msx Genes by a Bmp Gradient Is Essential for Neural Crest Specification.” *Development* 130(26).
- Tríbulo, Celeste, Manuel J. Aybar, Sara S. Sánchez, and Roberto Mayor. 2004. “A Balance between the Anti-Apoptotic Activity of Slug and the Apoptotic Activity of Msx1 Is Required for the Proper Development of the Neural Crest.” *Developmental Biology* 275(2).

- Vladoiu, Maria C. et al. 2019. "Childhood Cerebellar Tumours Mirror Conserved Fetal Transcriptional Programs." *Nature* 572(7767): 67–73.
<http://www.nature.com/articles/s41586-019-1158-7> (September 30, 2019).
- Wang, Fay et al. 2012. "RNAscope: A Novel in Situ RNA Analysis Platform for Formalin-Fixed, Paraffin-Embedded Tissues." *Journal of Molecular Diagnostics* 14(1): 22–29.
<https://pubmed.ncbi.nlm.nih.gov/22166544/> (July 8, 2020).
- Wang, Vincent Y., Matthew F. Rose, and Huda Y. Zoghbi. 2005. "Math1 Expression Redefines the Rhombic Lip Derivatives and Reveals Novel Lineages within the Brainstem and Cerebellum." *Neuron* 48(1): 31–43.
- Wang, Weidong, Xiaowei Chen, Hong Xu, and Thomas Lufkin. 1996. "Msx3: A Novel Murine Homologue of the Drosophila Msh Homeobox Gene Restricted to the Dorsal Embryonic Central Nervous System." *Mechanisms of Development* 58(1–2): 203–15.
- Wang, Zhen et al. 2013. "Automated Quantitative RNA in Situ Hybridization for Resolution of Equivocal and Heterogeneous ERBB2 (HER2) Status in Invasive Breast Carcinoma." *Journal of Molecular Diagnostics* 15(2): 210–19.
- Wassarman, Karen Montzka et al. 1997. "Specification of the Anterior Hindbrain and Establishment of a Normal Mid/Hindbrain Organizer Is Dependent on Gbx2 Gene Function." *Development* 124(15).
- Wingate, Richard J.T., and Mary E. Hatten. 1999. "The Role of the Rhombic Lip in Avian Cerebellum Development." *Development* 126(20).
- Wizeman, John W., Qiuxia Guo, Elliott M. Wilion, and James Y.H. Li. 2019. "Specification of Diverse Cell Types during Early Neurogenesis of the Mouse Cerebellum." *eLife* 8.
- Wu, Lan Ying et al. 2003. "Microphthalmia Resulting from Msx2-Induced Apoptosis in the Optic Vesicle." *Investigative Ophthalmology and Visual Science* 44(6): 2404–12.
- Yamada, Mayumi et al. 2014. "Specification of Spatial Identities of Cerebellar Neuron Progenitors by Ptf1a and Atoh1 for Proper Production of GABAergic and Glutamatergic Neurons." *Journal of Neuroscience* 34(14).
- Yao, Pu et al. 2015. "Coexpression Networks Identify Brain Region-Specific Enhancer RNAs in the Human Brain." *Nature Neuroscience* 18(8): 1168–74.
- Yeung, Joanna et al. 2014. "Wls Provides a New Compartmental View of the Rhombic Lip in Mouse Cerebellar Development." *The Journal of Neuroscience* 34(37): 12527–37.

<http://www.ncbi.nlm.nih.gov/pubmed/25209290> (October 30, 2018).

Yeung, Joanna, Thomas J. Ha, Douglas J. Swanson, and Dan Goldowitz. 2016. "A Novel and Multivalent Role of Pax6 in Cerebellar Development." *Journal of Neuroscience* 36(35): 9057–69.

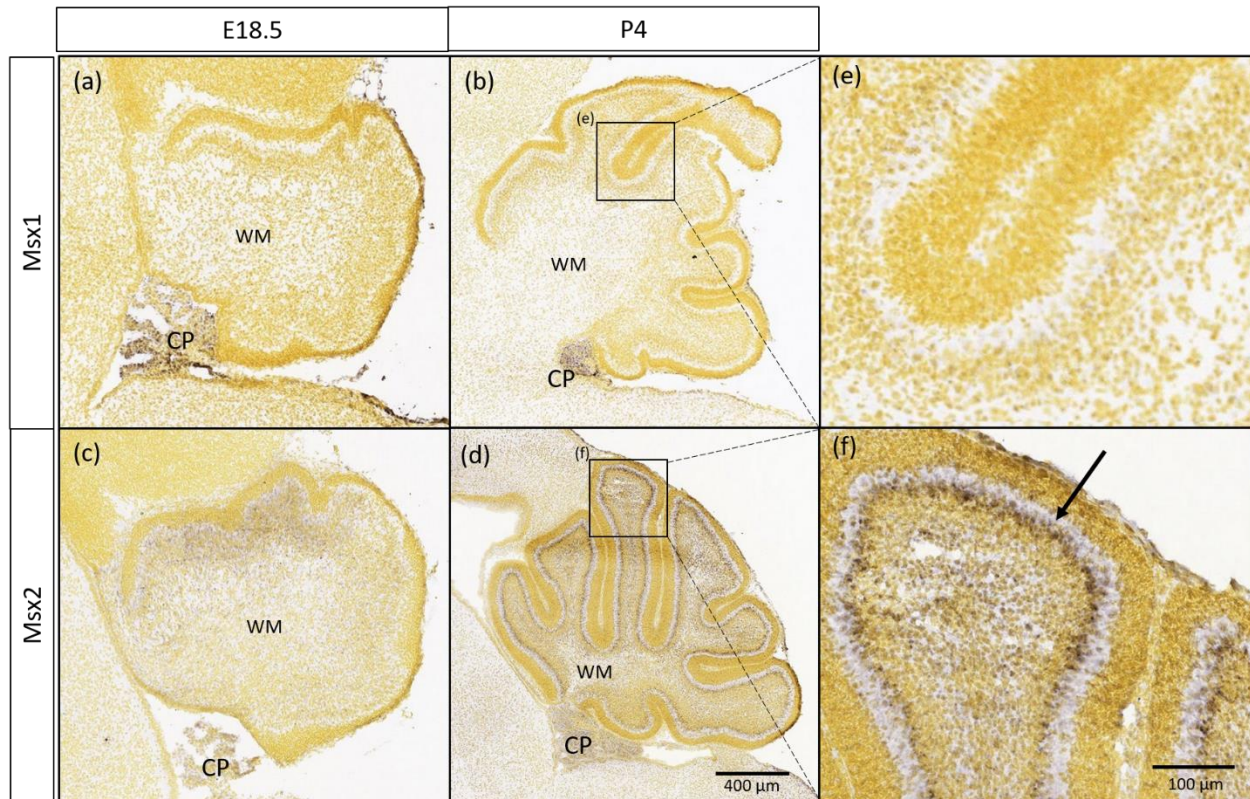
Zhang, Hailan, Katrina M. Catron, and Cory Abate-Shen. 1996. "A Role for the Msx-1 Homeodomain in Transcriptional Regulation: Residues in the N-Terminal Arm Mediate TATA Binding Protein Interaction and Transcriptional Repression." *Proceedings of the National Academy of Sciences of the United States of America* 93(5).

Zhou, Yong Xing et al. 2003. "Cerebellar Deficits and Hyperactivity in Mice Lacking Smad4." *Journal of Biological Chemistry* 278(43): 42313–20.

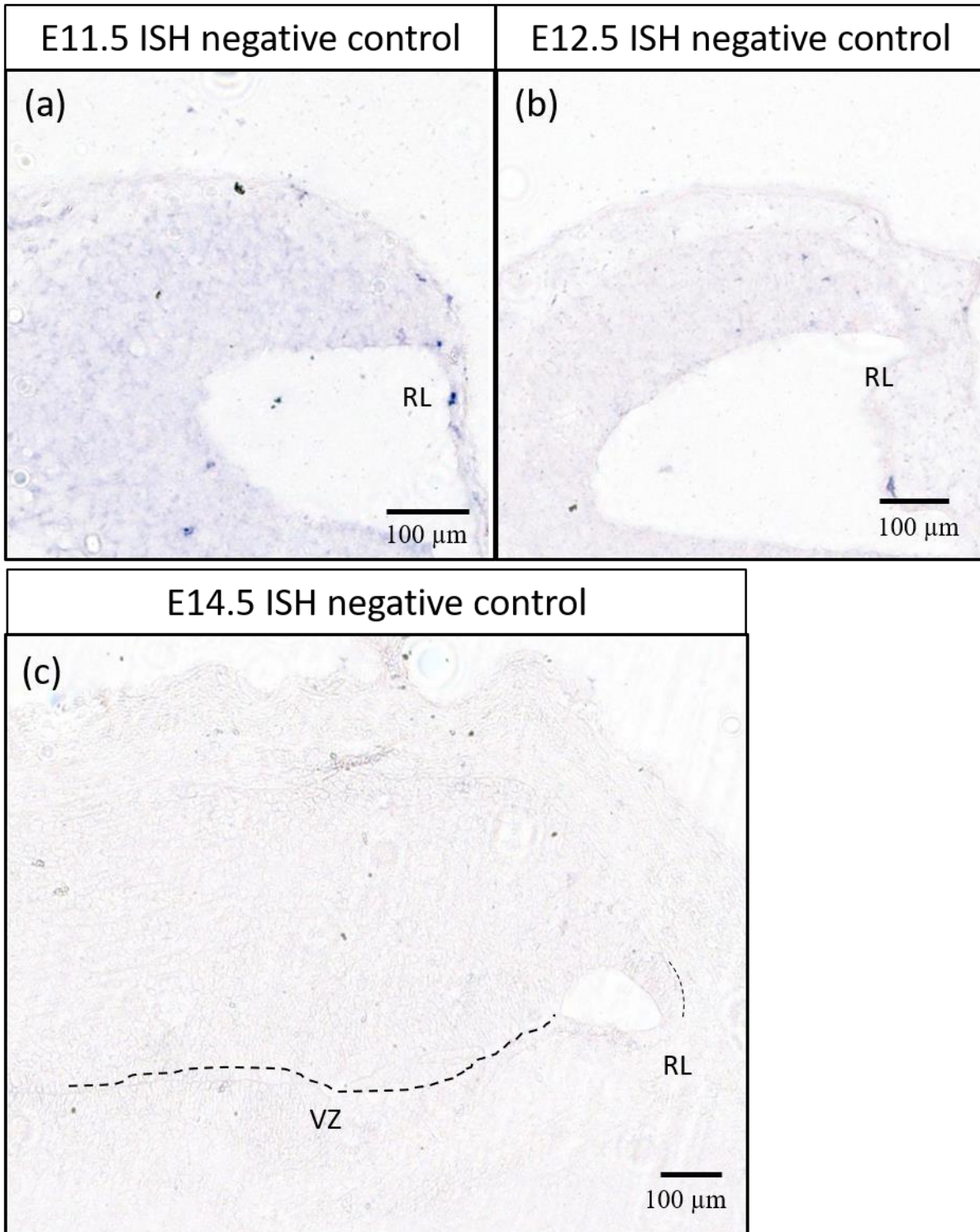
Zordan, Paola, Laura Croci, Richard Hawkes, and G. Giacomo Consalez. 2008. "Comparative Analysis of Proneural Gene Expression in the Embryonic Cerebellum." *Developmental Dynamics* 237(6).

Appendices

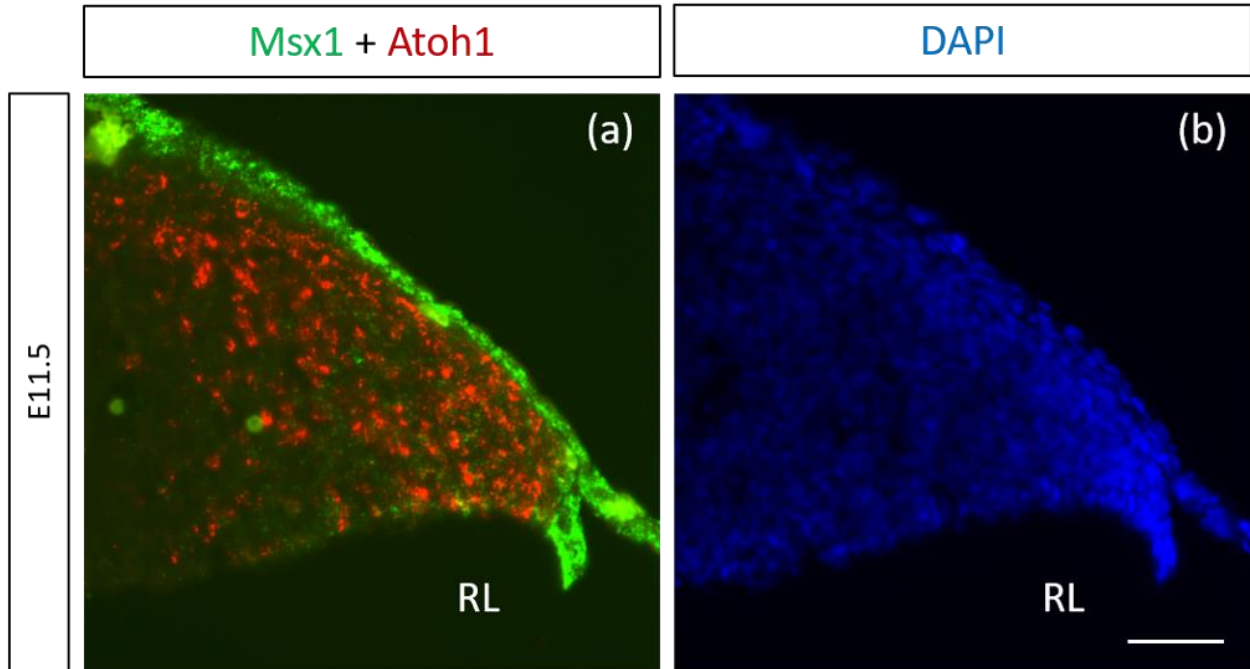
Appendix Figures



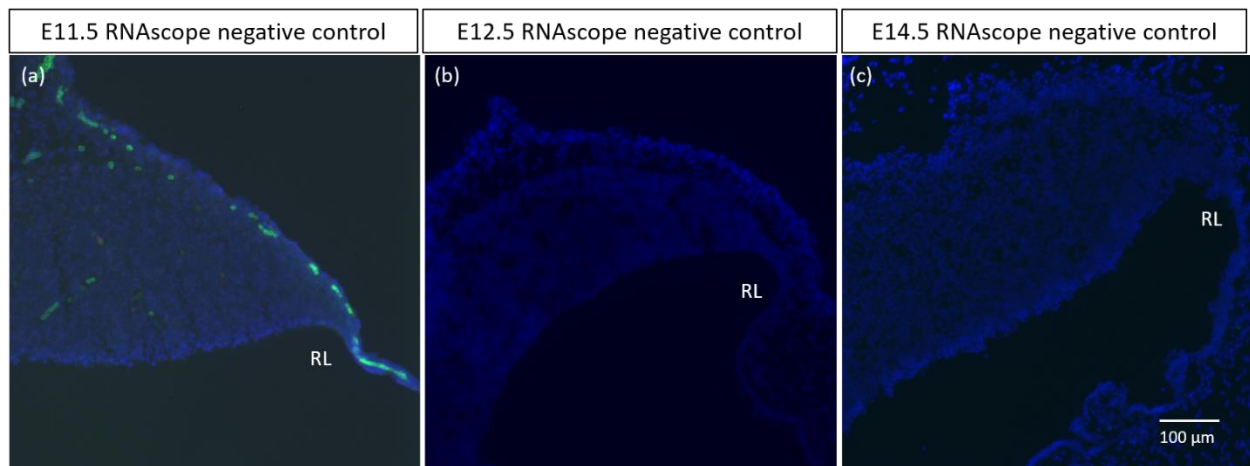
Appendix Figure 1. *Msx1* and *Msx2* expression in postnatal age. In situ hybridization images taken from the Allen Developing Mouse Brain Atlas (2008). (a-b) *Msx1* expression is largely limited to the choroid plexus (CP) and is missing from the cerebellar cortex visible at P4, seen clearly by closeup panel (e) (indicated). (c-d) *Msx2* expression is detected in the developing granule cells as they migrate to form the inner granular layer (IGL) from E18.5 to P4. The *Msx2*-positive cells in the IGL can be seen clearly in the closeup panel (f) (indicated) with signal in the IGL (arrow). CP, Choroid Plexus; WM, White Matter. Scale bars indicated.



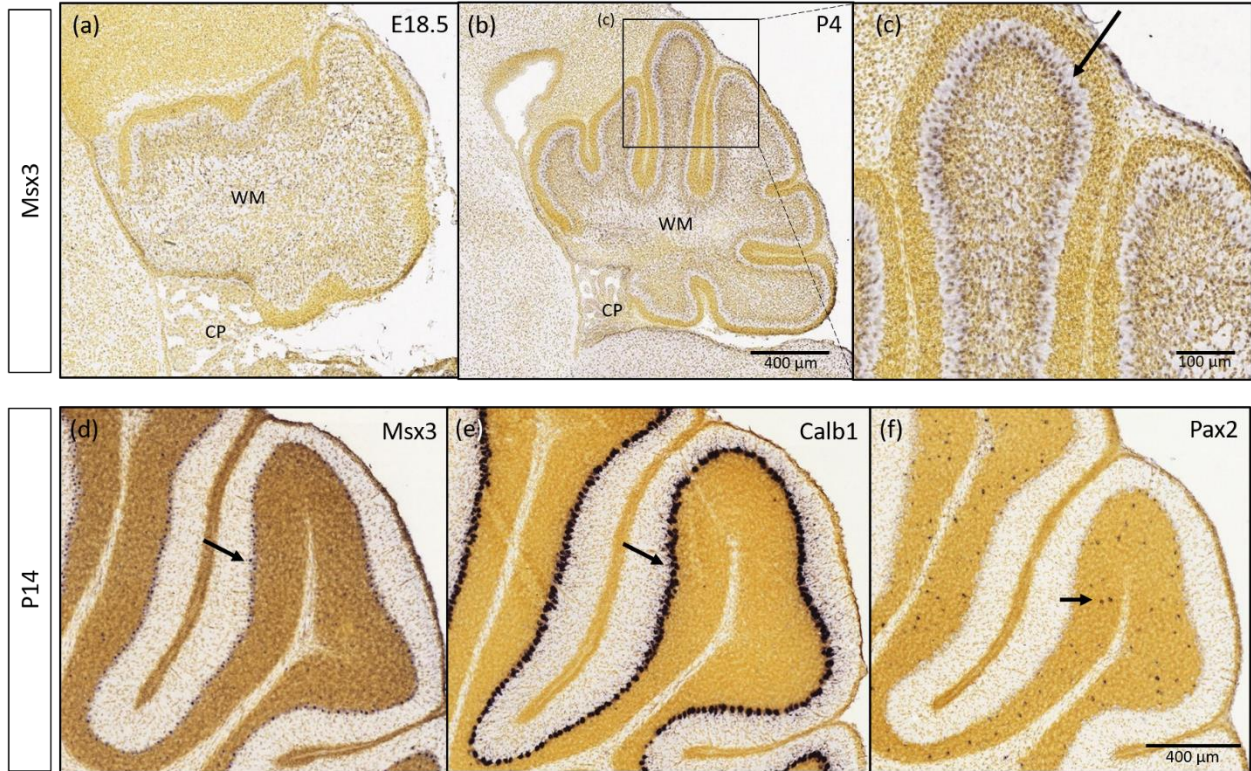
Appendix Figure 2. Negative control for RNA *in situ* hybridisation (ISH) for (a) E11.5, (b) E12.5 and (c) E14.5. Sagittal sections with right side denoting dorsal and bottom side caudal. Sense probes of *Msx1*, *Msx2* and *Msx3* were combined in equal amounts and used on these sections. RL, rhombic lip; VZ, ventricular zone. Scale bars, 100 μm .



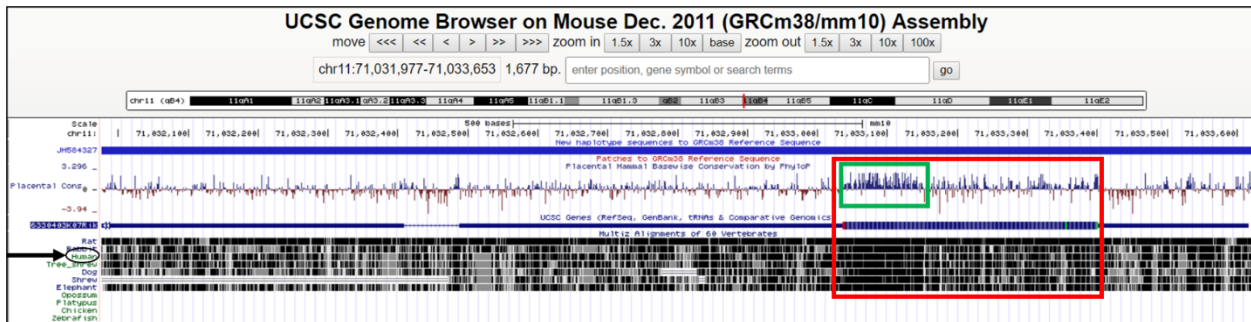
Appendix Figure 3. *Msx1* and *Atoh1* expression at E11.5. RNAscope FISH double-label on E11.5 sagittal section. (a) *Msx1* (green) is expressed strongest in the caudal-most tip of the RL that is *Atoh1* (red) negative. (b) DAPI (blue) counterstain for the same tissue section. RL, Rhombic Lip. Scale bar, 100 μm .



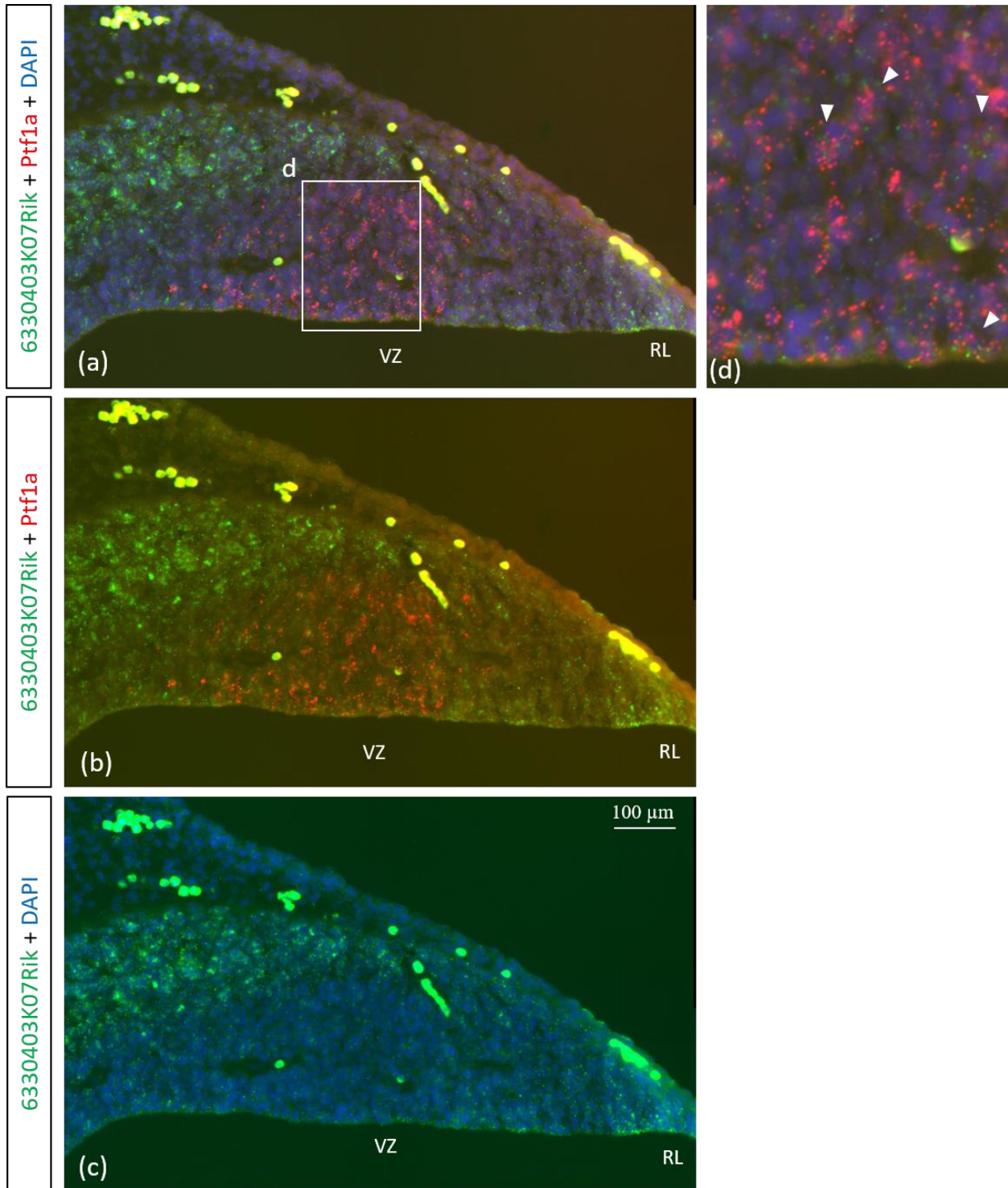
Appendix Figure 4. Negative control for RNAscope FISH for (a) E11.5, (b) E12.5 and (c) E14.5. (a-c) Sagittal sections with right side denoting dorsal and bottom side caudal. Probe for bacterial housekeeping gene (green) was used on these sections, with DAPI (blue) as counterstain. (a) At E11.5 the epithelial roof plate auto-fluoresces to produce the green blob-like artefacts. RL, rhombic lip. Scale bar, 100 μm .



Appendix Figure 5. *Msx3* expression in postnatal ages localises to Purkinje cells. RNA *in situ* hybridization images taken from the Allen Developing Mouse Brain Atlas (2008). (a-c) *Msx3* expression is detected in the cerebellum at (a) E18.5 and by (b) P4 *Msx3* expression is largely detected in the big cell bodies of the Purkinje cell layer as seen in the closeup panel (c) (arrow). (d-f) By P14, *Msx3* expression (d) is clearly visible in the Purkinje cell layer that can be identified by the post-mitotic marker, *Calbindin1* at P14 (e) (arrows). (f) shows *Pax2*-positive post-mitotic interneurons for comparison (arrow). CP, Choroid Plexus; WM, White Matter. Scale bars indicated.



Appendix Figure 6. lncRNA 6330403K07Rik is conserved across multiple species. Taken from the UCSC Genome Browser. 6330403K07Rik is on the negative strand on Chromosome 11 of the mouse. A sequence of ~350 bases in Exon 1 shows high positive conservation (red rectangle) across multiple species including humans (black arrow). A highly conserved stretch (~120 bases) of the lncRNA sequence occurs within this region in Exon 1 (green rectangle) indicative of a possible protein binding site.



Appendix Figure 7. Weak 6330403K07Rik expression in the VZ at E11.5. (a-c) RNAscope FISH double-label of lncRNA 6330403K07Rik (green) along with *Ptf1a* (red). Some expression of the lncRNA (green) in the VZ is detected. (d) is a close-up of (a) showing green punctate dots (arrowheads). NTZ, nuclear transitory zone; RL, rhombic lip. Scale bar, 100 μ m.

Appendix Tables

S. No.	p	Transcript ID	E11	E12	E13	E14	E15	E16	E17	E18	N00	N03	N06	N09	Average
1	p1	Malat1	2423.34	3032.36	6420.93	5080.72	5400.38	4309.52	3772.52	6458.96	7104.62	3816.58	3550.12	3647.78	4584.82
2	p1	Gas5	345.15	324.68	357.98	332.36	353.07	402.92	408.59	330.27	286.09	257.63	254.70	205.26	321.56
3	p1	Cct6a	271.33	254.71	219.83	226.12	207.94	189.86	187.18	190.43	201.87	183.69	191.76	179.88	208.72
4	p1	ENSMUST00000156068	155.31	287.72	313.10	282.61	242.39	236.22	220.17	190.57	171.05	103.56	80.44	74.46	196.47
5	p1	ENSMUST00000127786	106.64	104.49	176.76	163.85	185.56	148.20	154.70	48.19	198.12	248.54	141.58	130.47	150.59
6	p1	Snhg6	96.98	100.38	96.79	87.09	102.56	116.82	125.92	114.49	139.76	124.10	121.89	101.07	110.65
7	p1	1110038812Rik	137.42	133.57	117.79	110.05	108.89	101.85	104.08	93.51	98.98	85.73	75.24	57.24	102.03
8	p1	Miat	107.88	174.54	122.56	77.16	67.13	69.01	61.01	66.28	82.30	76.48	55.80	61.71	85.15
9	p1	Peg13	38.73	58.83	91.47	95.39	95.08	73.35	69.63	103.13	115.50	65.08	66.05	96.49	80.64
10	p1	1810026805Rik	55.24	65.77	75.05	60.89	63.21	62.26	68.79	71.50	69.89	65.30	63.79	71.71	66.20
11	p1	ENSMUST00000173314	31.53	25.47	60.59	72.10	66.82	73.65	61.08	99.60	53.50	67.84	66.33	72.00	62.54
12	p2	Cct6a	69.88	69.28	63.87	69.10	65.78	62.37	62.27	62.11	49.93	53.23	50.88	51.82	60.88
13	p1	Snhg8	57.72	49.28	44.32	54.92	61.00	63.70	70.54	70.29	55.20	70.45	70.79	60.51	60.73
14	p1	2410006H16Rik	49.81	56.06	62.23	55.02	54.24	56.61	65.30	54.61	56.31	60.98	62.76	59.16	57.76
15	p1	C130071C03Rik	69.18	73.47	69.92	56.71	54.07	51.56	42.58	41.34	61.79	49.79	48.68	36.30	54.62
16	p1	ENSMUST00000168978	38.23	40.08	42.23	47.64	48.01	52.86	58.23	53.52	59.94	47.21	50.81	49.86	49.05
17	p1	Meg3	13.01	4.79	27.33	24.56	54.25	92.21	46.38	133.96	79.91	61.75	29.08	18.62	48.82
18	p1	ENSMUST00000131907	25.86	43.84	61.59	50.44	50.93	37.78	39.48	42.01	42.98	42.82	52.58	66.38	46.39
19	p1	ENSMUST00000144852	40.13	38.31	37.84	45.35	46.22	42.55	46.68	46.66	40.73	39.62	36.22	38.06	41.53
20	p1	ENSMUST00000151374	49.84	34.97	34.10	35.95	44.00	45.74	49.27	45.78	36.92	40.81	33.72	30.38	40.12
21	p1	Gm2694	11.22	26.98	34.51	37.97	37.40	37.37	46.34	40.65	35.78	46.12	52.19	66.45	39.41
22	p1	C230004F18Rik	5.76	6.03	25.75	39.88	54.10	50.07	50.50	72.85	69.78	36.59	26.64	34.36	39.36
23	p1	Xist	25.91	25.50	45.24	43.96	47.17	32.94	32.83	11.82	61.79	58.65	36.47	32.35	37.89
24	p2	Peg13	20.52	33.64	54.03	52.42	48.86	35.13	29.37	44.53	44.62	23.11	22.79	30.23	36.60
25	p1	Snhg12	24.08	27.22	35.11	39.80	41.47	45.50	46.36	44.93	32.32	29.99	30.16	25.26	35.18
26	p1	ENSMUST00000112103	7.19	8.85	16.99	15.45	20.88	22.95	26.59	32.85	47.08	64.12	79.23	70.56	34.39
27	p1	2900097C17Rik	21.06	22.93	31.87	34.03	33.49	36.18	38.50	35.48	43.57	40.30	32.19	34.18	33.65
28	p1	2610203C20Rik	33.57	38.47	57.74	54.75	45.14	40.06	29.74	27.67	27.45	20.69	14.72	10.58	33.38
29	p1	2900060B14Rik	46.48	33.84	25.96	26.07	30.24	42.97	27.93	40.35	24.62	34.48	25.79	31.01	32.48
30	p1	ENSMUST00000098868	18.01	25.38	65.79	56.57	48.74	38.58	26.12	29.60	21.57	15.28	6.70	4.60	29.75
31	p2	1810058I24Rik	40.77	34.18	33.37	28.03	25.33	19.16	22.91	25.79	27.66	27.48	25.83	22.77	27.77
32	p1	Kcnq1ot1	30.69	35.66	34.98	25.49	23.50	24.42	19.86	31.76	20.27	19.92	18.24	13.82	24.88
33	p1	0630043F03Rik	8.26	14.73	34.86	52.57	48.62	29.22	25.26	24.17	13.82	13.96	12.64	11.45	24.13
34	p1	5330434G04Rik	22.76	23.98	35.49	26.92	26.85	22.17	23.07	30.28	21.48	16.52	16.34	12.15	23.17
35	p1	A730094K22Rik	3.37	6.49	17.28	22.03	27.76	22.70	25.13	31.61	25.94	30.11	37.15	25.47	22.92
36	p1	ENSMUST00000139356	20.70	26.29	27.38	25.20	20.80	19.36	21.70	22.94	27.39	23.14	21.19	18.25	22.86
37	p1	4632427E13Rik	26.47	27.89	29.46	27.59	23.98	22.25	20.63	20.90	13.31	13.18	15.99	17.28	21.58
38	p1	2810001G20Rik	21.89	21.72	22.52	25.44	22.63	22.86	19.68	20.07	20.56	21.21	16.51	22.14	21.43
39	p1	Zswim6	22.75	31.18	40.72	27.99	24.49	17.93	15.75	17.25	18.78	13.28	11.30	11.59	21.08
40	p1	1300002E11Rik	14.55	17.36	19.96	20.82	22.59	21.94	19.49	21.34	20.12	21.13	21.11	22.71	20.26
41	p2	Dlg2	1.77	1.56	12.28	24.02	31.07	24.13	28.34	28.63	29.17	16.66	18.94	24.85	20.12
42	p1	1700020I14Rik	13.99	15.45	15.02	16.92	15.73	19.74	21.44	23.50	22.36	23.43	19.39	29.53	19.71
43	p9	Dlg2	0.28	0.61	9.46	21.00	31.45	28.14	26.48	31.46	31.89	16.67	10.99	14.48	18.58
44	p3	Peg13	9.08	13.84	20.51	21.67	20.42	18.34	17.48	23.03	25.49	12.71	13.49	14.63	17.56
45	p2	ENSMUST00000098868	8.00	19.60	49.85	39.05	30.74	12.20	14.96	10.56	4.89	2.22	1.37	17.47	17.47
46	p1	ENSMUST00000128121	7.06	19.54	26.10	21.98	16.11	19.20	15.31	12.61	20.08	15.19	12.34	18.44	17.00
47	p1	ENSMUST00000137236	14.65	13.10	20.79	16.64	15.39	19.82	18.71	21.68	12.13	17.95	12.61	17.08	16.71
48	p1	2810013P06Rik	12.56	15.35	21.19	21.34	20.13	20.40	17.36	12.71	14.45	13.53	15.36	14.04	16.54
49	p1	ENSMUST00000133630	5.70	5.75	10.89	12.64	16.67	20.66	20.52	21.30	20.90	21.56	15.58	21.90	16.17
50	p1	Snhg3	11.21	11.57	15.20	15.27	15.48	17.45	17.05	15.62	19.81	15.10	16.24	17.62	15.64
51	p1	A930015D03Rik	13.60	11.98	16.84	19.01	16.07	18.66	17.66	20.23	12.26	13.36	12.87	13.02	15.46
52	p1	2900079G21Rik	0.77	1.70	8.38	8.30	9.85	10.61	11.13	14.81	22.25	19.83	32.65	41.65	15.16
53	p1	ENSMUST00000123850	16.71	17.73	20.25	18.03	18.23	15.56	14.20	11.43	15.97	10.84	10.00	12.16	15.09
54	p7	Dlg2	0.32	0.62	7.71	18.41	23.91	20.70	21.70	27.14	20.41	12.89	11.65	14.15	14.97
55	p1	2310009A05Rik	18.78	16.70	15.40	16.89	14.42	13.75	17.95	12.84	9.16	11.24	14.65	15.86	14.80
56	p1	ENSMUST00000139835	2.72	5.42	12.29	13.78	14.22	16.44	16.75	21.80	13.42	16.99	23.17	16.99	14.50
57	p2	Miat	8.75	12.07	17.39	13.08	11.64	12.97	11.51	12.13	18.57	15.19	17.76	14.97	13.84
58	p1	9530059O14Rik	4.30	10.50	18.56	14.40	15.88	19.88	15.69	18.62	12.29	9.75	10.51	14.35	13.73
59	p1	Snhg9	15.00	12.08	11.46	9.85	12.64	17.42	16.60	13.53	11.57	17.16	13.61	12.05	13.58
60	p3	ENSMUST00000131907	13.33	20.10	22.30	13.59	14.63	12.29	9.54	13.50	11.00	9.45	10.32	11.96	13.50
61	p1	ENSMUST00000159637	9.75	11.89	19.87	15.92	15.06	15.76	14.09	12.35	10.46	11.70	10.76	13.37	13.42
62	p1	2610035D17Rik	6.75	9.94	8.96	9.89	13.58	13.33	15.56	19.75	17.96	13.72	11.77	15.16	13.03
63	p1	ENSMUST00000127129	10.15	11.73	13.32	14.91	13.34	15.44	13.38	14.99	12.68	12.47	10.19	12.10	12.89
64	p1	ENSMUST00000136518	9.34	9.88	10.41	10.37	10.25	13.14	13.64	14.33	17.20	15.30	15.46	14.77	12.84
65	p1	ENSMUST00000128176	8.21	11.42	15.76	15.74	14.71	14.83	12.48	14.76	13.17	10.80	10.43	8.23	12.55
66	p1	1700012D14Rik	12.88	14.40	12.29	13.96	12.77	10.93	11.78	9.99	13.32	12.58	12.84	11.92	12.47
67	p2	4632427E13Rik	10.65	14.40	15.76	12.04	15.29	12.16	9.60	12.42	9.42	9.26	10.35	10.35	11.81
68	p1	ENSMUST00000134624	20.39	27.10	21.05	14.14	12.15	9.56	7.80	10.27	7.22	5.22	4.15	1.85	11.74
69	p5	Dlg2	0.20	0.74	8.43	7.34	7.96	7.89	9.20	14.46	17.28	18.38	19.39	26.46	11.48
70	p3	Cct6a	16.89	17.12	12.68	13.42	12.46	11.97	9.02	12.75	9.48	7.92	5.26	6.82	11.32
71	p1	2900076A07Rik	8.63	10.70	12.27	13.24	12.59	11.84	10.79	12.64	14.90	10.44	7.01	7.68	11.06
72	p1	ENSMUST00000155166	5.37	10.65	14.29	14.65	15.24	11.12	13.13	11.92	9.85	7.28	9.09	8.90	10.96
73	p1	Trmt61b	10.69	8.13	10.93	9.48	11.99	9.56	11.36	11.52	13.25	10.14	11.56	12.63	10.94
74	p1	Dleu2	18.41	12.15	7.45	8.78	9.63	10.92	11.95	8.58	5.38	10.67	15.73	9.92	10.80

75	p1	Tctn2	17.44	16.82	12.16	14.36	11.97	10.66	8.61	9.38	10.47	5.58	6.57	4.29	10.69
76	p1	Tmem134	9.26	9.03	8.79	9.61	8.22	8.45	9.13	9.91	10.98	12.53	13.40	15.31	10.39
77	p1	ENSMUST00000133570	3.50	4.30	7.39	9.51	10.86	11.14	12.20	14.63	14.24	13.21	11.28	11.96	10.35
78	p1	1810058124Rik	19.90	14.94	10.73	8.07	8.30	5.54	5.84	7.29	9.35	8.95	13.04	11.33	10.27
79	p1	2610316001Rik	6.40	7.71	11.39	11.92	12.49	10.84	13.26	13.27	9.75	9.25	9.22	5.90	10.12
80	p1	ENSMUST00000134527	11.52	7.79	8.35	8.50	9.33	9.71	8.67	12.19	13.24	12.23	9.37	8.54	9.95
81	p1	ENSMUST00000123016	2.22	6.58	16.54	19.31	14.76	12.76	9.71	11.05	8.68	6.44	6.02	4.87	9.91
82	p1	D130017N08Rik	5.35	6.80	11.67	13.18	14.11	12.17	11.17	11.47	10.28	8.44	7.51	4.98	9.76
83	p1	ENSMUST00000152147	12.47	9.80	11.65	11.84	10.19	12.76	9.14	7.09	5.73	8.98	8.61	7.37	9.64
84	p1	Tug1	10.09	9.49	10.69	10.71	10.23	9.96	10.26	11.57	9.87	7.45	7.02	7.69	9.59
85	p1	9330151119Rik	6.02	6.78	7.29	7.55	9.36	10.31	9.96	11.72	15.43	11.08	8.23	10.85	9.55
86	p1	ENSMUST00000151778	7.95	11.98	16.95	13.40	12.59	11.96	9.19	6.61	7.04	5.57	4.90	3.60	9.31
87	p1	F730043M19Rik	2.60	6.18	12.40	9.16	13.01	12.26	10.88	12.80	10.34	8.45	7.09	4.96	9.18
88	p1	ENSMUST00000128960	13.88	10.01	10.04	10.84	9.28	9.56	9.10	8.96	5.10	7.91	8.29	7.03	9.17
89	p1	1500015A07Rik	6.97	7.61	9.48	10.94	10.55	10.04	9.74	7.63	8.09	9.09	9.53	9.36	9.09
90	p3	ENSMUST00000098868	3.50	8.27	23.37	15.82	16.79	9.91	6.74	9.95	6.63	3.52	2.25	1.04	8.98
91	p1	ENSMUST00000174808	3.96	4.78	10.40	6.81	7.27	9.78	7.35	11.58	5.64	6.51	24.34	8.79	8.94
92	p1	ENSMUST00000129337	12.13	14.93	11.77	10.82	9.45	11.38	6.64	7.08	7.96	6.82	4.29	3.75	8.92
93	p1	Neepas	14.71	12.42	9.18	8.78	9.05	8.96	5.66	7.38	8.17	8.76	5.87	6.73	8.81
94	p2	ENSMUST00000131907	4.81	10.60	11.29	8.35	8.91	7.43	6.50	7.68	11.66	7.86	7.65	11.42	8.88
95	p1	Gm13375	11.84	14.08	8.14	8.36	8.15	4.71	4.02	8.13	11.03	8.50	7.81	8.99	8.65
96	p1	2810410L24Rik	9.79	10.23	10.19	7.82	5.89	8.56	6.36	6.41	12.58	8.59	7.85	8.35	8.55
97	p1	4632415L05Rik	7.08	7.79	8.76	9.50	9.56	9.70	9.73	7.77	6.96	7.04	8.61	9.10	8.47
98	p1	5rhg10	5.45	6.80	7.10	8.40	9.20	10.58	8.91	9.46	8.25	9.06	9.07	8.56	8.40
99	p1	ENSMUST00000170849	31.33	21.12	10.83	7.20	5.82	4.84	2.39	3.37	2.02	2.36	2.20	1.54	7.92
100	p1	A230056P14Rik	7.61	8.06	9.78	10.25	11.40	8.73	8.88	8.28	4.87	4.74	4.58	4.93	7.68
101	p1	1110002L01Rik	9.53	9.64	11.84	10.92	11.91	7.14	6.66	7.08	3.90	4.69	4.60	4.10	7.67
102	p1	ENSMUST00000064101	4.27	4.62	6.05	5.48	8.04	6.85	5.86	7.74	10.76	8.47	9.79	12.67	7.55
103	p1	5rhg1	13.07	6.94	6.68	8.89	6.63	7.15	5.77	10.53	6.46	6.27	6.77	5.12	7.52
104	p2	Meg3	2.24	0.85	4.60	3.35	9.12	13.88	6.98	18.16	15.75	7.91	4.39	2.67	7.88
105	p1	C430049B03Rik	9.98	4.41	9.12	7.65	7.48	8.16	7.59	11.54	5.10	7.09	6.50	5.25	7.49
106	p1	5730405015Rik	4.16	5.51	9.93	9.74	11.34	8.72	9.69	8.69	6.22	4.00	6.00	5.85	7.49
107	p1	ENSMUST00000159155	0.17	0.09	1.10	1.87	3.28	5.35	7.78	9.90	11.57	11.52	15.99	20.13	7.40
108	p1	ENSMUST00000144796	9.81	7.15	7.63	7.19	7.36	7.08	8.56	9.22	8.00	6.01	5.45	5.07	7.38
109	p1	9930104L06Rik	5.97	7.08	5.72	7.17	7.79	7.51	8.06	8.19	6.56	8.04	6.40	9.19	7.31
110	p1	D430036116Rik	5.41	3.72	1.84	3.34	6.70	8.54	10.33	11.40	15.90	9.60	4.46	5.51	7.23
111	p1	2610020C07Rik	8.18	7.29	7.38	6.96	7.17	5.24	7.59	6.95	6.77	7.42	6.64	6.15	6.98
112	p1	4933421010Rik	5.62	7.28	7.70	7.40	8.27	6.62	7.05	6.44	5.97	5.84	6.22	8.48	6.91
113	p1	A930005H10Rik	4.48	6.37	6.85	7.72	5.30	6.46	6.24	6.82	8.36	6.30	9.97	7.63	6.88
114	p1	ENSMUST00000148743	12.78	12.47	7.38	7.38	5.96	5.90	5.41	7.18	3.14	4.85	5.45	4.25	6.81
115	p1	Gm15545	8.00	8.70	8.31	7.12	9.48	5.61	5.86	7.73	5.45	3.35	7.13	3.92	6.72
116	p2	1810026B05Rik	5.62	7.15	7.53	7.15	7.17	8.76	6.97	6.55	6.20	5.25	6.75	4.86	6.86
117	p1	Ppmt1	7.87	7.21	4.01	5.04	6.12	6.83	7.87	5.50	6.70	6.59	7.43	7.67	6.57
118	p1	ENSMUST00000129089	18.02	13.70	9.43	8.31	8.14	4.63	4.29	4.93	2.30	1.98	1.69	0.70	6.51
119	p1	ENSMUST00000144350	0.22	1.46	4.42	3.57	5.12	6.26	6.99	10.57	8.01	7.19	12.40	11.07	6.44
120	p1	2810002D19Rik	6.41	6.93	6.96	8.84	8.22	7.05	7.22	7.49	3.44	5.23	4.80	4.29	6.41
121	p1	ENSMUST00000151229	18.52	14.24	9.91	9.14	8.06	3.92	2.88	3.62	3.70	1.07	0.59	0.81	6.37
122	p1	ENSMUST00000133808	4.35	3.42	3.13	4.82	4.99	5.32	6.24	5.86	6.23	9.48	9.98	10.63	6.20
123	p1	ENSMUST00000124378	2.04	2.25	8.02	7.82	10.27	8.52	9.46	6.37	6.53	5.52	3.21	3.38	6.11
124	p3	Meg3	1.91	0.38	3.36	2.89	8.89	14.03	4.80	17.24	9.32	4.42	2.69	2.27	6.00
125	p1	2810429104Rik	8.56	7.11	5.58	6.18	6.64	7.11	5.76	7.74	5.21	5.20	3.38	2.78	5.94
126	p4	Peg13	2.48	3.75	5.40	6.33	6.28	6.05	5.00	6.92	9.34	5.06	6.01	8.32	5.91
127	p1	ENSMUST00000129868	0.00	0.00	1.25	3.55	9.95	9.19	9.96	14.07	12.83	4.95	2.67	1.77	5.85
128	p1	0610040B10Rik	3.97	4.77	8.56	7.36	7.39	5.87	5.13	4.98	3.60	5.13	5.58	7.39	5.81
129	p1	ENSMUST00000126622	5.56	6.91	7.45	7.39	6.94	6.06	6.70	5.64	3.19	4.89	4.39	4.43	5.80
130	p1	2310015A10Rik	4.15	2.83	4.57	4.87	4.93	4.24	5.15	4.94	9.53	10.01	7.30	6.68	5.77
131	p1	ENSMUST00000172910	10.02	5.47	3.15	2.71	2.37	3.58	4.80	3.63	4.40	7.91	9.69	9.92	5.64
132	p1	6530402F18Rik	1.29	1.40	3.38	6.69	6.87	7.35	9.04	12.36	8.48	4.02	3.55	2.00	5.54
133	p1	If30	9.87	4.37	3.41	4.60	3.95	4.09	2.87	4.27	4.23	7.07	11.35	5.92	5.50
134	p1	ENSMUST00000079529	3.05	1.03	3.82	4.71	5.47	6.19	7.62	7.02	7.86	7.06	5.99	5.64	5.46
135	p2	ENSMUST00000173314	2.51	3.70	6.58	5.90	5.15	7.15	4.48	8.38	3.92	4.26	6.24	6.33	5.38
136	p1	E1300307A14Rik	2.34	3.63	5.56	7.11	8.74	8.04	6.30	7.64	4.57	3.86	3.25	3.21	5.36
137	p1	2610027F03Rik	12.57	21.91	14.22	8.13	3.57	1.82	1.01	0.24	0.37	0.07	0.00	0.00	5.32
138	p1	5930412G12Rik	8.18	10.37	7.05	6.00	5.14	7.37	6.46	5.32	3.90	1.74	0.98	0.50	5.25
139	p1	Gm15663	1.81	1.36	4.70	5.75	8.74	7.20	6.12	6.62	5.79	5.84	4.07	4.11	5.18
140	p4	ENSMUST00000098868	2.59	5.92	12.85	12.10	8.13	5.56	3.60	3.26	3.79	1.95	1.12	0.50	5.11
141	p1	ENSMUST00000146700	0.99	1.95	4.44	7.77	6.54	4.91	4.86	3.97	4.79	5.70	5.66	6.89	4.87
142	p1	ENSMUST00000122813	14.08	7.26	3.84	3.37	3.07	3.29	4.65	1.53	2.49	5.28	5.77	3.35	4.83
143	p3	Xist	2.68	3.77	4.23	3.28	5.01	4.36	4.67	1.63	6.44	11.44	6.39	4.03	4.83
144	p6	Malat1	2.56	2.28	4.26	3.55	3.91	6.04	4.74	6.40	4.04	3.74	9.21	5.80	4.71
145	p2	ENSMUST00000134624	8.95	11.06	7.33	5.99	4.88	3.57	3.25	4.26	1.81	1.87	1.80	1.04	4.65
146	p5	Meg3	1.21	0.71	2.64	2.30	5.49	10.30	3.49	9.19	9.93	4.58	3.91	0.65	4.53
147	p8	ENSMUST00000173314	1.51	1.83	4.69	3.98	3.09	5.15	2.99	5.16	4.19	3.62	13.62	4.09	4.49
148	p17	Dlg2	0.00	0.26	1.41	1.13	2.37	2.95	4.88	8.04	7.71	7.67	6.83	8.18	4.29
149	p1	ENSMUST00000098678	23.11	9.85	6.29	5.77	2.10	2.69	0.75	0.14	0.18	0.07	0.00	0.00	4.25

150	p12	Dlg2	0.10	0.12	2.43	2.49	2.81	3.27	3.11	5.49	7.57	6.27	8.04	8.24	4.16
151	p6	Meg3	1.30	0.41	1.78	3.29	3.73	7.29	4.11	8.85	6.74	4.47	3.63	2.89	4.04
152	p1	A330076H08Rik	0.15	0.91	1.08	2.00	1.97	1.96	1.83	3.31	5.17	4.74	5.77	17.07	3.83
153	p9	ENSMUST00000173314	1.77	1.30	3.64	2.79	3.74	4.58	1.64	3.30	3.56	3.74	11.01	4.05	3.76
154	p3	9430053009Rik	1.12	3.24	11.11	10.22	7.30	4.42	2.75	1.36	1.87	0.88	0.56	0.00	3.74
155	p1	ENSMUST00000134140	7.24	3.76	3.44	3.27	4.67	3.12	2.81	3.98	2.08	2.94	2.36	2.35	3.50
156	p1	ENSMUST00000126472	8.04	8.90	4.60	4.13	3.47	3.40	1.99	2.54	1.84	1.41	0.59	0.40	3.44
157	p2	2610027F03Rik	12.19	12.54	7.06	3.97	1.20	0.67	0.63	1.13	0.00	0.07	0.00	0.00	3.29
158	p20	Malat1	2.11	1.70	3.91	2.88	2.40	3.54	2.18	4.29	3.52	3.88	5.28	2.88	3.22
159	p6	ENSMUST00000173314	0.75	1.15	3.02	1.96	2.97	4.00	2.47	5.43	2.55	2.21	6.18	3.88	3.05
160	p1	ENSMUST00000163493	0.96	1.03	0.58	1.31	1.47	1.49	1.29	2.21	1.82	4.58	7.43	11.80	3.00
161	p1	ENSMUST00000147294	11.79	6.46	5.73	4.57	3.07	2.17	0.24	0.44	0.00	0.27	0.05	0.00	2.90
162	p1	ENSMUST00000137258	10.72	15.36	5.66	2.35	0.42	0.00	0.21	0.00	0.00	0.00	0.00	0.00	2.89
163	p9	Meg3	0.56	0.40	1.93	1.60	3.12	5.15	1.22	7.11	6.39	3.85	2.15	0.91	2.86
164	p4	2610203C20Rik	1.39	0.93	3.73	4.12	5.48	3.57	1.69	5.48	1.56	2.19	2.10	1.54	2.81
165	p1	ENSMUST00000128815	2.14	5.39	8.16	5.82	3.77	2.88	1.45	1.46	0.85	0.37	0.95	0.21	2.79
166	p2	ENSMUST00000174808	1.35	1.53	4.30	3.00	2.34	2.93	2.22	2.51	1.85	2.65	4.68	3.48	2.74
167	p3	ENSMUST00000173314	0.79	1.97	2.45	2.46	1.99	3.79	2.41	3.17	2.18	2.86	5.70	3.06	2.74
168	p9	Malat1	1.01	1.51	3.21	2.96	2.76	3.89	3.12	2.54	2.01	2.55	5.29	1.48	2.69
169	p6	ENSMUST00000174808	1.73	1.49	2.86	2.29	1.92	3.03	2.00	4.76	2.54	2.11	6.26	0.99	2.66
170	p1	ENSMUST00000160099	1.62	1.69	2.47	2.57	2.47	1.99	2.85	5.72	1.93	2.43	2.95	2.34	2.59
171	p4	ENSMUST00000174808	0.82	0.87	2.73	2.45	1.75	1.95	1.24	2.67	2.09	1.93	8.95	2.23	2.47
172	p7	ENSMUST00000174808	1.48	1.60	3.34	2.35	2.15	3.42	1.95	1.56	1.67	2.42	5.41	1.34	2.39
173	p8	Meg3	1.10	0.89	0.90	1.09	2.82	3.17	2.19	5.42	3.63	2.82	2.83	1.30	2.35
174	p5	ENSMUST00000174808	0.94	0.73	2.86	2.45	1.44	2.19	1.18	1.26	1.94	1.92	9.65	1.53	2.34
175	p3	2900079G21Rik	0.00	0.00	0.00	0.00	0.08	0.00	0.25	0.84	0.61	3.40	7.74	12.86	2.15
176	p1	ENSMUST00000130362	0.00	0.00	0.04	0.12	0.19	0.65	1.33	1.61	1.11	2.93	5.86	9.95	1.98
177	p8	ENSMUST00000174808	0.86	0.61	1.23	1.37	0.68	1.24	1.23	0.92	0.79	1.49	4.26	1.52	1.35
178	p1	ENSMUST00000159595	0.03	0.06	0.62	0.48	0.57	0.39	0.42	0.80	0.35	0.33	2.83	7.25	1.18
179	p18	Malat1	0.56	0.35	1.66	1.31	1.08	0.98	0.58	1.13	0.80	0.87	3.73	0.81	1.16
180	p20	Meg3	0.22	0.17	0.50	0.60	1.26	1.49	0.47	4.75	1.61	0.87	1.22	0.21	1.11

Appendix Table 1. Expression levels of robustly expressed lncRNAs during cerebellum development. FANTOM5 transcripts that are robustly expressed in the cerebellum were annotated as lncRNAs using GENCODE mouse lncRNA annotations (version M16) yielding a set of 180 transcripts, as listed here in the decreasing order of average expression levels (in TPM) across the cerebellar time-course. S.No., serial number; p, promoter number.